Development and application of standard molecules for Aβ oligomer quantification in CSF and human blood plasma in the sFIDA assay

Inaugural-Dissertation

zur Erlangung des Doktorgrades
der Mathematisch-Naturwissenschaftlichen Fakultät
der Heinrich-Heine-Universität Düsseldorf

vorgelegt von

Kateryna Kravchenko

aus Kowel, Ukraine

Jülich, Januar 2016

aus dem Institut für Physikalische Biologie
der Heinrich-Heine-Universität Düsseldorf

Gedruckt mit der Genehmigung der
Mathematisch-Naturwissenschaftlichen Fakultät der
Heinrich-Heine-Universität Düsseldorf

Referent: Prof. Dr. Dieter Willbold
Korreferent: Prof. Dr. Georg Groth

Tag der mündlichen Prüfung: 09.02.2016

EIDESSTATTLICHE ERKLÄRUNG

Hiermit erkläre ich, dass ich die vorliegende Arbeit selbständig angefertigt habe. Es wurden nur die in der Arbeit ausdrücklich benannten Quellen und Hilfsmittel benutzt. Wörtlich oder sinngemäß übernommenes Gedankengut habe ich als solches kenntlich gemacht.

Ort, Datum .....

Unterschrift .....

"If you change the way you look at things, the things you look at change."

- Dr. Wayne Dyer -

DANKSAGUNG

Mein Dank gilt meinem Doktorvater Prof. Dr. Dieter Willbold für die Möglichkeit der Anfertigung meiner Doktorarbeit auf einem spannenden Forschungsgebiet im Institut für komplexe Systeme am Forschungszentrum Jülich. Zusätzlich bedanke ich mich bei ihm für die hilfreichen Anregungen und Ideen, fachliche Diskussionen sowie exzellente Laborausstattung.
Des Weiteren bedanke ich mich bei Prof. D. Georg Groth für die Übernahme der Zweitkorrektur.
Bei meinem Gruppenleiter Oliver Bannach möchte ich mich für die Betreuung, die guten Ratschläge im Labor, die Hilfestellung beim Erstellen der Manuskripte, Motivation und seine positive und zuvorkommende Art bedanken.
Mein besonderer Dank gilt der sFIDA Gruppe. Insbesondere Katja Kühbach und Andreas Kulawik möchte ich für die zahlreichen fachlichen Diskussionen und ihre Geduld danken. Bei Katja bedanke ich mich für das Korrekturlesen und immer hilfreiche Ratschläge rund um das Thema Assay-Entwicklung. Bei Andreas bedanke ich mich für die Hilfestellung rund um das Thema Statistik und Vorbereitung der Vorträge für das Meeting ;). Kun Wang danke ich für die Einarbeitung in das Themengebiet und die zahlreichen Hilfestellungen im Labor. Christina Linnartz und Loreano Peters danke ich für ihre Unterstützung im Labor und ihre liebe und hilfsbereite Art. Bei Tuyen Bujnicki bedanke ich mich für immer ein offenes Ohr und motivierende Gespräche, bei Yvonne Herrmann für ihre herzliche und hilfsbereite Art und Aufmunterung, bei Christian Zafiu für zahlreiche Ideen und Diskussionen, bei Maren Hülsemann und Johannes Willbold für die angenehme Zusammenarbeit.
Weiterhin möchte ich mich bei meinen Bürokollegen Christina Dammers, Maren Thomaier und Volker Söhnitz für die angenehme Arbeitsatmosphäre bedanken. Maren's lustige und liebevolle Art hat immer die Stimmung im Büro aufgeheitert und die Arbeitsatmosphäre aufgelockert. Christinchen danke ich für die Freizeitgestaltung und unsere zahlreiche Gespräche außerhalb der Arbeitszeiten.
Ebenso bedanke ich mich für die Unterstützung und Freizeitgestaltung bei Tamar Ziehm, Tina Dunkelmann, Leonie Hofmann, Antonia Klein, Daniel Frenzel sowie Kristina Boxberger und Viktor Heinrichs.
Diese Arbeit wäre ohne die Unterstützung von meinen Liebsten nicht möglich gewesen. Ich bedanke mich ganz herzlich bei meiner besten Freundin Katharina Ebermann dafür,

dass sie mich auf meinem Lebensweg begleitet und mit unglaublich viel Einsatz mir viel Mut und Kraft insbesondere im letzten Jahr zugesprochen hat. Mein herzlicher Dank gilt auch dem Björn Kommoß für die Unterstützung und tolle Entspannung als Ausgleich zur Arbeit. Bei Valentina Brauer möchte ich mich für unsere jahrelange Freundschaft bedanken, die mir sehr viel bedeutet. Dennis Beckmann bin ich für die angenehme Freizeitgestaltung sowie seine positive und liebevolle Art dankbar.
Meinen Eltern Nina und Werner Richter und meiner Schwester Nataliya Kravchenko danke ich dafür, dass ihr mich in jeder Lebenslage unterstützt, an mich glaubt und immer für mich da seid. Ihr gebt mir viel Kraft und Motivation, meine Lebensziele zu verwirklichen.

SUMMARY

Alzheimer's disease (AD) is a neurodegenerative disorder and the most common form of dementia, with 100 mio. affected people predicted for 2050. Currently, neither a certain *pre mortem* diagnosis nor an effective causative therapy are available. The establishment of a reliable diagnostic assay for the early diagnosis of AD is of great importance for the development of effective therapeutics.

Several approaches have been proposed for AD diagnosis with oligomeric Aβ concentration in body fluids as a potential biomarker for AD. Aβ oligomers are considered to play a crucial role in the AD pathogenesis. However, these methods lack a reliable standard for assay calibration and inter-/intra-assay comparability. Molecules such as synthetic Aβ oligomers, Aβ dimers and multiple antigen peptides (MAPs) have been validated as standards in various assays, but no consensus has yet been achieved on which standard should be used for quantification of the pathologically relevant Aβ species.

In this study, the application of stabilized Aβ oligomers as standard molecules in the sFIDA assay (surface-based fluorescence intensity distribution analysis) was demonstrated. A correlation between the applied concentration of stabilized oligomers, diluted in PBS, CSF or blood plasma samples and the sFIDA readout was shown for a concentration range from 1 fM to 100 pM. The lower limits of detection for stabilized oligomers in PBS, CSF and plasma were 32 fM, 24 fM and 22 fM, respectively.

Additionally, a novel size-defined standard with a known number of epitopes in form of Aβ-coated silica nanoparticles (Aβ-SiNaP) was developed within the scope of this study. Silica nanoparticles were synthesized according to the Stöber process and biofunctionalized with Aβ via EDC/NHS coupling. The stability of this standard was shown by application of Aβ-SiNaP, diluted in water and CSF, in the sFIDA assay for at least four months at 4 °C.

Furthermore, Aβ-SiNaP were applied in order to assess the most suitable anti-coagulant for Aβ oligomer detection in blood plasma. A correlation between Aβ-SiNaP concentration and the sFIDA readout was demonstrated for Aβ-SiNaP diluted in PBS or EDTA, citrate and heparin plasma. Based on criteria such as reproducibility, linearity and sensitivity of the sFIDA assay, EDTA proved to be the anti-coagulant of choice for quantification of Aβ-SiNaP in blood plasma.

ZUSAMMENFASSUNG

Die Alzheimersche Demenz (AD) ist eine neurodegenerative Erkrankung, die einer Schätzung zufolge im Jahr 2050 ca. 100 Mio. Personen betreffen wird. Zur Zeit gibt es weder eine *pre mortem* Diagnose noch eine ursächliche Therapie. Die Etablierung eines zuverlässigen Assays ist von großer Bedeutung für die Entwicklung von wirksamen Therapeutika.

Einige Methoden wurden für die AD-Diagnostik vorgeschlagen, in welchen die Aβ-Oligomerkonzentration in Körperflüssigkeiten als Biomarker dienen, da diesen Molekülen die entscheidende Rolle in der AD-Pathogenese zugeschrieben wird. Allerdings fehlt diesen Methoden ein zuverlässiger Standard für die Assay-Kalibrierung und inter-/intra-Assay Vergleichbarkeit. Moleküle wie synthetische Aβ-Oligomere, Aβ-Dimere und multiple Antigen-Peptide (MAPs) wurden in verschiedenen Assays validiert, jedoch ohne Übereinstimmung darüber, welcher Standard den pathologisch relevanten Aβ-Oligomeren am nächsten kommt.

In dieser Arbeit wurde die Verwendung von stabilisierten Aβ-Oligomeren als Standardmolekül im sFIDA-Assay (*surface-based fluorescence intensity distribution analysis*) gezeigt. Die Konzentration von stabilisierten Oligomeren, die in PBS, CSF und Blutplasma verdünnt wurden, korreliert mit dem sFIDA-readout in einem Konzentrationsbereich zwischen 1 fM und 100 pM. Die untere Nachweisgrenze der Oligomere in PBS, CSF und Blutplasma lag bei 32 fM, 24 fM und 22 fM.

Zusätzlich wurde ein neuer Standard mit definierter Größe und bekannter Zahl an Epitopen im Rahmen dieser Arbeit entwickelt: Silika-Nanopartikel, an die kovalent Aβ gebunden ist (Aβ-SiNaP). Die Silika-Nanopartikel wurden nach dem Stöber-Prozess hergestellt und anschließend mit Aβ-Molekülen über EDC/NHS-Kopplung biofunktionalisiert. Anhand von sFIDA-Messungen wurde für Aβ-SiNaP eine Stabilität von mindestens vier Monaten nachgewiesen.

Des Weiteren wurde die erste Anwendung von Aβ-SiNaP an einer Studie zur Bestimmung der Eignung von verschiedenen Gerinnungshemmern für Aβ-Detektion in Blutplasma beschrieben. Es wurde gezeigt, dass der sFIDA-readout mit der Konzentration von Aβ-SiNaP verdünnt in PBS oder EDTA-, Zitrat- und Heparin-Plasma korreliert. Anhand von Kriterien wie die Reproduzierbarkeit, die Linearität und die Sensitivität des sFIDA-Assays hat sich EDTA als Gerinnungshemmer der Wahl für die Quantifizierung von Aβ-SiNaP in Plasma herausgestellt.

Contents

List of Figures

List of Tables

1 Introduction

1.1 Alzheimer's disease

1.1.1 Pathology of Alzheimer's disease

Alzheimer's disease (AD) was firstly described by the German psychiatrist Alois Alzheimer in 1906. He observed behavioral changes of his 51-year old patient Auguste D. such as cognitive decline, hallucinations, focal symptoms, delusions, disorientation and psychosocial impairment. At autopsy he found senile plaques and neurofibrillary tangles in her brain which today are considered the pathological hallmarks of the disease [1].
AD is a progressive neurodegenerative disorder and the most common form of dementia. Since age is considered to be the major risk factor for the disease and due to increasing aging of population the number of AD patients is predicted to reach 100 mio. people worldwide in 2050. Although a lot of research in the field has been done in the last century, important questions remain still unanswered. Neither a certain *pre mortem* diagnosis is available nor a causative therapy has yet been developed [2, 3].
Clinically, AD is divided in familial AD (fAD) with only 5 % of all cases and sporadic AD (sAD). The causes for familial AD are well established: mutations in amyloid precursor protein (APP), presenilin-1 (PSEN1) or presenilin-2 (PSEN2). In sporadic AD, a combination of genetic risk factors, e. g. possession of ApoE4 allele, and environmental risk factors as well as age have been linked to the onset of the disease. While fAD is characterized by early onset in 4th to 5th life decade, sAD develops mostly later in 6th to 7th decade [4, 5].
The pathology of sporadic AD starts 20 to 30 years before the clinical onset. According to disease progression, three stages of AD have been described: preclinical AD, mild

cognitive impairment (MCI) and clinical AD. At a preclinical stage, the degenerative processes are initiated in the brain including the increase of senile plaques and tangles. Years later first symptoms such as mild memory impairment are observed, which at this stage do not interfere with daily life. At clinical stage, severe memory impairment along with other symptoms such as disorientation, confusion, withdrawal from social activities, etc. appear. The differentiation of AD from other dementias or depression and the identification of MCI as a pre-stage of AD and not as a process associated with normal aging is of great importance for the development of therapeutical approaches [6, 7].
Pathological hallmarks of AD are brain atrophy, extracellular neuritic plaques composed of amyloid beta (Aβ) protein and intracellular neurofibrillary tangles composed of tau (τ) (1.1).

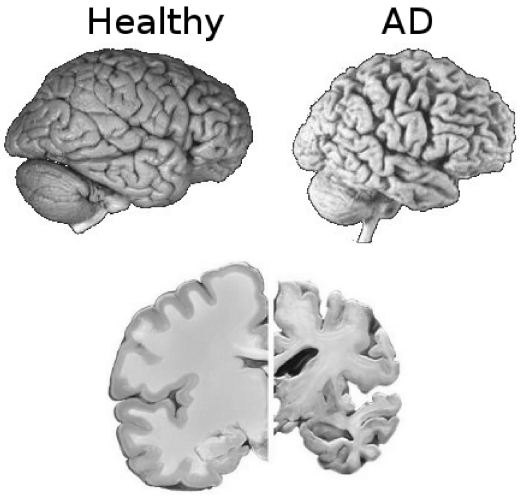

(a) Brain atrophy (adapted from [8])

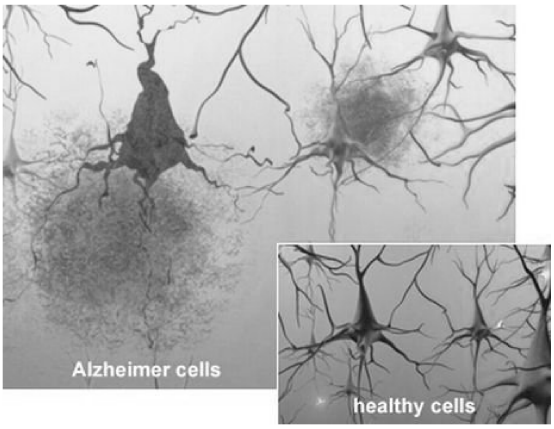

(b) Amyloid plaques and NFTs (adapted from [9])

Figure 1.1 Pathological hallmarks of Alzheimer's disease. a) On the left side a healthy brain is shown in comparison to AD affected brain on the right side. Significant brain volume loss is observed in the brains of AD patients. b) Brain lesions in form of amyloid plaques and neurofibrillary tangles (NFTs) occur throughout the brain in the course of AD progression. Amyloid plaques appear as bundles of amyloid beta (Aβ) peptide. Neurofibrillary tangles (NFTs) consist mainly of aggregated tau protein. Growth of NFTs within a cell causes neuronal death.

Shrinkage of the hippocampus, amygdala, frontal and temporal lobes caused by neuronal cell death were showed in numerous magnetic resonance imaging (MRI) studies [10–12] as well as in *post mortem* neuropathological examinations [13]. For a long time brain at-

rophy has been used in brain imaging techniques for AD diagnostics. However, recently the detection of molecular biomarkers in CSF has been shown to be a more reliable diagnostic tool [6, 14, 15].

Aβ plaque pathology is initiated with deposits in the neocortex, which spread gradually to hippocampus and finally to cerebellum [16]. These deposits consist of bundles of insoluble fibrillar structures. Mass spectrometric characterization of neuritic plaques by Portelius *et al.* showed that main components are Aβ_{1-42}, Aβ_{4-42} and Aβ_{1-40} and 3-pyroglutamate derivate of Aβ_{3-42}. Structural analysis revealed β-sheet rich content of the plaques which is closely linked to insolubility and neurotoxicity. [17] The link between amyloid plaques and disease progression remains not clear, since some studies show the presence of senile plaques, but the absence of AD symptoms [18–20].

Major components of neurofibrillary tangles (NFTs) are abnormally phosphorylated tau protein and ubiquitin. The main function of microtubule-associated protein τ is stabilization of axonal microtubules. In healthy individuals an equilibrium between dephosphorylated and phosphorylated tau (p-tau) exists. Upon increased hyperphosphorylation, p-tau dissociates from microtubules and forms aggregates. Bancher *et al.* describe three stages of NFT formation. At stage one, pathological fibers within a neuronal soma are formed which are called early tangles. At stage two, bundles of tightly packed paired helical filaments in form of flame-shaped inclusions are observed. Growth of these mature tangles causes dislocation and/or shrinkage of the cell nucleus. At last stage large filaments are found extracellularly, eventually causing the neuronal death [21]. Alonso *et al.* suggested a nucleation mechanism for NFT formation with hyperphosphorylated tau as seeds for tau aggregation [22].

1.1.2 Amyloid beta: production and neurotoxicity

The physiological role of Aβ is not fully understood. In its monomeric form it is present in healthy individuals suggesting certain physiological functions. There is evidence that Aβ is involved in modulation of synaptic activity by regulation of glutamate release. Moreover, neuronal cell death in absence of Aβ indicates its role in neuronal survival and implies its importance in cell processes of the central nervous system [23]. In animal trials a decreased Aβ expression was shown to impair learning abilities, whereas slight increase enhanced memory retention [24]. Also the role of Aβ as an anti-oxidant has

been proposed in literature based on its ability to chelate such metals as Cu, Fe and Zn which participate in redox cycles [25].

Aβ is 39 to 43 amino acids long protein with a molecular weight of approximately 4 kDa. It is derived from a 695 to 770 amino acid long amyloid precursor protein (APP), a type I transmembrane glycoprotein, that is coded on a chromosome 21 [26, 27].

APP is proteolytically processed either by α- and γ-secretase (non-amyloidogenic pathway) or by β- and γ-secretase (amyloidogenic processing) as illustrated in fig. 1.2.

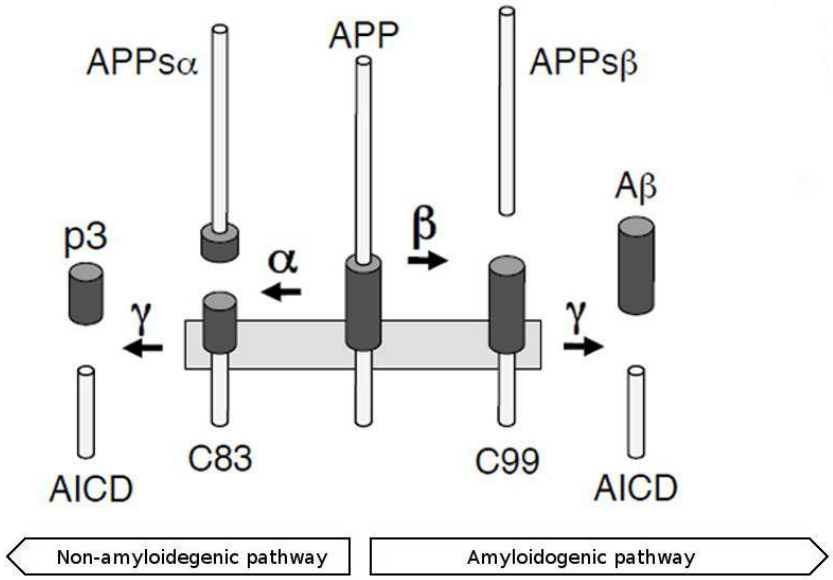

Figure 1.2 Processing pathways of amyloid precursor protein APP. Amyloidogenic and non-amyloidogenic pathways of APP cleavage are possible depending on secretases involved in the processing. APP can be cleaved by α secretase which leads to formation of a soluble APP domain APPsα and a transmembrane fragment C83. C83 is subsequently cut by γ secretase into P3 fragment and APP intracellular domain (AICD). Alternatively, APP is first cleaved by β-secretase and then by γ-secretase leading to release of a soluble APPsβ, AICD and amyloidogenic Aβ. Adapted from [28].

In the non-amyloidogenic pathway, APP is cleaved by α-secretase into a soluble APPsα fragment and transmembrane C83 fragment. The cleavage takes place within the Aβ region, thus preventing the formation of Aβ. C83 is subsequently cleaved by γ-secretase, which releases APP intracellular domain (AICD) and P3 fragment. In amyloidogenic processing, APP is first cleaved by β-secretase, the so called beta-site APP-cleaving enzyme (BACE), releasing a soluble APPsβ fragment. After that, γ-secretase cuts the

remaining C99 fragment within the transmembrane region into AICD and various Aβ isoforms between 17 and 42 amino acids as well as other truncated Aβ isoforms which are pathologically less important [17, 28].

The pathologically important Aβ isoforms with different COOH-termini are 40 and 42 amino acids long. The first 28 residues of Aβ are polar and the remaining 12 in Aβ_{1-40} or 14 in Aβ_{1-42} are non-polar. Due to the amphiphilic nature, Aβ peptide forms aggregates with hydrophobic cores *in vitro* [29, 30]. Interestingly, the two Aβ isoforms oligomerize through different pathways. Bitan *et al.* report formation of dimers, trimers and tetramers for Aβ_{1-40} and pentamer/hexamer units for Aβ_{1-42}. Moreover, the kinetics of the Aβ fibril formation showed significantly faster aggregation rates for Aβ_{1-42} compared to Aβ_{1-40} [31]. These differences may be caused by higher hydrophobicity of the longer Aβ_{1-42} isoform [32, 33].

A nucleation dependent mechanism for Aβ aggregation is demonstrated in fig. 1.3.

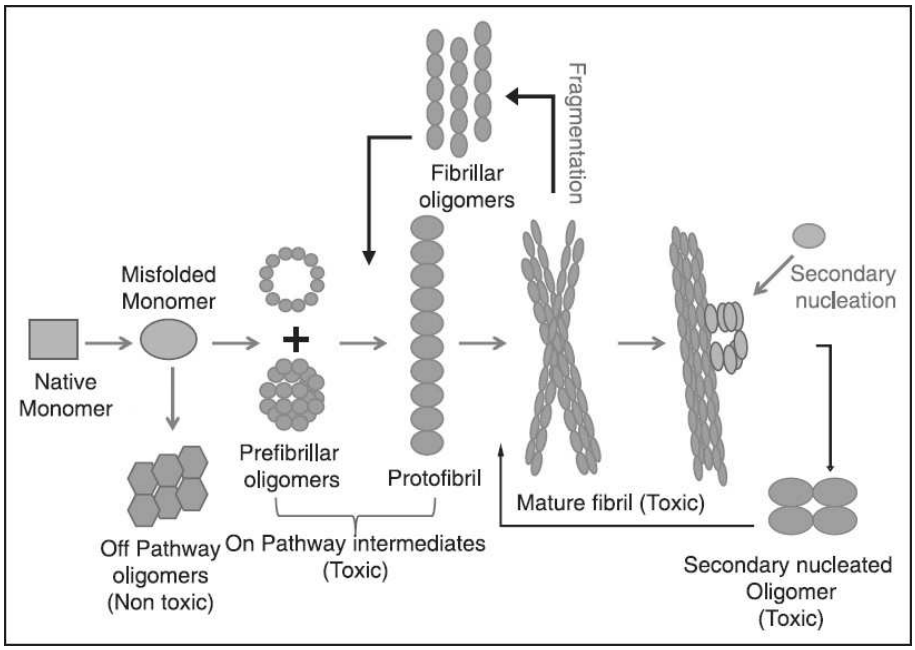

Figure 1.3 **Aβ aggregation mechanism.** Misfolding of native Aβ monomers leads to formation of non-toxic off-pathway oligomers and toxic on-pathway oligomers which form protofibrils. Protofibrils aggregate further to mature fibrils, which can dissociate to fibrillar oligomers which again end up in protofibrils and mature fibrils. Mature fibrils are also supposed to act as seeds for monomer association to secondary nucleated oligomers. Adapted from [34].

Misfolding of native Aβ causes conformational change from random coil to β-sheet structure. At a critical concentration of misfolded Aβ two types of oligomeric intermediates are formed: off-pathway oligomers and amyloidogenic oligomers. Whereas off-pathway oligomers do not develop to mature fibrils, amyloidogenic oligomers first form protofibrils which aggregate to mature fibrils. Oligomers are described as spherical or globular structures with an estimated diameter of approximately 140 Å. Protofibrils are ordered elongated aggregates with a diameter of approximately 200 to 700 Å. Fragmentation of mature fibrils leads to formation of fibrillar oligomers which will aggregate further and also end up in mature fibrils [35]. Recently Cohen *et al.* introduced a model for secondary nucleation of fibril formation. It suggests that mature fibrils act as catalysts for association of monomers [36].

Mature Aβ fibrils are ordered cross-β structures with diameters of approximately 2 to 20 nm and no defined length. For a long time Aβ fibrils were considered to cause neuronal death, however, the evidence from research of the last years indicates that Aβ oligomers are the most toxic species. Neurodegeneration caused by soluble Aβ was demostrated in numerous studies [30, 37–39]. Higher toxicity of oligomers can be explained by smaller size of oligomers which allows them to diffuse in tissues and interact with cellular targets and by structural instability in comparison to well-organized fibril molecules.

Several mechanisms were proposed for Aβ cytotoxicity with membrane interaction and perturbation of calcium homeostasis as most accepted. It is suggested that mature Aβ fibrils and oligomers initiate neurotoxic cascade by interaction with monosialotetrahexosylganglioside (GM-1)-rich membrane domains. Alternatively, it is believed that Aβ oligomers cause calcium homeostasis perturbance by ion channel formation in the cell membrane such as oxidative stress and inflammation, thus inducing the influx of Ca^{2+} into the cytoplasm. Elevated Ca^{2+} levels lead to production of reactive oxygen species, mitochondrial dysfunction, etc. which are closely associated with downstream events of AD pathology [34].

1.1.3 Amyloid cascade hypothesis

The most influential hypothesis of AD pathogenesis and pathology is the amyloid cascade hypothesis (ACH) formulated by Hardy and Higgins in 1992. The original ACH proposes that imbalance of Aβ production and clearance causes the formation of amyloid plaques and neurofibrillary tangles, death of neuronal cells and finally dementia. In over 20 years after its postulation ACH has been modified according to the stage of development in the research field. Fig. 1.4 illustrates ACH as adapted by K. Blennow *et al.* in 2010 [7].

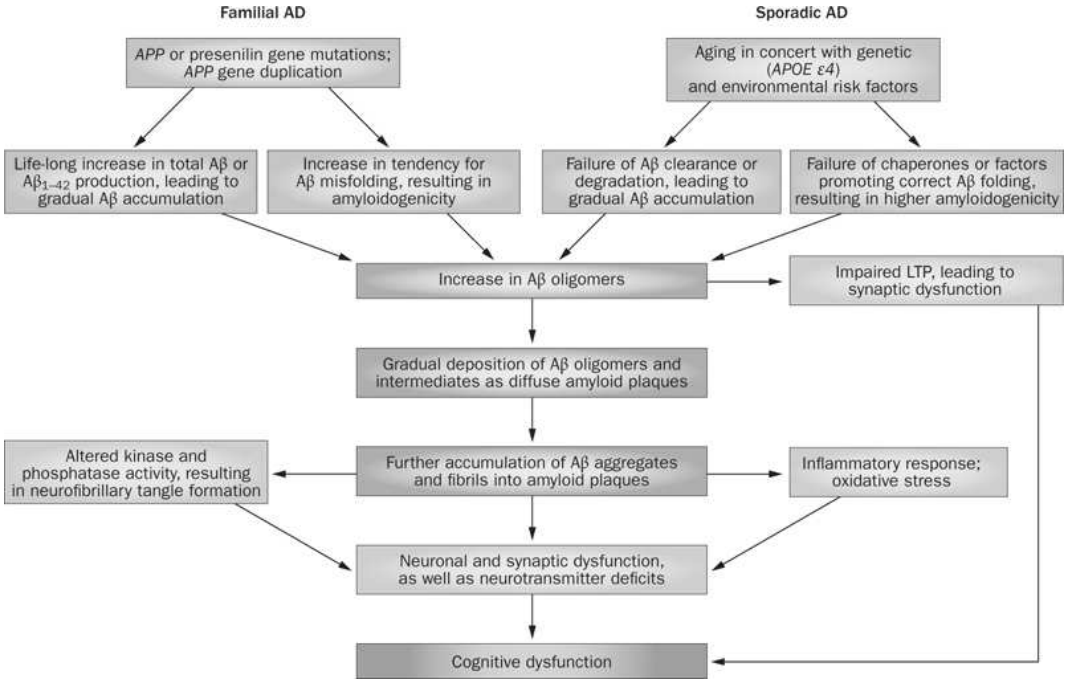

Figure 1.4 Amyloid cascade hypothesis (ACH). The ACH states that imbalance in production and clearance of Aβ causes the formation of amyloid plaques and neurofibrillary tangles, death of neuronal cells and finally cognitive impairment. In familial AD, the increase in Aβ concentration is caused either by life-long increase in Aβ or by increased tendency for Aβ misfolding. In sporadic AD, Aβ oligomer concentration increases due to failure of Aβ clearance, degradation or factors promoting correct Aβ folding. In both cases, Aβ accumulation precedes a cascade of down-stream events such as inflammatory response, oxidative stress, altered kinase and phosphotase activity which result in cognitive dysfunction. Adapted from [7].

In case of familial AD caused by mutations in APP or presenilin genes, total Aβ increases or Aβ has a higher tendency for misfolding, which leads to an increase in Aβ oligomers. Sporadic AD, caused by aging, genetic and environmental risk factors, is

characterized by failure of Aβ clearance or degradation or failure of factors promoting correct Aβ folding. In both familial and sporadic AD, increase of Aβ concentration and/or amyloidogenicity are according to ACH crucial events in disease formation and progression which is followed by an increase of Aβ oligomer concentration and a gradual deposition of Aβ aggregates and fibrils. The accumulation of insoluble Aβ causes inflammatory responses and oxidative stress and alters kinase and phosphatase activity which leads to formation of neurofibrillary tangles. These events trigger neuronal and synaptic dysfunction as well as neurotransmitter deficits leading finally to cognitive dysfunction. Although there is a considerable evidence supporting the ACH, inconsistencies are discussed in literature.

Evidence supporting the ACH includes studies on AD pathology and genetics. Amyloid beta being the main constituent of amyloid plaques seems closely linked to pathologic events in the disease progression. Overexpression of APP in transgenic mice results in amyloid deposits and neuronal loss which implies a pivotal role of amyloid beta in cell death. Also the increase of Aβ in fAD caused by gene mutations indicates that accumulation of this peptide causes a variety of downstream events which finally lead to dementia. Presence of NFTs in amyloid plaques indicates a link between Aβ deposition and NFTs formation.

However, following major objections question the increase of Aβ as the main cause of the AD: first, amyloid plaques and NFTs may be the reactive processes of the neurodegeneration. An increased expression of APP was shown in persons who suffered from head trauma as a protective mechanism to neuronal injury. Second, it is still not clear how amyloid deposits cause the formation of NFTs. There is evidence, that amyloid deposits may alter the phosphorylation state of tau, however, spatial and temporal separation of the lesions imply independent mechanisms of formation. Third, plaque load does not necessarily represent the degree of dementia. Some studies show presence of amyloid plaques in the brain, but absence of symptoms for cognitive impairment .

The finding that soluble oligomeric Aβ species are more toxic than fibrils resolves the inconsistencies regarding spatial distribution of Aβ deposits and NFTs. Small oligomeric Aβ can diffuse throughout the brain and cause NFT formation independently of Aβ plaques. Although insights in mechanism of formation and toxicity of oligomeric Aβ species has been gained, it remains unclear if Aβ indeed plays a crucial role or is *one* of the factors which contribute to AD pathogenesis [4, 40, 41].

1.2 AD diagnostics

1.2.1 Brain imaging techniques

The urgency of AD diagnostics for use in clinical studies and drug development led to development of various psychological, electrophysical and molecular approaches.
In 1975 mini-mental state examination (MMSE) was developed by M. F. Folstein to investigate cognitive deficits of demented patients [42]. Such cognitive functions as time and space orientation, memorizing and remembering abilities, concentration as well as understanding, speaking, reading and writing abilities are tested using 11 tasks which are afterwards scored with max. 30 points. The MMSE allows fast, simple and inexpensive prediction of cognitive impairment. However, it fails in differentiating AD from other dementia or depression and MCI from normal aging.
Starting at 1970s, AD has been diagnosed by structural imaging where brain atrophy is used as a marker for the degree of disease progression. In a non-invasive diagnostic imaging procedure computed tomography (CT), scans are obtained using a combination of X-rays and computer technology. However, this technique failed to produce consistent results in correlation between brain damage and behavioral changes [43, 44].
A more reliable technique is high-resolution magnet resonance imaging (MRI). Here, shrinkage of hippocampal region is the best established diagnostic marker for AD. This technique currently allows to differentiate AD patients from non-demented controls with 80 to 85 % sensitivity and specificity [11, 12].
Beginning at 1980s, positron emission tomography has been widely applied to measure fluorodeoxyglucose metabolism in cerebral cortex (FDG-PET) in AD patients. This technique considerably enhanced prediction of the disease by identifying brain regions with impaired local cerebral metabolic rate of glucose which showed reduced FDG uptake [45–47].
From 1990s onward, functional MRI (fMRI) has been applied to measure brain activities during certain tasks. In this brain imaging technique an initial MR signal is compared with MR signal during a task which involves certain thinking processes. For example, using episodic memory tasks, AD related decreased activity in hippocampus was reported. However, this method requires additional validation studies, especially for differentiating MCI from healthy controls [48, 49].
Since 2000s, amyloid positron emission topography (PET) has been used to identify amy-

loid plaques in the brain of AD patients. Invention of Pittsburgh compound B (PiB) allows detection of β-sheet rich structures within the brain *pre mortem*. This compound is Thioflavin T (ThT) which is modified in such a way that it is no longer charged and thus can pass the brain-blood-barrier. The binding of PiB is proportional to amyloid load in brain [50, 51]. Disadvantages of amyloid PET are injection of radioactive substances and limited clinical application due to short half-life of ^{11}C which was reported to be expensive and impractical [52, 53].

1.2.2 Molecular biomarkers in CSF and plasma

According to the Biomarkers Definitions Working Group of the US National Institutes of Health, a biomarker is defined as "an objectively measured feature that is assessed as an indicator of normal biological or pathogenic processes or pharmacological responses to a therapeutic intervention" [53]. It should also fulfill such criteria as reliability and non-invasive, simple and inexpensive procedure of sample collection.
Several molecular biomarkers were tested as candidates for AD diagnosis in body fluids. Table 1.1 summarizes some of them categorized due to the pathological processes they are associated with.

Table 1.1 Molecular biomarkers proposed for early AD diagnosis based on pathophysiological processes associated with disease progression

Pathology	**Biomarkers**
APP and Aβ metabolism	APP isoforms, truncated Aβ isoforms, monomeric Aβ_{1-40} and Aβ_{1-42}, Aβ oligomers, Aβ autoantibodies BACE1
NFT formation	total and/or phosphorylated tau
axonal and synaptic failure	VLP-1, RAB3A, GAP-43
cholesterol metabolism	cholesterol, 24S-Hydroxycholesterol
oxidative stress	antioxidant levels, F2-isoprostanes
inflammation	CRP, cytokinases, chemokinases

Detection of three biomarkers in cerebrospinal fluid (CSF) proved to be a reliable tool for diagnostics of early and incipient AD stages. A number of studies showed correlations between total tau (t-tau), phosphorylated tau (p-tau) and Aβ_{1-42} in CSF with molecular changes in brain. Levels of t-tau and p-tau which are used as biomarkers for neuronal

degeneration and NFT formation, respectively, are reported to considerably increase with AD progression, whereas Aβ_{1-42} levels as a biomarker for amyloid plaque formation, decrease. The specificity and sensitivity of these biomarkers is quite high as can be seen in table 1.2 [6].

Table 1.2 Specificity and sensitivity of molecular biomarkers t-tau, p-tau and Aβ_{1-42} for AD diagnosis at early and incipient stages.

biomarker	**specificity**	**sensitivity**
t-tau	90 %	80 %
p-tau	92 %	80 %
Aβ_{1-42}	90 %	85 %

AD prediction from MCI can be realized by combination of all three above mentioned biomarkers with additional tests and imaging techniques. At the preclinical stage of AD, Aβ was shown to decrease, but no significant change in t- and p-tau was observed. These findings suggest that Aβ_{1-42} concentration decline is the most promising biomarker at early stages of disease development [15].
Despite these convincing results, lumbar puncture is an invasive technique for sample collection, which may be accompanied by complications and post lumbar puncture headaches. Moreover, it is a time-consuming procedure which requires well-trained personal [7, 14]. Hence, growing interest has been observed for blood-based biomarkers due to less invasive sampling, less time-consuming and more cost-efficient sample handling compared to CSF.
Using protein array technology Ray *et al.* measured concentrations of 120 cell-signaling proteins in plasma of AD patients and healthy controls. Their study is considered one of the most influential on proteome-based biomarkers for AD in plasma. The choice of the proteins was based on association of immune and inflammatory pathways with AD progression. They reported 90 % accuracy in differentiating AD from healthy individuals for 18 plasma proteins such as cytokines, chemokines and growth factors. Also, they were able to predict AD in MCI specimens with 81 % accuracy [54].
Antioxidant levels, cholesterol and 24S-hydroxycholesterol and a variety of inflammatory molecules have been used as biomarkers for oxidative stress, lipid metabolism and inflammation in plasma. However, less consistent results for AD diagnosis were obtained in these studies [55, 56].
Based on the ACH, Aβ is the most promising biomarker for CSF and Aβ in plasma, since it plays a crucial role in AD pathogenesis and has been shown to be neurotoxic in

its oligomeric state. Whereas for CSF samples a correlation between Aβ concentration in brain and CSF has been shown, for plasma the results are inconsistent. Direct connection between the brain interstitial fluid and CSF allows more accurate correlation of Aβ levels in CSF with those in brain. Increase of senile plaques thus causes lowering of total Aβ concentration in CSF.
However, measuring Aβ levels in plasma is more complex. Oh *et al.* summarizes factors which can explain difficulties of quantifying Aβ in plasma compared to CSF [57]. Firstly, the activity of BACE1, an enzyme responsible for APP cleavage leading to Aβ formation, is observed not only in brain, but also in skeletal muscle, liver, kidney and lung. Secondly, Aβ has been detected in skin, subcutaneous tissue, intestine and muscle. Although this Aβ amount is smaller than Aβ originated from brain, it still may contribute to Aβ pool in blood. Thirdly, age-correlated increase of Aβ levels in plasma may interfere with accurate quantification of AD-related Aβ. Fourthly, the centrifugation of blood platelets, which are considered to be a source of Aβ in blood plasma, may lower Aβ amount [57]. Also, the interaction of Aβ with other proteins in plasma may confound Aβ level detection. Aβ is reported to be transported on lipoproteins and albumin in human plasma [58–60] and is sequestered by plasma proteins, e. g. α2-macroglobulin, amyloid P component, apoferritin, ApoJ and transthyretin [61, 62].
To overcome the above mentioned challenges in measuring Aβ levels several strategies for modulation of plasma Aβ levels have been proposed:

1. **Aβ levels modulation in plasma by Aβ-specific antibodies**. Elevation of Aβ levels in plasma may be achieved by shifting of equilibrium between soluble and sequestered Aβ. It was proposed that binding of plasma Aβ to an Aβ-specific antibody would cause an efflux of soluble Aβ from the brain to the blood. First studies showed that Aβ levels decreased in CSF and increased in serum upon infusion of intravenous immunoglobulin (IVIG) in individuals with neurological disorders [63].

2. **Aβ levels modulation in plasma by Aβ binding agents**. To avoid immunoreactivity towards injected antibodies, agents with high affinity for Aβ can be used instead. In animal trials few different Aβ binding agents such as gelsolin, ganglioside G_{M1}, Congo red derivatives and LPR-1 have been explored. However, these studies yielded inconsistent results.

3. **Aβ levels modulation in plasma by insulin infusion**. A different approach for modulation of Aβ levels in plasma is insulin infusion. It is based on *in vitro* data from Qui *et al.* which suggest that insulin elevates levels of extracellular Aβ by activation of insulin receptors in platelets [64]. Kulstad *et al.* showed encreased Aβ levels in plasma samples from AD patients, whereas no change was observed in plasma from healthy controls [65].

Finally, one of the major deficiencies of existing results for Aβ levels in plasma is the absence of standardized protocols for plasma treatment prior to Aβ detection [66]. Anti-coagulants such as EDTA and citrate, for example, inhibit blood coagulation by binding metal ions, thus inhibiting metal ion-dependent enzymes. Heparin, in contrary, activates anti-thrombin III, thus revealing a completely different mechanism of anti-coagulation [67], which may alter plasma composition and thus change the aggregation of Aβ or binding abilities of Aβ to other proteins.
Since recent studies have reported higher neurotoxicity of Aβ oligomers compared to fibrils, small soluble Aβ species gain growing interest as potential biomarkers for preclinical stages of AD. Several methods that have been introduced for Aβ oligomer detection in CSF are presented in fig. 1.5.

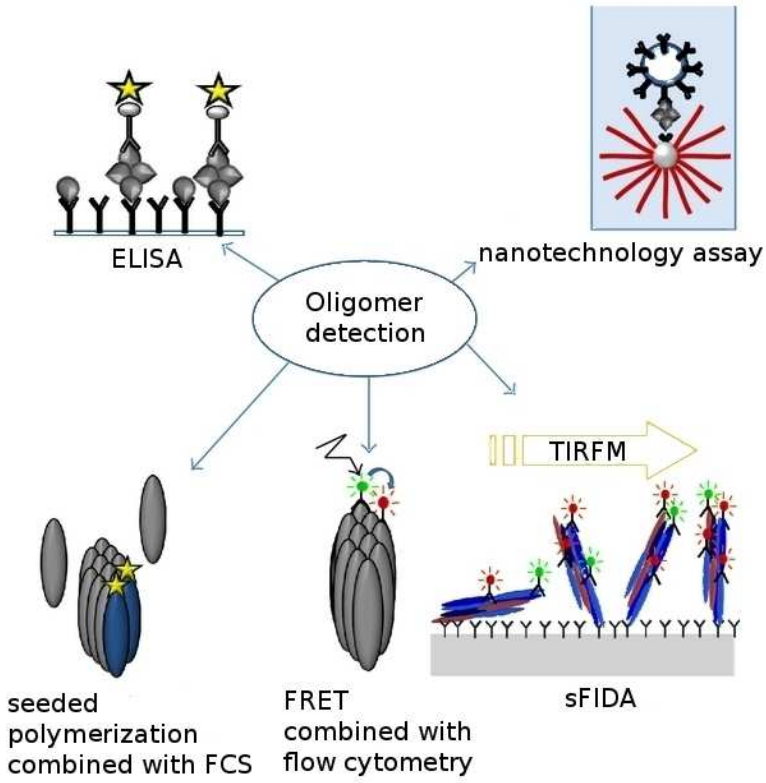

Figure 1.5 Methods used for the detection of soluble Aβ oligomers in CSF. In oligomer specific sandwich-ELISAs either conformational antibodies or the same monoclonal antibody for capture and detection are used. Within a nanotechnology-based bio-barcode assay oligomers are bound to magnetic beads and DNA labeled nanoparticles. The concentration of oligomers is determined based on a number of DNA barcodes. A principle of seeded polymerization is applied in combination with FCS for single particle detection. Here, fluorescent labeled monomers are added to the samples. If in a sample Aβ oligomers are present, they will act as seeds for aggregation of labeled monomers and stronger fluorescence signals compared to control are detected. Combination of fluorescence resonance energy transfer (FRET) and flow cytometry also allows detection of single oligomers. An energy transfer from a donor molecule takes place to an acceptor which emits energy that can be detected. In sFIDA, Aβ oligomers are captured on the glass surface and detected by different monoclonal Aβ specific antibodies and detected by total internal reflection microscopy (TIRFM). Adapted from [68].

The simplicity of performance of ELISA studies made this method most commonly used for Aβ oligomer detection. Using Aβ specific antibodies oligomers are captured on the surface and detected either by oligomer specific antibodies or by application of the same

antibody for capturing and detection. This approach allows to exclude signals from monomeric Aβ, which is present in the samples in much higher concentrations compared to oligomeric Aβ [69–72].
In a nanotechnology-based assay designated bio-barcode assay, oligomers are bound by a specific antibody to magnetic beads. The signal is amplified by binding of DNA labeled nanoparticles through a second Aβ specific antibody. Using a magnet Aβ oligomers are extracted from the sample. The concentration is estimated based on number of DNA barcodes [73].
Another method for detection of Aβ oligomers in CSF is based on the process of seeded polymerization. Fluorescence labeled Aβ monomers were added to the CSF of AD patients and control donors. In AD patients, oligomeric Aβ species acted as seeds for polymerization of the labeled monomeric Aβ. Fluctuations of the fluorescence intensities due to Brownian motion were measured by FCS [74].
A completely different method for counting of single particles is based on the combination of fluorescence resonance energy transfer (FRET) and flow cytometry for signal detection. Two fluorescence labeled Aβ specific antibodies are added to CSF sample. Only if both antibodies bind to the same oligomer, energy is transferred from an excited donor to an acceptor and emission of the acceptor molecule is detected by flow cytometry [75].
Surface-based fluorescence intensity distribution analysis (sFIDA) is a highly sensitive and specific method for Aβ oligomer quantification in body fluids in early AD diagnosis. In its setup, it basically mirrors sandwich-ELISA, however, in sFIDA different monoclonal N-terminal antibodies are used for Aβ capture and detection which makes this technique more specific. Furthermore, single-counting of Aβ oligomers is implemented by TIRFM which results in high sensitivity.

1.2.3 Surface-based fluorescence intensity distribution analysis (sFIDA)

In 2006, a method for the detection of single particles in a suspension of prion aggregates, obtained from BSE- and scrapie-infected animals, with two fluorescence labeled prion specific antibodies was published by Birkmann *et al.* [76]. The signal was measured by dual-color fluorescence correlation spectroscopy (FCS) and analyzed by plotting fluores-

cence intensities against their frequencies. At this stage of method development, the counting of single aggregates by fluorescence intensity distribution analysis designated 2D-FIDA was impeded by superposition of particle diffusion and the scanning of the sample.

In 2007, the sensitivity of the assay was considerably enhanced by immobilization of prion particles on the glass surface. Although the setup basically mirrors ELISA for protein detection, its major advantage is the counting of single particles on the scanned surface instead of measuring the overall integrated signal from the sample. The method was renamed to surface-FIDA implying the capturing of the target and measuring of the signal on the surface. Samples from scrapie-infected hamster and BSE-infected cattle could be identified considerably sensitiver compared to samples measured in solution [77].

Funke *et al.* adapted the method for the detection of Aβ aggregates. Synthetically prepared Aβ aggregates could successfully be detected both in solution via 2D-FIDA as well as on the glass surface applying surface-FIDA. Moreover, the authors detected synthetically prepared Aβ spiked in CSF and were able to differentiate CSF samples of AD patients from CSF of non-demented controls [78].

In 2010, the sensitivity of the method was further enhanced by scanning the immobilized target with laser scanning microscope (LSM). The amount of detected Aβ was derived from the number of colocalized pixels obtained in two channels and not from fluorescence intensity values over time. In comparison to 0.3 ng Aβ amount which could be differentiated from background signal using the FCS imaging setup, lowest amounts down to 0.36 pg Aβ were detected using LSM [79].

Lei Wang-Dietrich *et al.* optimized the assay in 2012 by coating the surface with CMD to reduce background noise caused by unspecific binding of detection antibodies to the glass. In this study, sFIDA readout revealed significantly higher values for 14 AD patients compared to 12 age-matched healthy controls [80].

Currently, the glass surface of multititer plates is covalently covered with PEG and an Aβ specific capture antibody is covalently bound to activated PEG binding sites. The sample is applied to the pretreated surface and after blocking step with BSA-free blocking solution, Aβ oligomers are detected by two fluorescence labeled antibodies. The images are obtained by total internal reflection fluorescence microscope (TIRFM) which enables exclusive excitation of fluorophores immobilized on the surface, thus considerably reducing the signals of the adjuscent molecules from the solution. The number of colocalized pixels is counted above the background. Cutoffs for the background are values for signal intensities which exceed a certain percentage of total analyzed pixels in

each channel in (unspiked) control samples. The setup of the sFIDA assay is illustrated in fig. 1.6

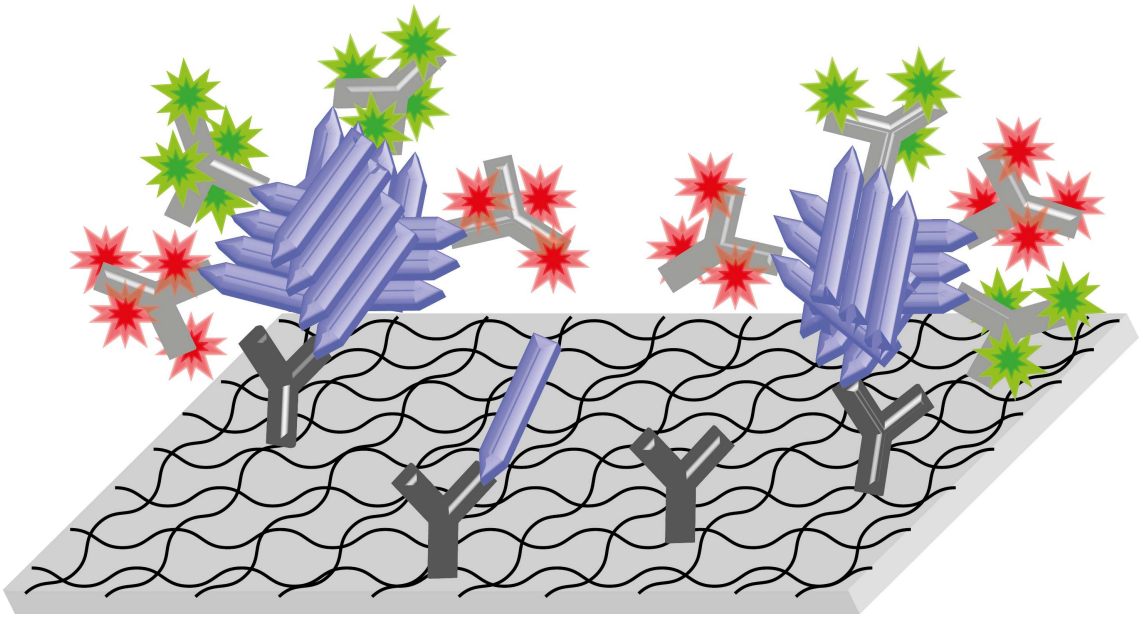

Figure 1.6 Surface-based fluorescence intensity distribution analysis (sFIDA). A monoclonal Aβ specific capture antibody (illustrated in dark grey) is covalently bound to PEG-coated surface of a glass chip. Oligomeric and monomeric Aβ species (illustrated in purple) from the sample bind to the capture antibody, but only oligomers are detected by two different fluorescence labeled anti-Aβ-antibodies (illustrated in light grey with red and green labels), which recognize the same or overlapping epitope at the N-terminus of Aβ molecules. Single Aβ oligomers are detected by total internal reflection microscopy (TIRFM).

1.2.4 Standards for validation and calibration of Aβ oligomer specific assays

A developed and optimized assay needs to be validated by experiments which evaluate its performance based on such criteria as specificity, accuracy, sensitivity, precision, detection limit, range and linearity, intra- and inter-assay ruggedness and robustness. Validation ensures that the assay is reliable under conditions of routine use for analysis of a defined target within a specified range [81].

For monitoring of assay performance over time, assay calibration and standardization

of different methods which detect the same analyte, standard molecules need to be developed, which represent an analyte in a defined range from low to high concentrations. Often, standards are prepared by spiking of molecules with known concentrations and characteristics similar to the analyte into the matrix in which the analyte is detected. Ideally, standards should fulfill certain requirements such as stability and inter- and intra-assay reproducibility. Furthermore, they should resemble the physicochemical properties of the analyte and the matrix-analyte interactions [82].

Development of standard molecules for Aβ oligomer specific assays is challenging due the nature of the analyte. First, the exact morphology and composition of soluble Aβ is not known. Aβ_{1-42} is more prone to aggregation compared to Aβ_{1-40}, however, small amounts of Aβ_{1-40} are also found in amyloid plaques. Second, the permanent dynamic equilibrium between various Aβ species in an oligomeric mixture does not allow a precise determination of Aβ oligomer size and composition. Third, the size range of potential neurotoxic oligomers varies from dimers to HMW oligomers composed of hundreds of molecules. It is a difficult task to cover the whole range with a certain standard of a defined oligomeric composition.

Several standard molecules have been developed for standardization and calibration of above mentioned Aβ oligomer specific methods. Most commonly used are Aβ oligomers also referred to as Aβ derived diffusible ligands (ADDLs). A number of protocols has been proposed for Aβ oligomer preparation, however, major defficiencies are the heterogeneous size distribution and instability of these Aβ species [83–85]. A mixture of Aβ oligomers often contains monomers and fibrils due to the dynamic equilibrium between these species.

Few studies use cross-linked Aβ dimers for assay calibration [69, 86], which are well-defined in size and morphology, however, do not exactly resemble the majority of Aβ oligomers in body fluids which were reported to be predominantly in the size range of 3- to 24-mers. Thus, this standard is most suitable for very small Aβ oligomers.

Also, multiple antigen peptides (MAPs) have been reported as a potential reference standard [71]. Stability and defined size of the molecules make them a reliable standard for Aβ oligomer quantification.

The detailed overview and critical review of currently used standards as well as a comparison with stabilized oligomers and Aβ-SiNaP, two molecules which are applied as standards in this study, can be found in the discussion.

1.3 Aims

Alzheimer's disease (AD) is a neurodegenerative disorder and the most common form of dementia. The number of AD patients is estimated to reach 100 mio. people in 2050 due to an increasing life expectancy of population and the fact that age is considered the major risk factor for the disease. Currently, neither certain *pre mortem* diagnostics nor a causative therapy is available.

Pathological hallmarks of AD are senile plaques composed of amyloid β (Aβ) protein and neurofibrillary tangles (NFTs) which mainly consist of protein tau. According to the amyloid cascade hypothesis, Aβ is suggested to play a crucial role in AD pathogenesis. Downstream events such as NFT formation, oxidative stress, inflammatory processes, neuronal loss and finally cognitive impairment are believed to be caused by increased concentration of Aβ. Since recent studies have shown, that small soluble oligomeric Aβ species are more toxic than Aβ monomers and fibrils, Aβ oligomers have gained increased interest as potential biomarkers. Several studies have already demonstrated significant differences in Aβ oligomer concentrations between CSF samples from AD patients and control donors.

Different methods have been developed for oligomeric Aβ detection in CSF: sandwich-ELISAs, nanotechnology-based methods, fluorescence correlation spectroscopy (FCS) combined with the process of seeded polymerization, flow cytometry applied for detection of fluorescence resonance energy transfer (FRET) signals and surface-based fluorescence intensity distribution analysis (sFIDA). The results obtained for Aβ detection in CSF and plasma by different technologies are inconsistent.

Among other challenges for the quantification of Aβ oligomers, the absence of a reliable standard makes the direct comparability of the obtained results hardly possible. Most commonly used standard molecules are Aβ oligomers, the so called Aβ-derived diffusible ligands (ADDLs). ADDLs were shown to exist in a dynamic equilibrium of numerous Aβ species ranging from monomers to low and high molecular weight oligomers. The stability of these standard molecules is often limited to 24 h and their characteristics vary strongly depending on preparation protocol and/or experimenter. Cross-linked Aβ dimers are used by some groups for quantification of low molecular weight (LMW) Aβ oligomers. Although Aβ dimers are stable and have a defined size, their usage as a standard is limited because they do not resemble high molecular weight (HMW) oligomers and, if composed of Aβ_{1-40} as reported, they differ in their hydrophobicity from Aβ_{1-42},

which is the main constituent of Aβ plaques. Lately, multiple antigen peptides consisting of a lysine core and 16 Aβ epitopes have been presented as a promising standard due to their stability, defined size and flexibility in number and choice of epitopes.
In this study, the performance of stabilized Aβ oligomers and Aβ-coated silica nanoparticles as standards in the sFIDA assay are presented. Three following tasks are the aim of this study. First, the performance of stabilized oligomers obtained from Crossbeta Bioscience will be validated as a standard in the sFIDA assay. Second, the development, characterization and validation of a stable and reliable standard for the detection of Aβ oligomers in body fluids in the sFIDA assay, Aβ_{1-42}-coated silica nanoparticles (Aβ-SiNaP), will be presented. Thirdly, the application of Aβ-SiNaP in the sFIDA assay will be demonstrated in a study for determination of the most appropriate anti-coagulant for detection of Aβ oligomers in blood plasma.

2 Results

2.1 Manuscript 1: Application of an amyloid beta oligomer standard in the sFIDA assay

2.2 Manuscript 2: Biofunctionalized silica nanoparticles: standards in amyloid-β oligomer-based diagnosis of Alzheimer's disease

2.3 Manuscript 3: Analysis of anticoagulants for blood-based quantitation of amyloid β oligomers in the sFIDA assay

frontiers in Neuroscience

TECHNOLOGY REPORT
published: 29 January 2016
doi: 10.3389/fnins.2016.00008

Application of an Amyloid Beta Oligomer Standard in the sFIDA Assay

*Katja Kühbach[1], Maren Hülsemann[1], Yvonne Herrmann[1], Kateryna Kravchenko[1], Andreas Kulawik[1], Christina Linnartz[1], Luriano Peters[1], Kun Wang[1], Johannes Willbold[1], Dieter Willbold[1,2] and Oliver Bannach[1,2]**

[1] ICS-6 Structural Biochemistry, Forschungszentrum Jülich GmbH, Jülich, Germany, [2] Institut für Physikalische Biologie, Heinrich-Heine-Universität Düsseldorf, Düsseldorf, Germany

Still, there is need for significant improvements in reliable and accurate diagnosis for Alzheimer's disease (AD) at early stages. It is widely accepted that changes in the concentration and conformation of amyloid-β (Aβ) appear several years before the onset of first symptoms of cognitive impairment in AD patients. Because Aβ oligomers are possibly the major toxic species in AD, they are a promising biomarker candidate for the early diagnosis of the disease. To date, a variety of oligomer-specific assays have been developed, many of them ELISAs. Here, we demonstrate the sFIDA assay, a technology highly specific for Aβ oligomers developed toward single particle sensitivity. By spiking stabilized Aβ oligomers to buffer and to body fluids from control donors, we show that the sFIDA readout correlates with the applied concentration of stabilized oligomers diluted in buffer, cerebrospinal fluid (CSF), and blood plasma over several orders of magnitude. The lower limit of detection was calculated to be 22 fM of stabilized oligomers diluted in PBS, 18 fM in CSF, and 14 fM in blood plasma.

Keywords: Alzheimer's disease, amyloid-β peptide, diagnostic biomarker, early diagnosis, sFIDA, surface-based fluorescence intensity distribution analysis, stabilized oligomers, standard molecule

OPEN ACCESS

Edited by:
Charlotte Elisabeth Teunissen, VU University Medical Center Amsterdam, Netherlands

Reviewed by:
Xifei Yang, Shenzhen Center for Disease Control and Prevention, China
Mary Josephine Savage, Merck and Company, USA

***Correspondence:**
Oliver Bannach
o.bannach@fz-juelich.de

Specialty section:
This article was submitted to Neurodegeneration, a section of the journal Frontiers in Neuroscience

Received: *10 November 2015*
Accepted: *11 January 2016*
Published: *29 January 2016*

Citation:
Kühbach K, Hülsemann M, Herrmann Y, Kravchenko K, Kulawik A, Linnartz C, Peters L, Wang K, Willbold J, Willbold D and Bannach O (2016) Application of an Amyloid Beta Oligomer Standard in the sFIDA Assay. Front. Neurosci. 10:8. doi: 10.3389/fnins.2016.00008

INTRODUCTION

Worldwide 5–7% of people older than 60 years are affected by dementia, with Alzheimer's disease (AD) being the most common type. Due to the aging population, the total number of demented people is predicted to increase even further (Prince et al., 2013). There is neither a cure nor a sufficiently reliable laboratory diagnostic test available for this fatal neurodegenerative disease (Lansdall, 2014). Early diagnosis of AD, however, is of great importance for the development of therapeutics and their future application at an early stage of the disease. It is believed that AD can be treated most effectively in preclinical stages, before cognitive functions become impaired and neurons and synapses are damaged irreversibly (Golde et al., 2011). Hitherto, the definitive diagnosis can only be made after the patients' death based on neuropathological hallmarks, like amyloid plaques, neurodegeneration and neurofibrillary tangles (Ballard et al., 2011).

The main component of amyloid plaques is amyloid β peptide (Aβ), which is formed from the amyloid precursor protein (APP) by β- and γ-secretases (Haass et al., 2012). Once released from the precursor, the Aβ peptide is prone to aggregation and can assemble into oligomeric structures and amyloid fibrils. It is widely accepted that soluble Aβ oligomers but not monomers are highly neurotoxic and that the pathological process in AD starts already years before the onset of clinical manifestation (Braak and Braak, 1991; McLean et al., 1999; Cleary et al., 2004; Lesné et al., 2006).

Currently, the total concentration of $A\beta_{42}$ in cerebrospinal fluid (CSF), which is lower in AD patients compared to healthy persons (Sunderland et al., 2003; Shaw et al., 2009), is used as a biomarker in clinical trials or academic settings to increase the accuracy of AD diagnosis. At the current stage of biomarker development, however, the total concentration of $A\beta_{42}$ in CSF, even in combination with other biomarkers such as tau protein, does not allow a clear distinction of AD patients from healthy controls or patients with other dementias (Humpel, 2011). Therefore, the development of more accurate biomarkers is of utmost importance.

Since Aβ oligomeric species are known to be directly involved in AD pathology or even to trigger the disease (Haass and Selkoe, 2007), Aβ oligomers are considered as promising biomarker for AD (Blennow et al., 2010). The main challenges for Aβ oligomer-based diagnostics in body fluids are the presumably very low concentrations of Aβ oligomers and the high background of monomeric Aβ (Rosén et al., 2013). To meet those requirements, we have previously developed an assay called sFIDA (surface-based fluorescence intensity distribution analysis; Birkmann et al., 2007; Funke et al., 2007, 2010; Bannach et al., 2012). The principle of sFIDA is illustrated in **Figure 1**. The biochemical setup of sFIDA resembles a conventional sandwich ELISA. All Aβ species are immobilized on a functionalized glass surface via Aβ-specific capture antibodies. After immobilization, Aβ aggregates are multiply loaded by at least two detection antibodies, each of them labeled with a different fluorochrome. Because capture and detection antibodies recognize the same or an overlapping epitope on Aβ, Aβ monomers cannot bind any detection antibodies while bound to the capture antibody. In contrast to a classical ELISA, the result of the measurement is not a single readout for the whole sample. Instead, the surface is imaged by high-resolution fluorescence microscopy, such as dual-color total internal reflection fluorescence microscopy (TIRFM). Only those pixels that show signal intensities above the background noise in both channels are counted. Thus, the number of colocalized pixels above the background noise is expected to correlate with the concentration of Aβ oligomers in the sample.

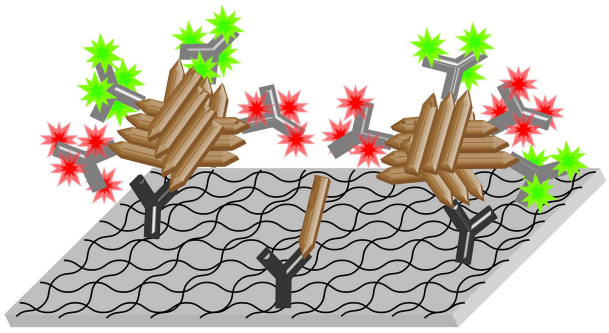

FIGURE 1 | Scheme of the sFIDA assay. Aβ-specific capture antibodies (dark gray Y symbols) are immobilized on a functionalized glass surface. Aβ oligomers (brown rods) present in the sample bind to the capture antibodies and are detected by fluorescence labeled (colored stars) anti-Aβ-antibodies (light gray Y symbols). The surface is then imaged by dual-color microscopy. In this version of the assay, all three of the applied antibodies (one capture and two different detection antibodies labeled with two different fluorochromes) bind to overlapping epitopes at the N-terminus of Aβ, which corresponds to the spiky ends of the brown rods in the scheme above. Thereby, only oligomers with multiple epitopes, but not monomers, are able to bind detection antibodies while bound to the capture and thus yield detectable signals.

Results showing increased sFIDA readouts for AD patients compared to non-demented controls have been reported previously (Wang-Dietrich et al., 2013). However, in this study no reliable Aβ oligomer standard was available to determine absolute concentrations from the assay readout. Due to both the dynamic aggregation and dissociation of Aβ, non-stabilized oligomers are not suited as standard in oligomer-based diagnostic assays.

Here, we demonstrate application of stabilized Aβ oligomers as standard molecules in the sFIDA assay. The sFIDA readout correlates with the applied oligomer concentration over five magnitudes down to a femtomolar range, which will allow the quantification of natural Aβ oligomer concentrations in body fluids.

MATERIALS AND METHODS

Biological Samples and PBS Spiked with Stabilized Oligomers

Four individual human EDTA-anticoagulated plasma samples (Zen-Bio, Research Triangle Park, USA) and one pooled human EDTA-anticoagulated plasma sample from three healthy donors were centrifuged for 15 min at 15,000 × *g*. The supernatant was collected and equal volumes from each sample were combined to obtain one large pool from several donors (from here on referred to as "plasma fraction"). Human cerebrospinal fluid sample (CSF; pooled from healthy donors/mixed gender) was purchased from Biochemed (Winchester, USA). Stabilized Aβ oligomers (Crossbeta Biosciences B.V., Utrecht, the Netherlands), from here on called "oligomers", were serially diluted from the stock solution (10 nM) to concentrations of 1 nM, 100 pM, 10 pM, 1 pM, 100 fM, 10 fM, and 1 fM in PBS (GE Healthcare, Chalfont St. Giles, UK), CSF or the plasma fraction as described above. All concentrations of Aβ oligomers in this publication refer to oligomer particle concentrations, if not stated otherwise. The oligomers consist of approximately 220 $A\beta_{1-42}$ monomers (manufacturer's data); further characterization of the stabilized oligomers, including data on the size homogeneity and stability, are available on the manufacturer's homepage (Crossbeta Biosciences, 2015).

sFIDA

Plate Preparation

384-well plates (SensoPlate Plus with 175 µm glass bottom; Greiner Bio-One, Kremsmünster, Austria) were used for sFIDA. Functionalization of the glass surface was performed as previously described in Janissen et al. (2009). The surface was treated with 5 M NaOH (AppliChem, Darmstadt, Germany) for 15 min, washed three times with water, neutralized with 1 M HCl (AppliChem, Darmstadt, Germany; 15 min), washed again three times with water and then twice with 70% ethanol (VWR International, Langenfeld, Germany). After drying the plate at room temperature, the wells were incubated in

10 M ethanolamine in DMSO (Sigma-Aldrich, St. Louis, USA) overnight. Afterwards, the wells were washed three times with DMSO, twice with 70% ethanol and the plate was dried again at room temperature. A solution of 50 mM SC-PEG-CM (MW 5000 Da, Laysan Bio, Arab, USA) in DMSO was heated shortly to 70°C until the PEG dissolved. After the solution cooled down, 2% (v/v) triethylamin (Fluka, Buchs, Switzerland) were added, the solution was quickly vortexed and 15 µl were applied per well. After an incubation time of 1 h the wells were washed five times with water.

The carboxymethyl groups of SC-PEG-CM on the glass surface were then activated by addition of 30 µl of 100 mM EDC (Fluka, Buchs, Switzerland)/100 mM NHS (Aldrich, Milwaukee, USA) in 0.1 M MES buffer, pH 3.5 (AppliChem) per well for 30 min. After flushing the wells three times quickly with MES buffer, 15 µl of 10 ng/µl capture antibody Nab228 in PBS (the supernatant after centrifuging 10 min at 18,000 g) was added to the surface. After incubating for 90 min, unbound antibody was removed and wells were washed three times with PBST (PBS + 0.05% Tween20, AppliChem Panreac, Darmstadt, Germany) and three times with PBS. Then 50 µl of blocking solution (SmartBlock, CANDOR Biosciences, Wangen, Germany) per well were incubated for 1 h. After washing the wells three times with PBST and three times with PBS, 15 µl sample was applied to each well and incubated overnight. The wells were washed once with PBST and twice with PBS. The detection antibodies 6E10 labeled with Alexa Fluor 488 (Covance, Princeton, USA) and Nab228 labeled with Alexa Fluor 647 (Santa Cruz, Dallas, USA) were combined to each 1.25 µg/ml in PBS and centrifuged for 1 h (100,000 g, 4°C). The supernatant was mixed and added to the wells (15 µl/well, 1 h). Finally, the wells were washed once with PBST and twice with PBS. The buffer was removed and 100 µl of water were applied to each well for image acquisition on TIRFM (AM TIRF MC, Leica microsystems, Wetzlar, Germany).

Image Data Acquisition

Using TIRF microscopy, 25 positions per well were imaged in two different channels (14 bit gray scale; channel 0: excitation at 635 nm, emission filter 705/72 nm; channel 1: excitation at 488 nm, emission filter 525/36 nm). Each image contains 1000 × 1000 pixels and represents an area of 116 × 116 µm. In total, 3.15% of the well surface was imaged.

Image Data Analysis

Prior to data analysis, images showing inhomogeneous surfaces, e.g., due to mechanical damage of the surface or impurities, were excluded from the analysis by automated artifact detection, which is briefly described in the following: Each original image was converted to a binary image by replacing all pixels having intensities above or equal the mean pixel intensity of the regarding image plus one standard deviation with the number one, all others with the number zero. In the next step, erosion was applied to these binary images by using a rectangular structuring element with a size of 31 × 31 pixels. After erosion, the binary image was dilated using the same structuring element as for erosion. Each cluster that consisted of connected pixels with the intensity one in the binary image after dilatation was then analyzed in the original image. Clusters showing either a mean pixel intensity of above 4000, a standard deviation of pixel intensities above 2800, or a skewness of <0 in the original images were defined as artificial and the whole image was excluded from the analysis. Images that had a mean pixel intensity of 16,383 over the whole image in at least one channel were included for image analysis although they were excluded by the artifact detection, because those images are estimated as being saturated, but not artificial.

To account for inhomogeneous illumination, only the central "region of interest" containing 500 × 500 pixels of each image were used for further analysis.

The remaining images were analyzed for colocalization: For both channels, intensity cutoffs for exclusion of background signal were determined. As the background signal might differ from one matrix (i.e., PBS, CSF, and plasma fraction) to another, the cutoff values were determined for each matrix individually, but—in order to compare sFIDA readouts achieved by diluting oligomers in the different matrices—in a reliable and unbiased way. The cutoff for each channel and each matrix was determined from the unspiked control sample to be the value, which is exceeded by only 0.01% of total image pixels. This value represents a reasonable compromise between efficient background removal and retention of assay sensitivity. For cutoffs used in this study, see **Table 1**.

Colocalized pixels with intensity values above the cutoffs in both channels were counted for each image. The number of colocalized pixels was determined for each picture and the average pixel count from all pictures from the same sample was referred to as "sFIDA readout". Please note that the sFIDA readout cannot exceed 250,000, which corresponds to the total number of pixels per analyzed image section.

Calculation of Calibration Curves

For the calibration of assay readout (number of colocalized pixels) to molecule concentration a weighted linear regression analysis was performed with Matlab (The MathWorks, Natick, USA) from experimental data points within the linear detection range (CSF: 100 pM to 10 fM; PBS: 10 pM to 10 fM; plasma fraction: 10 pM to 10 fM) with respective weights calculated as 1/readout. In cases of readout = 0 the weight was determined as 1.

Statistics

In order to statistically assess differences between sFIDA readouts of different concentrations of oligomers diluted in the same matrix, two-way omnibus Kruskal-Wallis test was used for comparison of more than two groups. *Post-hoc*

TABLE 1 | Cutoffs for the different body fluids.

Matrix	Cutoff channel 635 nm	Cutoff channel 488 nm
CSF	3268	2339
PBS	4082	2773
Plasma fraction	4259	2028

Cutoffs were obtained for each channel and matrix by allowing only 0.01% of all pixels to be above background signal for negative controls.

analysis was performed by using two-tailed Mann-Whitney-U test and *p*-value adjustment according to Benjamini and Hochberg (1995) in order to account for multiple testing. By Mann-Whitney-U test, sFIDA readouts from each concentration were compared to the next lower one. Additionally, sFIDA readouts from blank samples were compared to readouts from 10 to 100 fM. The false discovery rate controlling procedure after Benjamini and Hochberg was calculated for 0.05 (for significant results, indicated with *) and 0.01 (for very significant results, indicated with **). Kruskal-Wallis and Mann-Whitney-U test were calculated using the statistical software Origin (OriginLab Corporation, Northampton, USA), false discovery rate controlling procedure after Benjamini and Hochberg was calculated in Microsoft Excel (Microsoft Corporation, Redmond, USA).

RESULTS

Detection of Stabilized Oligomers by sFIDA

In a first set of experiments we sought to find out if the stabilized oligomers can be sensitively detected by the sFIDA assay. Therefore, a log10 dilution series of oligomers in PBS with concentrations ranging from 1 nM to 1 fM was subjected to sFIDA analysis in quadruplicate determination. As can be seen in **Figure 2**, the sFIDA readout correlated well with the applied concentration of stabilized oligomers in the range of 100 pM down to 1 fM. The readouts from 1 nM to 100 pM oligomers in PBS reached saturation, which means that all pixels were above cutoff in both channels. At the lower end of the dilution series, the sFIDA readout of the lowest oligomer concentration (1 fM) did not differ significantly from the readouts from 10 fM oligomers and the blank control. However, there was a significant difference in the sFIDA readouts from 10 fM oligomers and the blank control.

Spiking of CSF, PBS, and EDTA Plasma Fraction with Stabilized Oligomers

After demonstrating the ability to detect even femtomolar concentrations of stabilized oligomers diluted in buffer, we investigated if different body fluid environments affect the sensitivity of oligomer detection by sFIDA. To check for matrix effects that possibly attenuate the specific signal of Aβ oligomers, the oligomers were spiked into CSF and blood plasma from healthy, non-demented control subjects. All samples containing oligomers were determined fourfold by sFIDA analysis, while each blank sample was measured 21-fold. **Figure 3** shows the mean sFIDA readouts for all samples.

The sFIDA readout correlated well with the oligomer concentration down to 1 fM. However, there was no significant difference in the readouts of 10 fM as compared to 1 fM, as well as in the readouts from the blank sample compared to 1 and 10 fM oligomers spiked into CSF. sFIDA readouts from 100 fM and the blank sample differed significantly.

For plasma samples, there was even a very significant difference between the sFIDA readouts of 10 fM and blank sample.

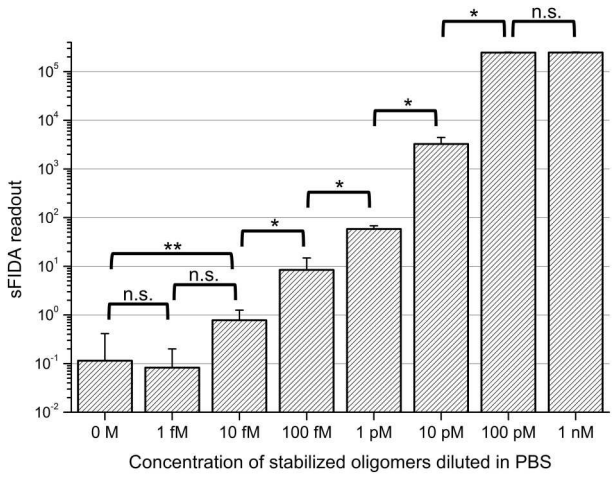

FIGURE 2 | sFIDA readout of stabilized oligomers diluted in PBS. Columns and error bars represent the mean values and standard deviations calculated from a fourfold determination of samples containing oligomers. The blank was determined 21-fold. Cutoffs for each channel were set to discard virtually all background from control samples except for 25 pixels, which are 0.01% of all pixels. This led to the following cutoff values (channel 635 nm/channel 488 nm): 4082/2773. Please note that the number of colocalized pixels (sFIDA readout) is lower than the number of pixels above background in the single channels. n.s., not significant; *$p \leq 0.05$; **$p \leq 0.01$.

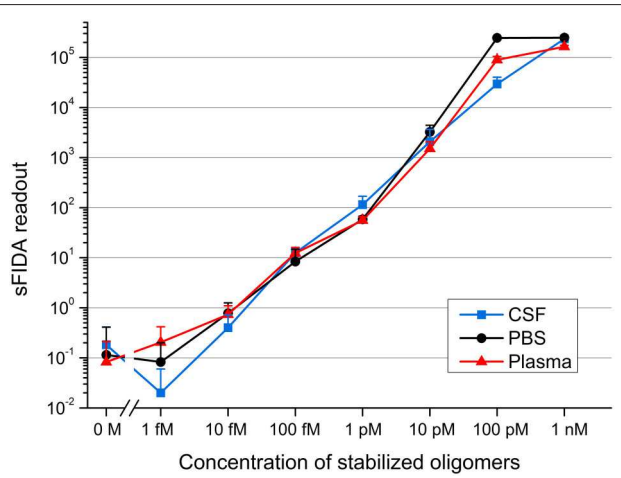

FIGURE 3 | sFIDA readout of stabilized oligomers diluted in CSF, PBS, and a plasma fraction. Shown are mean values and standard deviations from fourfold (samples containing stabilized oligomers) or 21-fold (all blanks) determinations. Cutoffs for channel 635 nm/channel 488 nm: CSF, 3268/2339; PBS, 4082/2773; plasma fraction, 4259/2028.

Lower Limits of Detection and Lower Limits of Quantification for Stabilized Oligomers Diluted in PBS, CSF, and the Plasma Fraction

As the concentration of Aβ oligomers in body fluids like CSF and blood is presumably very low (Bruggink et al., 2013; Hölttä et al., 2013; Savage et al., 2014), the lower limit of detection (LLOD) is an important characteristic of every assay for the determination

of Aβ oligomer concentration. To identify the LLOD for each matrix used in this report, each blank sample was determined 21-fold. The LLOD was calculated as the mean sFIDA readout from all blank samples plus three times the standard deviation. By establishing a calibration curve from the dilution series, the Aβ oligomer concentration corresponding to the calculated sFIDA readout was then determined. The resulting LLODs were 22 fM for stabilized oligomers diluted in PBS, 18 fM in CSF, and 14 fM in the plasma fraction.

The lower limits of quantification (LLOQ) were calculated as the mean sFIDA readout from all blank samples plus ten times the standard deviation. The same calibration curves as used for determination of LLOD were applied, leading to the following concentrations: 32 fM for stabilized oligomers diluted in PBS, 24 fM for dilution in CSF, and 22 fM for dilution in the plasma fraction.

DISCUSSION

In the present work we applied stabilized Aβ oligomers as standard in the sFIDA assay. For dilutions in PBS, CSF from control donors, and blood plasma from control donors, the sFIDA readout correlated with the oligomer concentration over five to six orders of magnitude. Although oligomer concentrations in the upper picomolar range are presumably not physiologically relevant, the observed linearity over several orders of magnitude is useful to check assay functionality and to facilitate assay calibration. The calculated LLODs for oligomers diluted in PBS, CSF, and a plasma fraction were in the range of 14–22 fM particle concentration. We can exclude that endogenous Aβ oligomers, which are possibly present also in healthy subjects, contribute significantly to the assay readout, since the intensity cutoff was determined based on the non-spiked control samples.

For the lower concentrations from 1 pM down to 1 fM, a linear relation between the sFIDA readout and concentrations of Aβ oligomers was observed. We expect that to be the relevant concentration range for analysis of biological samples, as published concentrations of oligomers in CSF are in the femtomolar to low picomolar range (stated as monomeric concentrations of Aβ; oligomeric concentrations are even lower; Bruggink et al., 2013; Hölttä et al., 2013; Savage et al., 2014).

LLODs often refer to the concentration or mass of the total applied peptide, although the actual portion of oligomerized Aβ and the size of Aβ oligomers in the preparations is mostly unknown (Santos et al., 2007; Sancesario et al., 2012). The concentration of 14 fM of the stabilized oligomers used in this study corresponds to 3.1 pM (13.9 ng/L) monomeric $A\beta_{1-42}$. The LLOD given in mass per volume is roughly in the same range or above the limits of detection published for some Aβ oligomer specific ELISA (Fukumoto et al., 2010; Bruggink et al., 2013; Hölttä et al., 2013; Savage et al., 2014). In principle, sFIDA allows detection and quantification of single particles of oligomers consisting of approximately 220 Aβ monomers.

Although the stabilized oligomers used in this study might not accurately reflect the properties of native Aβ oligomers in terms of composition, mass, and structural heterogeneity, they are nevertheless a valuable tool for assay development, assay calibration, and determination of inter- and intra-assay variation due to their stability and homogenous size. While heterogeneous Aβ oligomer standards would resemble endogenous conditions more closely, it is hardly possible to reliably produce such standards with minimal batch-to-batch-variations thus limiting their use in assay validation.

The stabilized oligomers are advantageous with regard to long term stability and they can easily be distributed to compare inter-laboratory results. This enables to thoroughly validate and calibrate an assay, which is a very important feature in assay development. However, the applicability of this standard for biological samples will have to be addressed in future studies. Quantification of very small oligomers in body fluids might emphasize the need for even smaller standard oligomers than the ones used in this study.

We have previously shown that monomers of synthetic Aβ give not rise to significant signals in the sFIDA assay by using overlapping epitopes in the capture and detection system (Wang-Dietrich et al., 2013). When analyzing native CSF samples in diagnostic setups, however, experimental conditions (i.e., pH, incubation times, freeze/thaw cycles) have to be carefully adjusted to avoid false-positive signals due to artificial aggregation of endogenous Aβ monomers.

In the present version of the assay, two N-terminal antibodies were used for capturing and detection of Aβ, i.e., Nab228 (epitope Aβ1-11) and 6E10 (epitope Aβ3-8). By using alternative capture and probe antibodies, it is not only possible to detect oligomers composed of different Aβ isoforms, but also to detect hybrid aggregates composed of different peptides or proteins. Therefore, sFIDA assay can in future be applied for scientific purpose in order to investigate the presence and pathological relevance of different oligomeric species in body fluids or brain homogenates of patients with different neurodegenerative diseases, such as AD. Additionally, after thorough investigation and validation of the assay and the measured targets, sFIDA might either give extra information useful for diagnostics or even measure oligomeric biomarkers that allow a reliable diagnosis, and might be useful for disease monitoring in clinical trials during treatment.

AUTHOR CONTRIBUTIONS

KKU, MH, YH, KKR, AK, CL, LP, KW, JW conducted experiments. KKU, DW, and OB designed experiments and wrote the manuscript.

ACKNOWLEDGMENTS

This work was supported by the Federal Ministry of Education and Research within the projects VIP (03V0641), KNDD (01GI1010A), and JPND/BIOMARKAPD (01ED1203H).

REFERENCES

Ballard, C., Gauthier, S., Corbett, A., Brayne, C., Aarsland, D., and Jones, E. (2011). Alzheimer's disease. *Lancet* 377, 1019–1031. doi: 10.1016/S0140-6736(10)61349-9

Bannach, O., Birkmann, E., Reinartz, E., Jaeger, K. E., Langeveld, J. P., Rohwer, R. G., et al. (2012). Detection of prion protein particles in blood plasma of scrapie infected sheep. *PLoS ONE* 7:e36620. doi: 10.1371/journal.pone.0036620

Benjamini, Y., and Hochberg, Y. (1995). Controlling the false discovery rate: a practical and powerful approach to multiple testing. *J. R. Stat. Soc. B* 57, 289–300.

Birkmann, E., Henke, F., Weinmann, N., Dumpitak, C., Groschup, M., Funke, A., et al. (2007). Counting of single prion particles bound to a capture-antibody surface (surface-FIDA). *Vet. Microbiol.* 123, 294–304. doi: 10.1016/j.vetmic.2007.04.001

Blennow, K., Hampel, H., Weiner, M., and Zetterberg, H. (2010). Cerebrospinal fluid and plasma biomarkers in Alzheimer disease. *Nat. Rev. Neurol.* 6, 131–144. doi: 10.1038/nrneurol.2010.4

Braak, H., and Braak, E. (1991). Neuropathological stageing of Alzheimer-related changes. *Acta Neuropathol.* 82, 239–259. doi: 10.1007/BF00308809

Bruggink, K. A., Jongbloed, W., Biemans, E. A. L. M., Veerhuis, R., Claassen, J. A. H. R., Verbeek, M. M., et al. (2013). Amyloid-β oligomer detection by ELISA in cerebrospinal fluid and brain tissue. *Anal. Biochem.* 433, 112–120. doi: 10.1016/j.ab.2012.09.014

Cleary, J. P., Walsh, D. M., Hofmeister, J. J., Shankar, G. M., Kuskowski, M. A., Selkoe, D. J., et al. (2004). Natural oligomers of the amyloid-β protein specifically disrupt cognitive function. *Nat. Neurosci.* 8, 79–84. doi: 10.1038/nn1372

Crossbeta Biosciences (2015). *Crossbeta Oligomer Publications* [Online]. Available online at: http://www.crossbeta.com/technology/publications/ (Accessed December 07, 2015).

Fukumoto, H., Tokuda, T., Kasai, T., Ishigami, N., Hidaka, H., Kondo, M., et al. (2010). High-molecular-weight β-amyloid oligomers are elevated in cerebrospinal fluid of Alzheimer patients. *FASEB J.* 24, 2716–2726. doi: 10.1096/fj.09-150359

Funke, S. A., Birkmann, E., Henke, F., Görtz, P., Lange-Asschenfeldt, C., Riesner, D., et al. (2007). Single particle detection of Abeta aggregates associated with Alzheimer's disease. *Biochem. Biophys. Res. Commun.* 364, 902–907. doi: 10.1016/j.bbrc.2007.10.085

Funke, S. A., Wang, L., Birkmann, E., and Willbold, D. (2010). Single-particle detection system for Aβ aggregates: adaptation of surface-fluorescence intensity distribution analysis to laser scanning microscopy. *Rejuvenation Res.* 13, 206–209. doi: 10.1089/rej.2009.0925

Golde, T. E., Schneider, L. S., and Koo, E. H. (2011). Anti-aβ therapeutics in Alzheimer's disease: the need for a paradigm shift. *Neuron* 69, 203–213. doi: 10.1016/j.neuron.2011.01.002

Haass, C., Kaether, C., Thinakaran, G., and Sisodia, S. (2012). Trafficking and proteolytic processing of APP. *Cold Spring Harb. Perspect. Med.* 2:a006270. doi: 10.1101/cshperspect.a006270

Haass, C., and Selkoe, D. J. (2007). Soluble protein oligomers in neurodegeneration: lessons from the Alzheimer's amyloid β-peptide. *Nat. Rev. Mol. Cell Biol.* 8, 101–112. doi: 10.1038/nrm2101

Hölttä, M., Hansson, O., Andreasson, U., Hertze, J., Minthon, L., Nägga, K., et al. (2013). Evaluating amyloid-β oligomers in cerebrospinal fluid as a biomarker for Alzheimer's disease. *PLoS ONE* 8:e66381. doi: 10.1371/journal.pone.0066381

Humpel, C. (2011). Identifying and validating biomarkers for Alzheimer's disease. *Trends Biotechnol.* 29, 26–32. doi: 10.1016/j.tibtech.2010.09.007

Janissen, R., Oberbarnscheidt, L., and Oesterhelt, F. (2009). Optimized straight forward procedure for covalent surface immobilization of different biomolecules for single molecule applications. *Colloids Surf. B Biointerfaces* 71, 200–207. doi: 10.1016/j.colsurfb.2009.02.011

Lansdall, C. J. (2014). An effective treatment for Alzheimer's disease must consider both amyloid and tau. *Biosci. Horizons* 7:hzu002. doi: 10.1093/biohorizons/hzu002

Lesné, S., Koh, M. T., Kotilinek, L., Kayed, R., Glabe, C. G., Yang, A., et al. (2006). A specific amyloid-β protein assembly in the brain impairs memory. *Nature* 440, 352–357. doi: 10.1038/nature04533

McLean, C. A., Cherny, R. A., Fraser, F. W., Fuller, S. J., Smith, M. J., Vbeyreuther, K., et al. (1999). Soluble pool of Aβ amyloid as a determinant of severity of neurodegeneration in Alzheimer's disease. *Ann. Neurol.* 46, 860–866.

Prince, M., Bryce, R., Albanese, E., Wimo, A., Ribeiro, W., and Ferri, C. P. (2013). The global prevalence of dementia: a systematic review and metaanalysis. *Alzheimer's Dement.* 9, 63–75. doi: 10.1016/j.jalz.2012.11.007

Rosén, C., Hansson, O., Blennow, K., and Zetterberg, H. (2013). Fluid biomarkers in Alzheimer's disease - current concepts. *Mol. Neurodegener.* 8:20. doi: 10.1186/1750-1326-8-20

Sancesario, G. M., Cencioni, M. T., Esposito, Z., Borsellino, G., Nuccetelli, M., Martorana, A., et al. (2012). The load of amyloid-β oligomers is decreased in the cerebrospinal fluid of Alzheimer's disease patients. *J. Alzheimers Dis.* 31, 865–878. doi: 10.3233/JAD-2012-120211

Santos, A. N., Torkler, S., Nowak, D., Schlittig, C., Goerdes, M., Lauber, T., et al. (2007). Detection of amyloid-β oligomers in human cerebrospinal fluid by flow cytometry and fluorescence resonance energy transfer. *J. Alzheimers Dis.* 11, 117–125.

Savage, M. J., Kalinina, J., Wolfe, A., Tugusheva, K., Korn, R., Cash-Mason, T., et al. (2014). A sensitive Aβ oligomer assay discriminates alzheimer's and aged control cerebrospinal fluid. *J. Neurosci.* 34, 2884–2897. doi: 10.1523/JNEUROSCI.1675-13.2014

Shaw, L. M., Vanderstichele, H., Knapik-Czajka, M., Clark, C. M., Aisen, P. S., Petersen, R. C., et al. (2009). Cerebrospinal fluid biomarker signature in Alzheimer's disease neuroimaging initiative subjects. *Ann. Neurol.* 65, 403–413. doi: 10.1002/ana.21610

Sunderland, T., Linker, G., Mirza, N., Putnam, K. T., Friedman, D. L., Kimmel, L. H., et al. (2003). Decreased β-amyloid1-42 and increased tau levels in cerebrospinal fluid of patients with Alzheimer disease. *JAMA* 289, 2094–2103. doi: 10.1001/jama.289.16.2094

Wang-Dietrich, L., Funke, S. A., Kühbach, K., Wang, K., Besmehn, A., Willbold, S., et al. (2013). The amyloid-β oligomer count in cerebrospinal fluid is a biomarker for Alzheimer's disease. *J. Alzheimers Dis.* 34, 985–994. doi: 10.3233/JAD-122047

Conflict of Interest Statement: The authors declare that the research was conducted in the absence of any commercial or financial relationships that could be construed as a potential conflict of interest.

Journal of Alzheimer's Disease 54 (2016) 79–88
DOI 10.3233/JAD-160253
IOS Press

Biofunctionalized Silica Nanoparticles: Standards in Amyloid-β Oligomer-Based Diagnosis of Alzheimer's Disease

Maren Hülsemann[a,1], Christian Zafiu[a], Katja Kühbach[a], Nicole Lühmann[b], Yvonne Herrmann[a], Luriano Peters[a], Christina Linnartz[a], Johannes Willbold[a], Kateryna Kravchenko[a], Andreas Kulawik[a], Sabine Willbold[b], Oliver Bannach[a,c] and Dieter Willbold[a,c,*]
[a]*Forschungszentrum Jülich, ICS-6, Institut für Strukturbiochemie, Jülich, Germany*
[b]*Forschungszentrum Jülich, ZEA-3, Zentralinstitut für Engineering, Elektronik und Analytik, Jülich, Germany*
[c]*Heinrich-Heine-Universität Düsseldorf, Institut für Physikalische Biologie, Düsseldorf, Germany*

Handling Associate Editor: Piotr Lewczuk

Accepted 23 May 2016

Abstract. Amyloid-β (Aβ) oligomers represent a promising biomarker for the early diagnosis of Alzheimer's disease (AD). However, state-of-the-art methods for immunodetection of Aβ oligomers in body fluids show a large variability and lack a reliable and stable standard that enables the reproducible quantitation of Aβ oligomers. At present, the only available standard applied in these assays is based on a random aggregation process of synthetic Aβ and has neither a defined size nor a known number of epitopes. In this report, we generated a highly stable standard in the size range of native Aβ oligomers that exposes a defined number of epitopes. The standard consists of a silica nanoparticle (SiNaP), which is functionalized with Aβ peptides on its surface (Aβ-SiNaP). The different steps of Aβ-SiNaP synthesis were followed by microscopic, spectroscopic and biochemical analyses. To investigate the performance of Aβ-SiNaPs as an appropriate standard in Aβ oligomer immunodetection, Aβ-SiNaPs were diluted in cerebrospinal fluid and quantified down to a concentration of 10 fM in the sFIDA (surface-based fluorescence intensity distribution analysis) assay. This detection limit corresponds to an Aβ concentration of 1.9 ng l^{-1} and lies in the sensitivity range of currently applied diagnostic tools based on Aβ oligomer quantitation. Thus, we developed a highly stable and well-characterized standard for the application in Aβ oligomer immunodetection assays that finally allows the reproducible quantitation of Aβ oligomers down to single molecule level and provides a fundamental improvement for the worldwide standardization process of diagnostic methods in AD research.

Keywords: Alzheimer's disease diagnosis, Aβ oligomer standards, assay standardization, biofunctionalized nanoparticles

INTRODUCTION

Alzheimer's disease (AD) is the most common form of dementia, affecting more than 33 million people worldwide and the case number is expected to triple over the next four decades [1, 2]. AD represents a multifactorial disorder with a yet poorly understood pathogenesis, which makes its early and accurate diagnosis a difficult challenge [3]. Currently, there is no causal therapy available and a reliable diagnosis can only be achieved by post mortem analysis of brain samples.

The 'amyloid cascade' hypothesis is widely accepted to explain development and progression of AD. It mainly postulates an imbalance between

[1]Current address: Albert Einstein College of Medicine, Institute of Anatomy and Structural Biology, Laboratory of Molecular and Cellular Biophysics, New York City, USA.

*Correspondence to: Prof. Dr. Dieter Willbold, ICS-6, Institut für Strukturbiochemie, Forschungszentrum Jülich, 52428 Jülich, Germany. Tel.: +49 2461 61 2100; Fax: +49 2461 61 2023; E-mail: d.willbold@fz-juelich.de.

expression and clearance of amyloid-β (Aβ) peptides in the brain. The Aβ overload favors Aβ aggregation, ultimately inducing neuronal and synaptic degeneration and leading to dementia [4]. More recent data suggest that soluble oligomers of Aβ, in particular, directly correlate with disease severity [5, 6]. Thus, Aβ oligomers represent a popular target in drug development as well as a promising biomarker candidate for both early diagnosis of AD and therapy monitoring, respectively. A broad range of diagnostic methods for detection and quantitation of Aβ oligomers is currently applied or under evaluation. The concentration of Aβ oligomers in human body fluids is commonly assayed by ELISA methods, using capture antibodies and detection antibodies that bind to the same or overlapping epitopes, or by application of oligomer-specific antibodies [7–14].

We previously described the surface-based fluorescence intensity distribution analysis (sFIDA) technology as a highly oligomer-specific detection and quantitation method for the early diagnosis of AD [15, 16].

In sFIDA, a glass surface is covalently coated with anti-Aβ capture antibodies (Nab228, Epitope $Aβ_{1–11}$) which immobilize Aβ species from the sample. In the next step, Aβ oligomers are labeled by at least two different fluorophore-coupled anti-Aβ antibodies. Since all three applied antibodies recognize overlapping epitopes in the N-terminal part of Aβ, only oligomeric structures can be immobilized and bound by both detection antibodies at the same time, which makes the sFIDA technique insensitive against Aβ monomers. The use of different antibodies with affinities to a pan-epitope (6E10-488, Epitope $Aβ_{3–8}$ and IC16-633, Epitope $Aβ_{1–8}$) enhances the specificity of the assay, since only co-localized signals are counted but not signals caused by cross-reactivity of the individual antibodies. Finally, the chip surface is imaged by dual-color TIRF microscopy. After application of an intensity threshold the number of colocalized pixels from both channels is counted and correlates with the number of oligomers in the samples and is referred to as sFIDA readout.

While assays quantitating total Aβ can readily be calibrated with synthetic Aβ monomers, it is very difficult to establish standards for oligomer-based diagnostic tests. Furthermore, there are large variations in Aβ oligomer measurements among and within laboratories [17].

Therefore the development of a reliable oligomer standard is highly needed, since the readouts of these quantitation tests are dependent on calibration curves of standard molecules. The use of oligomers or aggregates from synthetic Aβ is limited, as these structures are metastable, heterogeneous and in dynamic equilibrium with other assembly states, and hence do not have defined sizes or consistent molecular weights. Additionally, oligomers from synthetic Aβ are prone to further aggregation and susceptible to freeze/thaw cycles, making long-term storage and constant performance, as pre-requirements for any standard, impossible.

In this work we present a novel concept for the synthesis of Aβ oligomer standards, suitable for the application in Aβ oligomer-specific quantitation assays. The core and size-determining component of the standard is a SiNaP, which can be adjusted to any size required with nearly a monodisperse size distribution [18, 19]. SiNaPs are chemically inert, non-toxic, easy to modify and stable over months. These features make SiNaPs a highly favored substructure in the design of the standard. To simulate characteristics of a native oligomer, the size of the SiNaPs was tuned to the described size range of native oligomers of 3 to 20 nm [20–22]. The surface of the SiNaPs was functionalized, activated and finally coated with $Aβ_{42}$ peptides. These biofunctionalized Aβ-SiNaPs exhibit a defined number of Aβ epitopes on the surface and allow their application in quantitative oligomer-based detection assays.

To our knowledge no other available Aβ oligomer standard presents as defined characteristics as our standard, which will therefore have a major impact on the accurate and reproducible quantitation of Aβ oligomers in human samples. Aβ-SiNaPs are a helpful accomplishment for the urgently needed standardization process between different operators, laboratories, and clinical studies in AD research worldwide [17].

MATERIAL AND METHODS

Synthesis of SiNaPs according to the Stöber process

200 ml absolute ethanol (VWR, Darmstadt, Germany), 2.7 ml water, and 4.49 ml ammonia solution (25%, Carl Roth, Karlsruhe, Germany) were vigorously stirred in a round bottom flask. After 5 min 4.43 ml TEOS (tetraethylorthosilicate, Aldrich Chemistry, St. Louis, USA) were added and the solution was stirred further for 2 days at room temperature. The resulting SiNaPs were dialyzed (MWCO

3,500, Tubing Spectral Por7 Dialysis Membrane, Spektrum Laboratories, Rancho Dominguez, CA, USA) against fivefold the volume of ethanol for 2 days to remove non-reacted chemicals and the catalysts. The SiNaPs reached a concentration of about 10 g l^{-1} and were stored at 4°C in ethanol until further usage.

Particle characterization by TEM, XPS, and FTIR

The morphology of the SiNaPs was determined by transmission electron microscopy (TEM). TEM images were recorded using a Zeiss Libra 120 Transmission Electron Microscope (Carl Zeiss AG, Jena, Germany). The copper grids (S160, Plano GmbH, Wetzlar, Germany) were prepared without staining by placing a 5 µl drop of SiNaPs (1 to 0.1 mg ml^{-1}) in ethanol on the carbon film of the grid and letting it dry at room temperature for at least 3 h before measurement.

The different SiNaP functionalization steps were monitored by Fourier transformed Infrared Spectroscopy (FTIR) and X-ray photoelectron spectroscopy (XPS). FTIR spectra were obtained by a Bruker Tensor 27 (Bruker Optik GmbH, Ettlingen, Germany) equipped with an attenuated total reflection (ATR) unit (Golden Gate, diamond crystal, Specac Ltd, UK). A film of the particles was prepared by drop casting dispersion in ethanol onto the diamond crystal. The spectra were collected with 128 scans at resolution of 4 cm^{-1} after the solvent signals in the IR spectrum vanished. The beam path was purged with argon during the measurements.

XPS spectra were obtained by a PHI 5000 VersaProbe II emitting monochromatic Al-kα radiation at an angle of 46°. A film of particles was drop casted on glass slides and the solvent was evaporated over night before measurement. Spectra were obtained from three individual positions on the glass slides.

Calculations and assumptions

After size determination of the SiNaPs by TEM micrographs, the particle surface was calculated, assuming a spherical surface. The molecular weight of the SiNaP was calculated assuming an average density of 1.85 g cm^{-3} [23]. The concentration of the SiNaP solution was determined gravimetrically in triplicate and the mean concentration of the SiNaP was calculated after every functionalization step, so that chemicals for further functionalization steps were added accordingly.

The number of potential binding sites on the SiNaP surface was determined under the assumption that one APTES molecule occupies a surface of 0.6 nm^2 [24].

Synthesis of amino-functionalized SiNaPs

Amino-functionalized SiNaP were prepared via silanization with APTES ((3-aminopropyl) triethoxysilane, Sigma-Aldrich, St. Louis, USA). A 5-fold molar excess of APTES in relation to the number of potential binding sites on the particle surface was added to the SiNaPs in ethanol. The dispersion was sonicated for 10 min and incubated overnight on a shaker at ambient temperature. The resulting amino-functionalized SiNaPs were centrifuged (5,000 × *g*, 2 h) and the resulting pellet was dispersed in ethanol by sonication for 15 min. This washing step was repeated three times.

Synthesis of carboxylated SiNaPs

A pellet containing amino-functionalized SiNaP was re-dispersed in 0.1 M succinic anhydride (Aldrich Chemistry, St. Louis, USA) in DMF (AppliChem, Darmstadt, Germany) under argon atmosphere and stirred overnight. The resulting carboxylated SiNaPs were alternately washed with water and ethanol for three times by centrifugation (5,000 × *g*, 2 h) and pellet resuspension.

Peptide coupling to the SiNaP surface

The carboxylated SiNaPs (cSiNaP) were re-dispersed in 10 mM MES buffer, pH 5.7 (Sigma Aldrich, St. Louis, USA) and were activated by EDC (1-ethyl-3-(3-dimethylaminopropyl) carbodiimide, Fluka, Sigma Aldrich, St. Louis, USA) and NHS (N-hydroxysuccinimide, Aldrich Chemistry, St. Louis, USA). The chemicals were added to the particle solution in a 16-fold and 4-fold molar excess respectively, compared to the potentially bound APTES molecules, and the mixture was sonicated for 10 min. The dispersion was centrifuged for 1 h at 10,000 × *g* and the pellet was re-dissolved in 10 mM MES buffer (pH 5.7) again. The washing procedure was repeated once before the NHS-ester activated SiNaPs were added to the peptides.

The concentration of the pre-activated SiNaPs was gravimetrically determined and the theoretical number of NHS ester groups on the SiNaP surface was

calculated. The pre-activated SiNaPs were added to the peptide resulting in a 1 : 1 ratio of potential binding sites (i.e., NHS ester groups) versus peptides, whereas a complete binding of all peptides to the particle surface cannot be expected due to the size of the peptide. The Aβ monomer has a hydrodynamic radius of 0.9 nm ± 0.1 nm [25] which would allow a maximum surface coverage of 645 peptides per SiNaP.

The dispersion of SiNaPs and peptide was sonicated for 20 min and incubated under shaking overnight. On the next day the Aβ-coated SiNaPs were centrifuged again and the pellet was re-dispersed in aqueous 50% HFIP solution (hexafluoroisopropanol, Merck, Darmstadt, Germany) to remove non-covalently bound protein. The SiNaPs were sonicated in HFIP for 5 min, followed by centrifugation (5,000 × *g*, 1 h). The last washing step was performed in water and the peptide-coated SiNaPs were stored in water at 4°C until further usage.

Peptide preparation

1 mg $A\beta_{42}$ lyophilisates (Bachem, Bubendorf, Switzerland) were dissolved in 500 µl HFIP and incubated overnight. On the next day another 500 µl HFIP were added to the peptide solution and 200–500 µl (1 µg μl^{-1}) Aliquots were prepared and the solvent was evaporated. The dry aliquots were frozen at –20°C until further usage.

Determination of the peptide concentration by BCA assay

The Kit Extra Sense BCA Assay Protein Assay Kit (BioVision Incorporated, Catolog number K814-2500, *Microplate Procedure*) was used to determine the peptide load on the SiNaPs surface. Therefore 150 µl of $A\beta_{42}$ SiNaP were mixed with 150 µl 6 M Urea (Urea crystalline, AppliChem, Darmstadt, Germany) and the solution was incubated at 60°C for 30 min. 150 µl of working solution was added and the mixture was heated at 60°C for 1 h, before the absorption at 562 nm was measured by UV/VIS spectrometry. The protein concentration was calculated according to Beer-Lambert equation.

sFIDA protocol

Custom-made 96 well plates were manufactured by gluing a 170 µm thick glass bottom (Menzel Gläser, Thermo Fisher Scientific, MS, USA) to a 0.5 cm glass plate which was perforated with 96 holes. Prior to use, plates were cleaned with ethanol and water. For further purification and hydroxylation of the glass surface the wells were treated with 5 M NaOH (Karl Roth, Karlsruhe, Germany) for 3 h. Further washing with water and drying of the plate at 90°C was followed by H_2O-Plasma treatment (Diener electronics GmbH, Ebhausen, Germany). Afterwards a desiccator was flushed with argon gas and two trays containing 1 ml of APTES and 200 µl of TEA (triethylamine, Sigma Aldrich, St. Louis, USA), respectively, were added to the chamber. The 96 well full glass plate was placed into the desiccator with the wells facing the filled trays. The chamber was flushed with argon again and vapor deposition of APTES on the glass surface was performed overnight. Next day the chemicals were removed and the desiccator was again flushed with argon and the plate got cured inside for at least 4 h (storage possible up to one week).

Carboxyl groups of 20 mg ml^{-1} carboxymethyldextrane (CMD, Sigma Aldrich, St. Louis, USA) in water were activated by 200 mM EDC and 50 mM NHS for 0.5 h under shaking. Afterwards the mixture was added to the amino-functionalized glass plates to establish amide bonds between the CMD network and the glass surface. After 1.5 h the CMD solution was removed and the wells were washed with water three times.

The remaining carboxyl groups of the bound CMD were activated by 200 mM EDC and 50 mM NHS in water again for 0.5 h. After removing EDC/NHS and performing two washing steps with water, 1 mg l^{-1} anti-Aβ capture antibody (Nab 228, epitope $A\beta_{1-11}$, Sigma Aldrich, St. Louis, USA) in PBS was added to the wells. The incubation for 1.5 h led to the covalent binding of the capture antibody to the surface.

After removing the antibody solution the remaining active NHS-ester groups on the functionalized surface were quenched by 0.1 M ethanolamine hydrochloride (Sigma Aldrich, St. Louis, USA) in Tris-buffered saline, pH 7.4 (TBS). The solution was removed after 30 min and the wells were washed with TBS three times. Until sample application the plates were stored in TBS.

15 µl of samples were applied to the plate in triplicates and incubated overnight on the capture-antibody coated glass surface. Afterwards the wells were washed once with TBS-T (TBS supplemented with 0.05% Tween-20) and twice with TBS. In the next step, 1.25 mg/l of two fluorescence-labeled anti-Aβ antibodies IC16-Alexa 633 and 6E10-ATTO 488 (6E10: epitope $A\beta_{3-8}$, Covance, Princeton, USA;

dye: ATTO-Tec, Siegen, Germany) were added to the wells and incubated for 2 h. mAB IC16 (epitope $A\beta_{1-8}$) was kindly provided by the groups of Prof. Carsten Korth and Prof. Sascha Weggen, Heinrich Heine University Düsseldorf Medical School and labeled with Alexa 633 dye according to the manufactures instructions (Life Technologies, Carlsbad, USA). Finally, the wells were washed twice with TBS-T and twice with TBS. Prior to TIRF microscopy the wells were filled with water and sealed with a plastic foil.

Application of Aβ-SiNaPs in sFIDA

Aβ-SiNaPs were stored in water at 4°C until use. For sFIDA analysis, Aβ-SiNaPs were serially diluted in water and human AD-negative CSF (biochemed, Winchester, USA) to concentrations ranging from 100 pM down to 10 fM and analyzed by sFIDA in threefold determination.

Data acquisition

The surface of the sFIDA well plates was imaged by total internal reflection fluorescence (TIRF) microscopy (AM TIRF MC Leica TIRF microscope, Leica Microsystems, Wetzlar, Germany). The measurement was performed by the Leica Matrix screener software using a 100 × objective lens (1.47 oil CORR TIRF Leica), which enabled the detection of surface-near fluorescence. For each well, 25 images (112 × 112 μm, 1000 × 1000 pixels, 200 nm distance between the scan areas, 14 bit) were taken in channel 0 (Ex/Em 635/705 nm), and channel 1 (Ex/Em 488/525 nm), detecting IC16-Alexa 633 and 6E10-ATTO 488 respectively. Microscope settings of gain, laser power and exposure time were adjusted in a way that the intensity histogram still showed a detectable fluorescence signal for the lowest standard concentration. The microscope settings included a gain between 800 and 1000, a laser power of 100% and an exposure time between 1 and 1.8 s.

Data analysis

After data acquisition at the TIRF microscope the images were exported as tiff files and analyzed with a self-developed software designated sFIDAta. The performed image analysis was applied only to the central 700 × 700 pixels of each image. By this procedure, the border regions of all images, which are not uniformly illuminated, were excluded from the analysis. The software performed a separated histogram analysis for each channel and each SiNaP concentration. To exclude the background signal, intensity cutoffs were determined for each channel. Since the background signal can differ between different matrices (water or CSF), cutoffs were calculated individually for each matrix. The cutoff is defined as an intensity threshold that leaves 0.1% of the total pixel number in the images from the blank control measurement (i.e., 1,000 pixels out of a million pixels). Finally, images from both channels were merged and the number of colocalized pixels above the determined cutoffs was counted for each well. The mean number of colocalized pixels from the images of each concentration is referred to as 'sFIDA readout'.

RESULTS

Synthesis of SiNaPs

SiNaPs were produced as the core component of the standard. Synthesis of the SiNaPs was performed via the Stöber process, which describes a condensation reaction of tetraethylorthosilicate (TEOS) to a siloxane polymer network in the presence of water and ammonia, resulting in nearly monodisperse SiNaPs [18]. Since the diameter of a native oligomer is in the range of 3 to 20 nm, we aimed to synthesize the SiNaP core in an according size range. To determine the size and morphology of the obtained SiNaPs, transmission electron micrographs were recorded. Figure 1 shows SiNaPs with a mean diameter of 24 ± 4.6 nm exhibiting a rather polyhedral shape. It has been previously reported that the shape of very small SiNaPs (<50 nm) is not spherical due to the mechanism of particle formation [18, 23].

Synthesis strategy of biofunctionalized SiNaPs

For biofunctionalization of SiNaPs, three functionalization steps were performed as described in Fig. 2a-e. After synthesis of SiNaPs via the Stöber process (Fig. 2a) a primary amine group was introduced to the SiNaP surface by silanization with APTES (3-(aminopropyl)triethoxysilane) (Fig. 2b, aminated SiNaP = aSiNaP). In the next step aSiNaPs were transferred to a solution of succinic anhydride in DMF (dimethylformamide) under dry conditions. The amine group on the SiNaP surface attacked the succinic anhydride which led to a ring-opening of the anhydride, the formation of an amide bond and

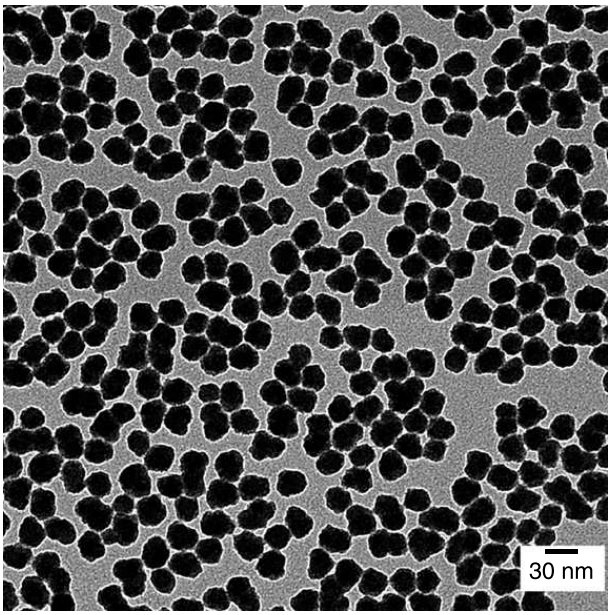

Fig. 1. Transmission electron micrographs of bare SiNaPs. A mean Feret diameter of 24 ± 4.6 nm was calculated from at least 250 SiNaPs.

the exposure of free carboxyl groups on the SiNaP surface (Fig. 2c, carboxylated SiNaP = cSiNaP) [26].

The activation of the exposed carboxyl groups by EDC/NHS (1-ethyl-3-(3-dimethylaminopropyl) carbodiimide / N-hydroxysuccinimide) resulted in the formation of NHS ester groups (Fig. 2d, activated SiNaP) which could react with primary amine groups of chosen biomolecules (Fig. 2e) and led to their covalent binding on the SiNaP surface.

The successful modifications of the SiNaP surface was monitored by XPS and attenuated total reflection Fourier transform infrared spectroscopy (ATR-FTIR). Figure 3a shows the atomic composition of SiNaP and aSiNaP obtained from XPS spectra. Both nanoparticles exhibited high levels of oxygen and silicon atoms which originated from the dense silica core of the materials. Elevated levels of carbon and nitrogen in aSiNaP spectra suggest the surface modification with APTES as these signals were absent in the case of unmodified SiNaP.

Figure 3b shows full range FTIR spectra of different modification steps of SiNaP and a predominant band ranging from 1300 and 1000 cm^{-1} which corresponds to the Si-O and Si-OH bonds of amorphous silicate material. Another common feature of the spectra is a broad band between 3800 and 2700 cm^{-1} (Fig. 3c) which represents the O-H vibrations within the SiNaP core.

Unmodified SiNaP show two characteristic bands, one at 3650 cm^{-1} (free -O-H strech) and in Fig. 3d

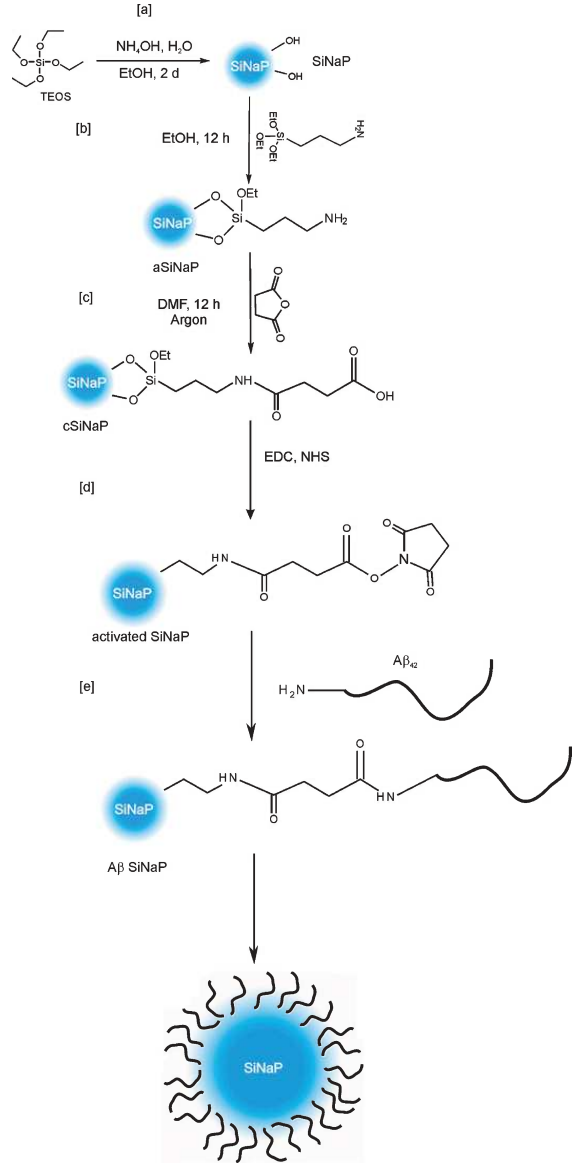

Fig. 2. Synthesis strategy of biofunctionalized SiNaPs. a) Stoeber synthesis of SiNaPs was followed by (b) silanization of the SiNaP surface with APTES (aSiNaP). c) Primary amines reacted with succinic anhydride via a nucleophilic addition and led to the introduction of carboxy functions on the SiNaP surface (cSiNaP). d) Carboxy groups became activated to reactive NHS esters by EDC/NHS (activated SiNaP) which (e) reacted with amine groups of biomolecules, such as Aβ peptides and led to their covalent binding on the SiNaP surface.

at 1650 cm^{-1} (-O-H bend) that represent the -O-H surface functionalities. Furthermore, the spectrum consisted of a broad band at 1450 cm^{-1} which could be assigned to carbonate anions as an insertion product of CO_2 into the silanol group of the silica surface.

After exposing SiNaP to APTES CH_2 scissoring bands at 1395 and 1445 cm^{-1} were observed together with C-H stretching bands between 2900 and 2980 cm^{-1}. In addition a weak band at 1620 cm^{-1}

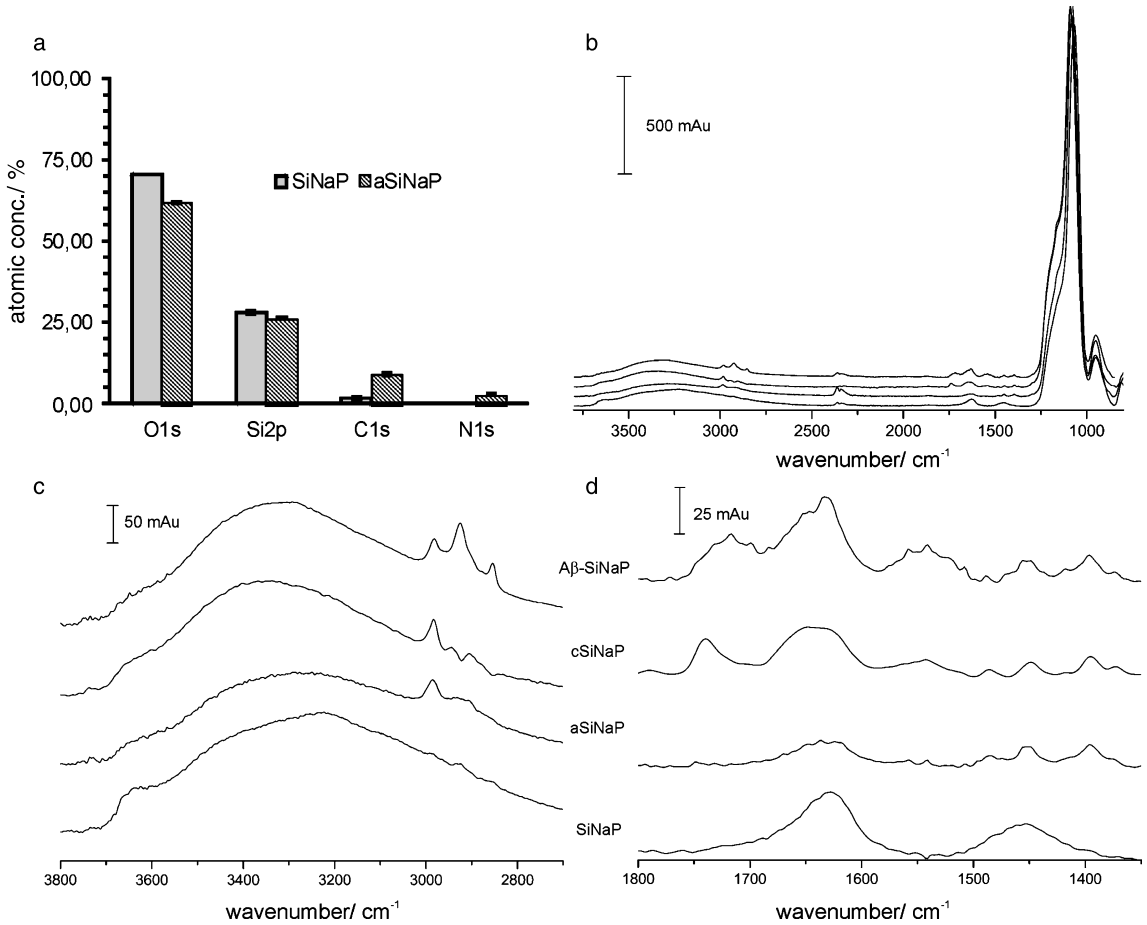

Fig. 3. a) XPS data analysis of SiNaP (grey) and aSiNaP (striped). b) ATR-FTIR spectra of different SiNaP functionalization steps. SiNaP: unmodified SiNaP, aSiNaP: aminated SiNaP functionalized with APTES, cSiNaP: carboxylated SiNaP functionalized with succinic anhydride; Aβ-SiNaP: SiNaP coated with Aβ. c) Expanded spectra from (b) in the range of 2700 – 3800 cm^{-1}. d) Expanded spectra from (b) in the range of 1300 – 1800 cm^{-1}.

represents the -N-H surface functionality which was also observed by XPS (Fig. 3a).

The modification of the SiNaPs by succinic acid was confirmed in the FTIR spectra by the appearance of two new bands at 1655 and 1723 cm^{-1} (COOH and COO^- vibrations respectively). The band at 1655 cm^{-1} overlaps with an additional one at 1630 cm^{-1}, which is typical for the amide I vibration.

Bioconjugation of SiNaPs with synthetic Aβ

The bioconjugation of SiNaPs with chosen biomolecules was enabled by previous functionalization and activation of the surfaces of SiNaPs by EDC/NHS treatment and the formation of NHS ester groups as reactive intermediates (Fig. 2d, e). The NHS esters on the surfaces of SiNaPs formed amide bonds with the exposed lysine residues of $A\beta_{42}$ at position 16 and/or 28 and led to coating of SiNaPs with Aβ peptides. An additional binding site is the N-terminus of the peptide, which we consider less reactive for the coupling reaction due to its vicinity to acidic amino acids and steric restraints. The successful attachment of $A\beta_{42}$ to the particles was demonstrated by FTIR (Fig. 3). Not only the bands assigned to CH_2 stretching vibrations (2925 cm^{-1} and 2855 cm^{-1}) showed an increased intensity for the peptide coated SiNaPs, but also the signals between 1580 and 1750 cm^{-1}. The increase of the band at 1720 cm^{-1} (COOH) appeared due to the presence of additional carboxyl groups by the amino acids of $A\beta_{42}$. Whereas the amide I vibration of the COOH-terminated SiNaPs was only visible as a shoulder which was increased to a maximum for the $A\beta_{42}$ functionalized SiNaPs. A new band positioned at 1542 cm^{-1} could be assigned to the amide II vibration of the peptide as well. Peptide quantitation by BCA assay revealed an $A\beta_{42}$ concentration of 24 μg ml^{-1} in a 1 mg ml^{-1} SiNaPs solution. This corresponds to an average load of 44 peptides per 24 nm SiNaP,

which is only 7% of the theoretical maximal load of 645 peptides, probably as a consequence of repulsive interactions on the nanoparticle surface.

Aβ-SiNaP quantitation in water and cerebrospinal fluid by sFIDA

The sFIDA assay is designed to specifically determine the Aβ oligomer concentration in body fluids, such as cerebrospinal fluid (CSF). Apart from quantifying Aβ-SiNaPs in aqueous environment, we also analyzed possible matrix effects on the sFIDA readout by spiking Aβ-SiNaPs into CSF from AD-negative donors (Fig. 4).

Aβ-SiNaP concentrations ranging from 100 pM to 10 fM were subjected to sFIDA analysis, and the respective non-spiked fluids served as controls. All samples including blank controls were determined three-fold by sFIDA analysis. Aβ-SiNaPs diluted in water as well as in CSF revealed a correlation between the sFIDA readout and the Aβ-SiNaP concentration down to 10 fM. A concentration of 10 fM Aβ-SiNaPs in water and 100 fM in CSF could still be differentiated from the control demonstrating that Aβ-SiNaPs are a suitable standard in CSF-based AD diagnostics.

Considering a load of 44 $A\beta_{42}$ peptides per Aβ-SiNaP, 10 fM Aβ-SiNaP corresponded to an $A\beta_{42}$ peptide concentration of 1.9 ng l^{-1}. This limit of detection of $A\beta_{42}$ peptides is in the same range or one order of magnitude higher as reported for oligomer-specific ELISA-based assays [13, 14, 27]. By repetition of the experiment with the same Aβ-SiNaP batch stored at 4°C over a period of four months, we demonstrated constantly stable sFIDA readouts from the Aβ-SiNaP dilution series and therefore confirmed long-term stability of the standard (Fig. 5).

DISCUSSION

In this work we presented the synthesis and application of Aβ-SiNaPs as standard in sFIDA diagnostics. The successful synthesis and biofunctionalization of SiNaPs was shown by TEM, XPS micrographs and ATR-FTIR spectra. By sFIDA analysis we quantified Aβ-SiNaPs diluted in water and CSF over several orders of magnitude down to the femtomolar concentration range. A SiNaP standard of tunable, defined size and with an adjustable number of epitopes on the SiNaP surface might significantly contribute to the development, optimization and calibration of immuno-based diagnostic

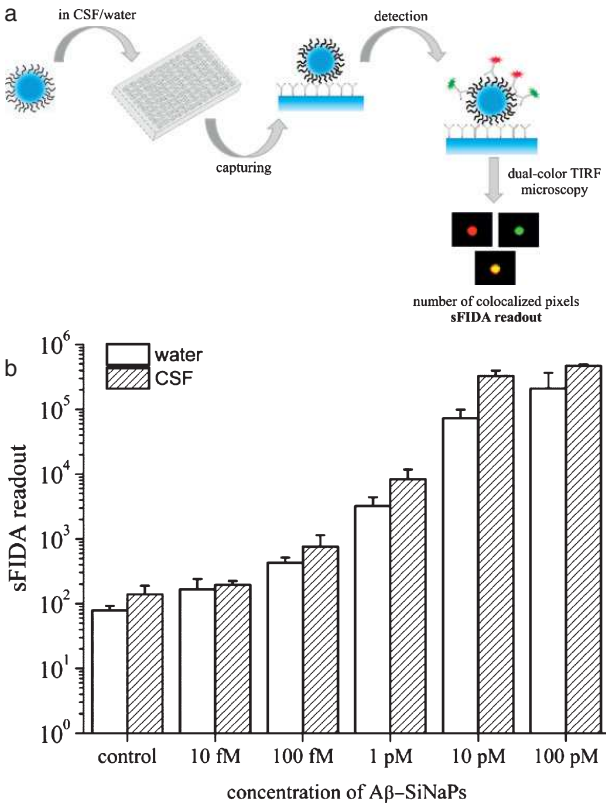

Fig. 4. sFIDA analysis of Aβ-SiNaPs. a) Schematic illustration of the experimental procedure of detecting Aβ-SiNaPs in the sFIDA assay. b) sFIDA analysis of Aβ-SiNaPs diluted in water and CSF sFIDA readout of Aβ-SiNaPs diluted in water and human CSF to concentrations of 100 pM to 10 fM. The respective diluent lacking Aβ-SiNaPs served as negative control. Shown are mean values and standard deviations from threefold determination.

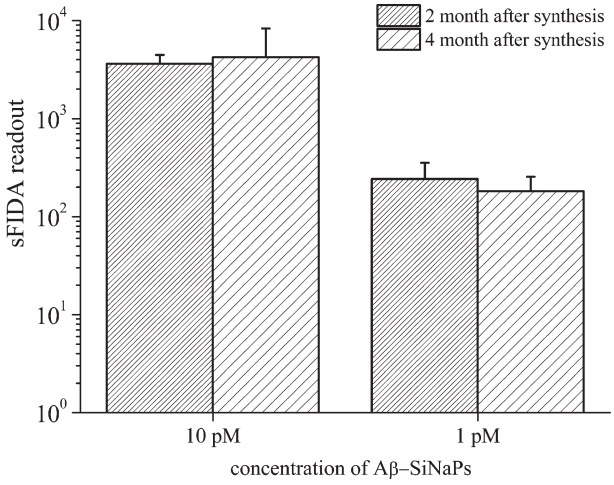

Fig. 5. sFIDA analysis of Aβ-SiNaPs diluted in water. sFIDA readout of Aβ-SiNaPs diluted in water to concentrations of 10 pM and 1 pM. Shown are two measurements of the same SiNaP batch at different time points, 2 and 4 months after synthesis. Plotted are mean values and standard deviations from threefold determination.

assays for protein misfolding diseases based on single-molecule detection.

In contrast to any other standard of Aβ aggregates, Aβ-SiNaPs exhibit a measurable number of accessible Aβ peptides on the SiNaP surface. These defined characteristics render Aβ-SiNaPs superior to the more heterogeneous oligomer standards prepared from a stochastic aggregation reaction of synthetic Aβ, as they have been used so far. In the presented case we bound 44 peptides per SiNaP.

In addition, Aβ-SiNaPs prepared by this method showed no observable aggregation after the excessive and non-covalently bound monomer was removed. This observation suggests that Aβ bound to the particle surface is not able to transmit to a conformation that is prone to form aggregates. Since the mid and C-terminal sections of the Aβ sequence are involved in the aggregation mechanism it appears very likely that the coupling of Lys16 and/or Lys28 is responsible for the inhibition of the aggregation of Aβ-SiNaP.

The chemically activated SiNaPs can be easily coated with any peptide of choice to serve also as standard in oligomer-based assays of other protein misfolding diseases, such as prion diseases or Parkinson's disease [28–31]. Additionally, hybrid aggregates consisting of different peptides, such as tau and Aβ, could be mimicked by a SiNaP standard to support explorative studies on hybrid oligomers as biomarkers, which might reflect the clinical diversity of many neurodegenerative disorders [32, 33]. For the described synthesis of biofunctionalized SiNaPs the chosen peptide needs to have a free primary amine group for the covalent coupling to the SiNaP outside the epitope, to enable detection of the peptide on the SiNaP. Alternatively other coupling methods, such as Biotin/Streptavidin could link peptides to the SiNaP platform.

Different approaches are developed for the oligomer-specific diagnosis of Alzheimer's disease based on immunodetection in liquid, such as ELISA-like methods as described above or flow cytometry combined with FRET [34]. However, these methods lack an appropriate standard molecule to enable the accurate and reproducible quantitation of Aβ oligomers in human samples. A calibration curve of a serial dilution of Aβ-SiNaPs in the respective body fluid should allow the quantitation of the analyte and also the number of detected epitopes by comparing the obtained fluorescence signals of the clinical sample and the standard.

We envisage the Aβ-SiNaP standard as an essential tool to cross-validate Aβ oligomers as AD biomarker on different platform technologies. It will allow the accurate determination of inter-assay variability and thereby be a valuable tool in the standardization process of various Aβ oligomer immunodetection assays.

ACKNOWLEDGMENTS

This work was supported by the Federal Ministry of Education and Research within the projects VIP (03V0641), KNDD (01GI1010A), and JPND/BIOMARKAPD (01ED1203H).

Authors' disclosures available online (http://www.j-alz.com/manuscript-disclosures/16-0253r2).

REFERENCES

[1] Prince M, Albanese E, Guerchet M, Prina M (2014) *World Alzheimer Report 2014, Dementia and Risk Reduction: An Analysis of Protective and Modifiable Factors*.

[2] Barnes DE, Yaffe K (2011) The projected effect of risk factor reduction on Alzheimer's disease prevalence. *Lancet Neurol* **10**, 819-828.

[3] Hardy J, Selkoe DJ (2002) The amyloid hypothesis of Alzheimer's disease: Progress and problems on the road to therapeutics. *Science* **297**, 353-356.

[4] Hardy J (2006) Has the amyloid cascade hypothesis for Alzheimer's disease been proved? *Curr Alzheimer Res* **3**, 71-73.

[5] Haass C, Selkoe DJ (2007) Soluble protein oligomers in neurodegeneration: Lessons from the Alzheimer's amyloid beta-peptide. *Nat Rev Mol Cell Biol* **8**, 101-112.

[6] Lesne S, Koh MT, Kotilinek L, Kayed R, Glabe CG, Yang A, Gallagher M, Ashe KH (2006) A specific amyloid-beta protein assembly in the brain impairs memory. *Nature* **440**, 352-357.

[7] El-Agnaf OM, Mahil DS, Patel BP, Austen BM (2000) Oligomerization and toxicity of beta-amyloid-42 implicated in Alzheimer's disease. *Biochem Biophys Res Commun* **273**, 1003-1007.

[8] Klaver AC, Patrias LM, Finke JM, Loeffler DA (2011) Specificity and sensitivity of the Abeta oligomer ELISA. *J Neurosci Methods* **195**, 249-254.

[9] Savage MJ, Kalinina J, Wolfe A, Tugusheva K, Korn R, Cash-Mason T, Maxwell JW, Hatcher NG, Haugabook SJ, Wu GX, Howell BJ, Renger JJ, Shughrue PJ, McCampbell A (2014) A sensitive A beta oligomer assay discriminates Alzheimer's and aged control cerebrospinal fluid. *J Neurosci* **34**, 2884-2897.

[10] Sian AK, Frears ER, El-Agnaf OM, Patel BP, Manca MF, Siligardi G, Hussain R, Austen BM (2000) Oligomerization of beta-amyloid of the Alzheimer's and the Dutch-cerebral-haemorrhage types. *Biochem J* **349**, 299-308.

[11] Xia W, Yang T, Shankar G, Smith IM, Shen Y, Walsh DM, Selkoe DJ (2009) A specific enzyme-linked immunosorbent assay for measuring beta-amyloid protein oligomers in human plasma and brain tissue of patients with Alzheimer disease. *Arch Neurol* **66**, 190-199.

[12] Yang T, O'Malley TT, Kanmert D, Jerecic J, Zieske LR, Zetterberg H, Hyman BT, Walsh DM, Selkoe DJ (2015) A

highly sensitive novel immunoassay specifically detects low levels of soluble A beta oligomers in human cerebrospinal fluid. *Alzheimers Res Ther* **7**, 14.

[13] Holtta M, Hansson O, Andreasson U, Hertze J, Minthon L, Nagga K, Andreasen N, Zetterberg H, Blennow K (2013) Evaluating amyloid-beta oligomers in cerebrospinal fluid as a biomarker for Alzheimer's disease. *PLoS One* **8**, e66381.

[14] Fukumoto H, Tokuda T, Kasai T, Ishigami N, Hidaka H, Kondo M, Allsop D, Nakagawa M (2010) High-molecular-weight beta-amyloid oligomers are elevated in cerebrospinal fluid of Alzheimer patients. *FASEB J* **24**, 2716-2726.

[15] Funke SA, Birkmann E, Henke F, Goertz P, Lange-Asschenfeldt C, Riesner D, Willbold D (2007) Single particle detection of A beta aggregates associated with Alzheimer's disease. *Biochem Biophys Res Commun* **364**, 902-907.

[16] Wang-Dietrich L, Funke SA, Kuhbach K, Wang K, Besmehn A, Willbold S, Cinar Y, Bannach O, Birkmann E, Willbold D (2013) The amyloid-beta oligomer count in cerebrospinal fluid is a biomarker for Alzheimer's disease. *J Alzheimers Dis* **34**, 985-994.

[17] Mattsson N, Andreasson U, Persson S, Carrillo MC, Collins S, Chalbot S, Cutler N, Dufour-Rainfray D, Fagan AM, Heegaard NH, Robin Hsiung GY, Hyman B, Iqbal K, Kaeser SA, Lachno DR, Lleo A, Lewczuk P, Molinuevo JL, Parchi P, Regeniter A, Rissman RA, Rosenmann H, Sancesario G, Schroder J, Shaw LM, Teunissen CE, Trojanowski JQ, Vanderstichele H, Vandijck M, Verbeek MM, Zetterberg H, Blennow K, Alzheimer's Association QCPWG (2013) CSF biomarker variability in the Alzheimer's Association quality control program. *Alzheimers Dement* **9**, 251-261.

[18] Stober W, Fink A, Bohn E (1968) Controlled growth of monodisperse silica spheres in micron size range. *J Colloid Interface Sci* **26**, 62-69.

[19] Thomassen LC, Aerts A, Rabolli V, Lison D, Gonzalez L, Kirsch-Volders M, Napierska D, Hoet PH, Kirschhock CE, Martens JA (2010) Synthesis and characterization of stable monodisperse silica nanoparticle sols for *in vitro* cytotoxicity testing. *Langmuir* **26**, 328-335.

[20] Glabe CG (2008) Structural classification of toxic amyloid oligomers. *J Biol Chem* **283**, 29639-29643.

[21] Mastrangelo IA, Ahmed M, Sato T, Liu W, Wang C, Hough P, Smith SO (2006) High-resolution atomic force microscopy of soluble Abeta42 oligomers. *J Mol Biol* **358**, 106-119.

[22] Sakono M, Zako T (2010) Amyloid oligomers: Formation and toxicity of Abeta oligomers. *FEBS J* **277**, 1348-1358.

[23] Masalov VM, Sukhinina NS, Kudrenko EA, Emelchenko GA (2011) Mechanism of formation and nanostructure of Stober silica particles. *Nanotechnology* **22**, 275718.

[24] Graf C, van Blaaderen A (2002) Metallodielectric colloidal core-shell particles for photonic applications. *Langmuir* **18**, 524-534.

[25] Nag S, Chen J, Irudayaraj J, Maiti S (2010) Measurement of the attachment and assembly of small amyloid-beta oligomers on live cell membranes at physiological concentrations using single-molecule tools. *Biophys J* **99**, 1969-1975.

[26] Qhobosheane M, Santra S, Zhang P, Tan W (2001) Biochemically functionalized silica nanoparticles. *Analyst* **126**, 1274-1278.

[27] Bruggink KA, Jongbloed W, Biemans EA, Veerhuis R, Claassen JA, Kuiperij HB, Verbeek MM (2013) Amyloid-beta oligomer detection by ELISA in cerebrospinal fluid and brain tissue. *Anal Biochem* **433**, 112-120.

[28] Bannach O, Birkmann E, Reinartz E, Jaeger KE, Langeveld JP, Rohwer RG, Gregori L, Terry LA, Willbold D, Riesner D (2012) Detection of prion protein particles in blood plasma of scrapie infected sheep. *PLoS One* **7**, e36620.

[29] Bannach O, Reinartz E, Henke F, Dressen F, Oelschlegel A, Kaatz M, Groschup MH, Willbold D, Riesner D, Birkmann E (2013) Analysis of prion protein aggregates in blood and brain from pre-clinical and clinical BSE cases. *Vet Microbiol* **166**, 102-108.

[30] Hubinger S, Bannach O, Funke SA, Willbold D, Birkmann E (2012) Detection of alpha-synuclein aggregates by fluorescence microscopy. *Rejuvenation Res* **15**, 213-216.

[31] Hansson O, Hall S, Ohrfelt A, Zetterberg H, Blennow K, Minthon L, Nagga K, Londos E, Varghese S, Majbour NK, Al-Hayani A, El-Agnaf OM (2014) Levels of cerebrospinal fluid alpha-synuclein oligomers are increased in Parkinson's disease with dementia and dementia with Lewy bodies compared to Alzheimer's disease. *Alzheimers Res Ther* **6**, 25.

[32] Clinton LK, Blurton-Jones M, Myczek K, Trojanowski JQ, LaFerla FM (2010) Synergistic Interactions between Abeta, tau, and alpha-synuclein: Acceleration of neuropathology and cognitive decline. *J Neurosci* **30**, 7281-7289.

[33] Guo JP, Arai T, Miklossy J, McGeer PL (2006) A beta and tau form soluble complexes that may promote self aggregation of both into the insoluble forms observed in Alzheimer's disease. *Proc Natl Acad Sci U S A* **103**, 1953-1958.

[34] Santos AN, Torkler S, Nowak D, Schlittig C, Goerdes M, Lauber T, Trischmann L, Schaupp M, Penz M, Tiller FW, Bohm G (2007) Detection of amyloid-beta oligomers in human cerebrospinal fluid by flow cytometry and fluorescence resonance energy transfer. *J Alzheimers Dis* **11**, 117-125.

Biological Chemistry `Just Accepted' Papers

Biological Chemistry `Just Accepted' Papers are papers published online, in advance of appearing in the print journal. They have been peer-reviewed, accepted and are online published in manuscript form, but have not been copy edited, typeset, or proofread. Copy editing may lead to small differences between the Just Accepted version and the final version. There may also be differences in the quality of the graphics. When papers do appear in print, they will be removed from this feature and grouped with other papers in an issue.

Biol Chem `Just Accepted' Papers are citable; the online publication date is indicated on the Table of Contents page, and the article's Digital Object Identifier (DOI), a unique identifier for intellectual property in the digital environment (e.g., 10.1515/hsz-2011-xxxx), is shown at the top margin of the title page. Once an article is published as **Biol Chem `Just Accepted' Paper** (and before it is published in its final form), it should be cited in other articles by indicating author list, title and DOI.

After a paper is published in **Biol Chem `Just Accepted' Paper** form, it proceeds through the normal production process, which includes copy editing, typesetting and proofreading. The edited paper is then published in its final form in a regular print and online issue of **Biol Chem.** At this time, the **Biol Chem `Just Accepted' Paper** version is replaced on the journal Web site by the final version of the paper with the same DOI as the **Biol Chem `Just Accepted' Paper version.**

Disclaimer

Biol Chem `Just Accepted' Papers** have undergone the complete peer-review process. However, none of the additional editorial preparation, which includes copy editing, typesetting and proofreading, has been performed. Therefore, there may be errors in articles published as **Biol Chem `Just Accepted' Papers that will be corrected in the final print and online version of the Journal. Any use of these articles is subject to the explicit understanding that the papers have not yet gone through the full quality control process prior to advanced publication.

Biological Chemistry **'Just Accepted' paper**
ISSN (online) 1437-4315
DOI: 10.1515/hsz-2016-0153

Research Article

Analysis of anticoagulants for blood-based quantitation of amyloid β oligomers in the sFIDA assay

Kateryna Kravchenko[1], Andreas Kulawik[1,2], Maren Hülsemann[1], Katja Kühbach[1], Christian Zafiu[1], Yvonne Herrmann[1], Christina Linnartz[1], Luriano Peters[1], Tuyen Bujnicki[1], Johannes Willbold[1], Oliver Bannach[1,2] and Dieter Willbold[1,2,*]

[1]ICS-6 Structural Biochemistry, Forschungszentrum Jülich, Wilhelm-Johnen-Str., D-52425 Jülich, Germany

[2]Institut für Physikalische Biologie, Heinrich-Heine-Universität Düsseldorf, Universitätsstraße 1, D-40225 Düsseldorf, Germany

*Corresponding author

e-mail: d.willbold@fz-juelich.de

Abstract

Early diagnostics at the preclinical stage of Alzheimer's disease is of utmost importance for drug development in clinical trials and prognostic guidance. Since soluble Aβ oligomers are considered to play a crucial role in the disease pathogenesis, several methods aim to quantify Aβ oligomers in body fluids such as cerebrospinal fluid (CSF) and blood plasma. The highly specific and sensitive method surface-based fluorescence intensity distribution analysis (sFIDA) has successfully been established for oligomer quantitation in CSF samples. In our study, we explored the sFIDA method for quantitative measurements of synthetic Aβ particles in blood plasma. For this purpose, EDTA, citrate and heparin treated blood plasma samples from five individual donors were spiked with Aβ coated silica nanoparticles (Aβ-SiNaPs) and were applied to the sFIDA assay. Based on the assay parameters linearity, coefficient of variation and limit of detection, we found that EDTA plasma yields the most suitable parameter values for quantitation of Aβ oligomers in sFIDA assay with a limit of detection of 16 fM.

Keywords: Alzheimer's disease diagnostic biomarkers; Amyloid beta oligomers; neurodegenerative diseases; blood plasma; sFIDA, silica nanoparticles.

Introduction

Alzheimer's disease (AD) is the most frequent form of dementia which affects more than 35 million people worldwide (Wimo *et al.*, 2013). Since age is considered to be the major risk factor for AD, the case number is expected to dramatically increase in the next decades as a consequence of the aging society. The clinical onset of AD is preceded by pathophysiological changes years before outbreak of the disease (Blennow, 2004). Early diagnostics at the preclinical stage of the disease is highly desired for drug development in clinical trials and prognostic guidance.

Major pathological hallmarks of AD are extracellular amyloid plaques consisting mainly of amyloid beta (Aβ) peptide as well as intracellular neurofibrillary tangles composed of tau protein (Selkoe, 1991). More recent data indicate that oligomeric Aβ is the most toxic species and is therefore of interest both as drug target and candidate biomarker (Haass and Selkoe, 2007; Blennow *et al.*, 2015).

On that account, we developed a highly sensitive oligomer-specific diagnostic assay designated surface-based fluorescence intensity distribution analysis (sFIDA) (Birkmann *et al.*, 2006; Birkmann *et al.*, 2007; Funke *et al.*, 2007; Funke *et al.*, 2010; Bannach *et al.*, 2012; Wang-Dietrich *et al.*, 2013; Kühbach *et al.*, 2016). In sFIDA, Aβ is captured to a functionalized glass surface by Aβ specific antibodies which recognize the N-terminus of the molecule. Subsequently, Aβ is decorated by two fluorescently labeled antibodies. Since the same or overlapping epitopes are recognized by both capture and detection antibodies, the assay is insensitive for monomeric Aβ which is omnipresent also in healthy subjects. Images from the surface are obtained using dual-color total internal reflection fluorescence microscopy (TIRFM). The number of colocalized pixels with signal intensities above background is referred to as sFIDA readout, which correlates with the number of Aβ oligomers in the sample. As a calibration standard in the sFIDA assay, 30 nm silica nanoparticles coated with $A\beta_{1\text{-}42}$ peptides (Aβ-SiNaPs) are used. Aβ-SiNaPs have been shown to be a suitable standard in Aβ oligomer quantitation due to their uniform size and defined number of accessible epitopes. Moreover, the particles are not prone to aggregation and are stable over several months (Hülsemann *et al.*, 2016).

sFIDA has been proven as a capable tool for the quantitation of Aβ oligomers from cerebrospinal fluid with a large sensitive range of detection. However, lumbar puncture,

though generally considered as safe, goes along with risks and is often experienced as uncomfortable for patients. Hence, the diagnosis from blood preparations after venipuncture is a worthwhile aim.

Blood can be processed either as serum or as plasma, which is the noncoagulated liquid component of blood after centrifugation. Coagulation is prevented by addition of anticoagulants of which EDTA, citrate, and heparin are the most commonly used in clinical practice (Jambunathan and Galande, 2014). EDTA and citrate prevent the formation of thrombin by chelating calcium required for the blood clotting cascade (Davie and Ratnoff, 1964), whereas heparin functions by activating antithrombin (Olson and Chuang, 2002).

The choice of anticoagulant for blood plasma preparation is an important factor in the preanalytical phase of assay development and can have a considerable effect on the identification of biomarkers as shown for a variety of assays concerning the detection of e.g. cytokines (Riches *et al.*, 1992), miRNA (Leidinger *et al.*, 2015), proteins (Banks *et al.*, 2005; Hsieh *et al.*, 2006), enzymes (Gerlach *et al.*, 2005), amino acid analysis (Parvy *et al.*, 1983; Hubbard *et al.*, 1988; Chuang *et al.*, 1998) and other analytes (Fendl *et al.*, 2016; Ribeiro *et al.*, 2016).

The goal of the present study was to compare the effect of different anticoagulants on the sFIDA assay and identify the most suitable anticoagulant regarding assay standardization. Therefore, a dilution series of Aβ-SiNaPs was spiked in blood plasma supplemented with different anticoagulants (EDTA, citrate and heparin, respectively) and were subsequently applied to the sFIDA assay. Based on the assay parameters linearity, coefficient of variance and limit of detection, the effect of the anticoagulants on the assay outcome was investigated.

Results

Aβ-SiNaPs were spiked in a log 10 dilution series to EDTA, citrate and heparin plasma, each of five individual healthy donors and subjected to sFIDA assay. As a preprocessing procedure all images underwent artifact detection. For Aβ-SiNaPs spiked in EDTA plasma, citrate plasma, heparin plasma and PBS 81.4%, 87.9%, 88.0% and 89.2% of the total number of images passed quality control, respectively.

Inspection of the images for sFIDA analysis revealed differences for the different anticoagulants (Figures 1 and 2). For channel 0 (em. 635 nm / exc. 705 nm) the major peak in intensity distribution for EDTA was approximately at 2400, for citrate at 1700 and for heparin at 900 on a 14-bit grayscale, and for channel 1 (em. 488 nm / exc. 525 nm) at approximately 1300, 1300 and 1000, respectively (Figure 2), as shown for blood plasma samples spiked in 1 pM Aβ-SiNaPs. This indicates that the overall intensity of images obtained from heparin treated blood plasma are considerably lower compared to EDTA and citrate, as can also be seen in representative images (Figure 1, left hand column). Furthermore, the variation in intensity distribution between the images is higher for heparin compared to EDTA and citrate plasma (Figure 1, middle and right hand column).

For deeper analysis, sFIDA readout was calculated which is the number of colocalized pixels above background. A correlation between Aβ-SiNaP concentration and sFIDA readout was observed from 100 pM down to the lowest concentration of 10 fM for all plasma samples (Figure 3). In order to further characterize the effect of different anticoagulants on the sFIDA readout of Aβ-SiNaP spiked plasma samples, the linearity of the data was assessed as well as the coefficient of variation (CV) as a criterion for intra-assay precision and limit of detection (LOD) as a criterion for assay sensitivity were calculated.

Linearity

The sFIDA assay is known to have a wide sensitive detection range for Aβ oligomers. However, the linearity of the assay's readout is influenced by a variety of factors. To investigate the impact of anticoagulants in blood plasma samples on the linearity of the sFIDA readout, the Pearson's correlation coefficient, Mandel's fitting test as well as Lack-of-fit test were calculated (Table 1).

Nearly ideal linear relationship in terms of Pearson's correlation of $\rho = 0.94$ was found for EDTA blood plasma and PBS diluents, whereas considerably lower values of $\rho = 0.37$ and $\rho = 0.64$ were obtained for dilutions in citrate and heparin blood plasma, respectively (table 2). Since Pearson's correlation coefficient ρ has very limited significance as a criterion for linearity, Mandel's fitting test as well as Lack-of-fit test for the first and second order calibration curve was performed which are recommended and well established methods for testing linearity (Van Loco *et al.*, 2002; Sanagi *et al.*, 2010). Likewise, Mandel's fitting test and Lack-of-fit test,respectively, indicate good linearity for EDTA plasma and PBS control,

whereas for citrate and heparin a second order calibration curve is the function preferred (Table 1).

Coefficient of variation

Coefficient of variation (CV) was calculated to assess intra-assay precision, which differs between the anticoagulants (Figure 4). The lowest mean CV of 28% was obtained for EDTA plasma followed by 39% for citrate plasma and 67% for heparin plasma. For PBS a CV of 51% was obtained.

Limit of detection

Limit of detection (LOD) was calculated to investigate the effect of different anticoagulants on assay sensitivity as the mean for five donors. As each donor was measured in six replicates, the mean LOD calculation is based on 30 negative controls. Significant differences in mean LOD for Aβ-SiNaP dilution series in EDTA, citrate and heparin plasma as well as in PBS were observed (Figure 5). The lowest mean LOD of 16 fM was obtained for Aβ-SiNaPs spiked in EDTA plasma followed by 19 fM (incl. outlier: 34 fM) for citrate, 27 fM for PBS and 34 fM (incl. outlier: 280 fM) for heparin. Additionally, the median LOD was calculated being more robust towards outliers as observed for citrate and heparin. In agreement with mean LOD the lowest median LOD of 16 fM was obtained for Aβ-SiNaP spiked in EDTA plasma followed by 22 fM for citrate plasma, 23 fM for PBS and 31 fM for heparin plasma (data not shown).

Summary

Mean Pearson's correlation coefficient between spiked Aβ-SiNaPs and sFIDA readout, mean CV [%] and mean LOD for all three anticoagulants and PBS are summarized in Table 2. Highest linearity, highest intra-assay precision and highest sensitivity of the sFIDA assay was obtained for Aβ-SiNaP-spiked EDTA plasma.

Discussion

The choice of anticoagulants for blood plasma preparation can have a significant impact on the detection of biomarkers. The aim of the present study was to compare the effect of different anticoagulants on the sFIDA readout and identify the most suitable anticoagulant

regarding assay standardization. For this purpose, a dilution series of Aβ-SiNaPs was spiked in human blood plasma samples supplemented with different anticoagulants (EDTA, citrate and heparine, respectively) and was subsequently applied to the sFIDA assay. The assay outcome was evaluated by means of three parameters: the linearity of the sFIDA readout as a function of applied Aβ-SiNaP concentration, the coefficient of variation as well as the limit of detection.

The highest linearity for mean Pearson's correlation coefficient ρ of 0.94 was calculated for Aβ-SiNaPs spiked in EDTA plasma followed by heparin (ρ=0.94) and citrate (ρ=0.37) plasma. The lowest mean CV of 28% was obtained for EDTA followed by citrate (CV=39%) and heparin plasma (CV=67%). The lowest LOD of 16 fM was obtained for quantitation of Aβ-SiNaPs spiked in EDTA plasma followed by LOD of 19 fM and 34 fM for citrate and heparin plasma, respectively.

EDTA, citrate and heparin are the most common anticoagulants for blood plasma treatment in clinical practice. Whereas the anticoagulative effect of EDTA and citrate is attributed to the prevention of thrombin formation by chelating calcium required for the blood clotting cascade (Davie and Ratnoff, 1964), heparin functions by activating antithrombin (Olson and Chuang, 2002). Apart from this, heparin is known to bind to a variety of proteins including proteases, growth factors, chemokines, lipid binding proteins and adhesion proteins as summarized in Capila and Linhardt (2002) and thus might modulate matrix effects significantly by affecting the biochemical constitution of blood plasma. Moreover, it has been shown in several studies that heparin binds directly to Aβ species (Watson *et al.*, 1997; Madine *et al.*, 2012; Nguyen and Rabenstein, 2016) possibly interfering with Aβ oligomer quantitation and accounting for the attenuating effects in sFIDA assay presented here.

Altogether, this is in line with studies on quantitation of total Aβ levels from blood plasma. Vanderstichele *et al.* (2002) reported that plasma collected in citrate and heparin tubes did not result in any measurable Aβ levels, whereas Aβ levels in EDTA plasma could be readily detected (Vanderstichele *et al.*, 2000). Lachno *et al.* (2009) determined total Aβ levels in serum, EDTA, citrate, heparin and fluoride plasma with highest Aβ levels in EDTA treated plasma (Lachno *et al.*, 2009).

The well-described binding of Aβ to various plasma proteins (Koudinov *et al.*, 1994; Biere *et al.*, 1996; Koudinov *et al.*, 1998) might lead to a masking of epitopes and ultimately result

in signal attenuation due to impaired capturing and probe detection. Previously, an interaction between prion protein aggregates and low density lipoproteins has been reported, making pretreatment with lipases and detergents necessary to counteract signal loss in sFIDA measurements (Safar *et al.*, 2006; Bannach *et al.*, 2012). In the present study, however, the presence of EDTA plasma did not have any adverse effect on detection and quantitation of Aβ-SiNaP down to the low femtomolar range.

The achieved coefficient of variation of 28% is a severe issue for further improvement. Also, more validation parameters as suggested by Andreasson *et al.* (2015) (Andreasson *et al.*, 2015) need to be addressed in future.

We conclude that EDTA is the most suitable anticoagulant for Aβ-SiNaP quantitation in blood plasma using the sFIDA assay. We therefore suggest that plasma samples for AD diagnosis in the sFIDA assay should be collected in EDTA tubes to ensure most accurate determination of Aβ oligomer levels in human blood plasma. Future investigations, however, will reveal, whether humans do contain detectable amounts of Aβ oligomers and whether they correlate with disease progression or prognosis. Thus, further work will focus on sFIDA measurements of clinical EDTA plasma samples from AD patients and controls in order to assess if Aβ oligomers can be exploited as a blood-based biomarker for AD.

Materials and methods

Plasma samples

A total of 15 blood plasma samples from 5 healthy donors were purchased from ZenBio, Inc. (BioCat GmbH, Heidelberg, Germany). Plasma samples were collected in BD Vacutainer tubes containing 12.15 mg K_2EDTA per 7.0 ml sample, 158 USP Units Heparin per 10.0 ml sample or 1 ml acid-citrate-dextrose solution B (4.8 g/l citric acid; 13.2 g/l Na_3Citrate; 14.7 g/l dextrose) per 6 ml sample, respectively. To avoid repeated freeze/thaw cycles, plasma samples were directly aliquoted and stored at -80°C until usage. Prior to aliquoting, plasma samples were centrifuged for 10 min at 20 000 *g* and the supernatant was preserved.

Silica nanoparticles coated with $A\beta_{1-42}$ (Aβ-SiNaPs)

Aβ-SiNaPs were prepared as described previously (Hülsemann *et al.*, 2016). Briefly, bare silica nanoparticles (SiNaPs) were synthesized via Stöber process and silanized with APTES to cover the surface with primary amino groups. Subsequent reaction with succinic anhydrid resulted in carboxylated SiNaPs, which were activated by EDC/NHS for covalent coupling of $A\beta_{1-42}$. The same batch of Aβ-SiNaPs was used for all spiking experiments to ensure equal size (diameter of approx. 30 nm) of the particles and Aβ distribution on the surface. 1 nM Aβ-SiNaP stock solution was serially diluted to 100 pM, 10 pM, 1 pM, 100 fM and 10 fM in plasma samples and PBS.

sFIDA protocol

For sFIDA assay a 384-well multititer plate (SensoPlate plus, Greiner Bio-One International, Frickenhausen, Germany) was used. All of the protocol steps were carried out under the clean bench to avoid dust and microbial contamination. Prior to functionalization of the glass surface, wells were cleaned with sodium hydroxide and hydrochloric acid. 5 M NaOH (Carl Roth, Karlsruhe, Germany) was applied for 15 min to the wells (95 µl/well) followed by three washing steps with the same volume of water. Immediately, 1 M HCl (32%, AnalaR NORMAPUR, VWR Chemicals, France) was incubated for 15 min in the wells (95 µl/well) followed by three washing steps with water and two washing steps with 70% ethanol (AnalaR NORMAPUR, VWR Chemicals, France). Shortly after wells dried at room temperature (RT), 45 µl of a DMSO (Sigma-Aldrich, Steinheim, Germany) ethanolamine mixture (Sigma-Aldrich, Steinheim, Germany) (v/v 2:3) was added to the wells and incubated overnight at RT. Afterwards, the wells were washed twice with DMSO and twice with 95 µl/well 70% ethanol and let dry. In the meantime, NHS-PEG-COOH (MW 5000, Laysan Bio, USA) was solved at 70°C in DMSO and cooled down to RT. 15 µl of 2 mM PEG solution were applied per well for 1 h followed by three washing steps with water. Activation of the PEG carboxyl groups was then performed by applying 30 µl/well of 100 mM EDC (Fluka, Buchs, Switzerland) and 100 mM NHS (Aldrich, Milwaukee, USA) mixture (v/v 1:1) in 0.1 M MES (Carl ROTH, Karlsruhe, Germany) buffer (pH 3.5) for 30 min. After washing the wells three times quickly with MES buffer, 15 µl/well capture antibody was added immediately for 1 h to the wells. As capture antibody, monoclonal anti-β-amyloid antibody NAB228 (Sigma-Aldrich, Steinheim, Germany) was diluted in PBS (Dulbecco's phosphate buffered saline 10×, Sigma-Aldrich, Steinheim, Germany) to a final concentration of 10 ng/µl and

centrifuged at 15 000 *g* for 10 min to remove the unsoluble components. Hereafter, the wells were washed twice with PBS-T (PBS + 0.05% Tween-20, Sigma-Aldrich, Steinheim, Germany) and twice with PBS. Next the surface was blocked with 50 µl/well Smart Block solution (Candor Bioscience, Wangen, Germany) followed by two washing steps with PBS-T and two steps with PBS. 15 µl/well sample was then applied to the surface and incubated overnight. Unbound sample components were removed by two washing steps with PBS-T and two washing steps with PBS. Finally, fluorescently labeled detection antibodies 6E10 Alexa Fluor 488 (Covance, Princeton, USA) and NAB228 Alexa Fluor 647 (Santa Cruz, Dallas, USA) were combined to the final concentration of 1.25 ng/µl each, centrifuged at 100 000 *g* for 1 h and applied to the wells (15 µl/well). After final washing twice with PBS-T and twice with PBS, wells were filled with 95 µl PBS.

Data acquisition

Acquisition of 14-bit grayscale images was performed using total internal reflection microscopy (AM TIRF MC, Leica Microsystems, Wetzlar, Germany). A total of 50 images per well (25 positions per channel) containing 1000 × 1000 pixels each were obtained for channel 0 (excitation at 635 nm, emission filter 705/72 nm) and channel 1 (excitation at 488 nm, emission filter 525/36 nm). The image size represents an area of 116 µm × 116 µm, thus in total 3.15% of the well surface (approx. 10 nm^2) were scanned. Laser intensity of 100%, exposure time between 1 s and 1.5 s and gain between 900 and 1000 were applied for image acquisition.

Artifact detection

Prior to data analysis, artificial images were removed from raw data pool applying two algorithms based on histogram analysis and cluster detection, respectively.

First, images were subjected to histogram artifact detection. This method is based on calculating the histogram for each image and counting the peaks by determination of local maxima in the histogram. Images with multimodal histograms (histograms containing more than one histogram maximum) were considered artificial and were excluded from further analysis. The image histogram was smoothed using 800 values for binning to eliminate background noise and thus avoid detection of local maxima. Via numerical differentiation the derivative of the smoothed histogram was calculated, which was then smoothed in the same way as the original histogram. After smoothing procedures, some rest noise can still cause

local maxima especially at points where function overlaps with x-axis. In order to determine the parameters for exclusion of images based on their histogram, a threshold was defined which includes two components: α and β. α is the number of pixels which form a maximum, β is a number of pixels which form a minimum. Only if α and β of adjacent maximum and minimum are high enough to meet α and β limits, a maximum was treated as a maximum. α limit of 400 and β limit of 300 were chosen as parameters for maxima determination.

Second, images with unimodal histograms (histograms with a single maximum) can still contain artifacts in form of large and/or bright spots. To detect these spots a cluster detection algorithm was applied to the images. This method is based on finding of agglomerations of pixels with intensities above a certain threshold. Depending on such parameters as cluster size, mean pixel intensity and standard deviation within a cluster, bright spots are identified as artifacts. Obtained grayscale images were transformed into binary images. The grayscale values with intensities ≤ mean grayscale value plus one standard deviation were set to 0, all others to 1. Using a rectangular structuring element with the size of 15 pixels × 15 pixels the images were eroded to identify large clusters and eliminate the small ones which represent Aβ-SiNaPs. To compensate pixel loss caused by erosion, dilation was applied to eroded images using the same structuring element.

An image was considered artificial and was excluded from further analysis, if at least one cluster fulfilled one of the following criteria: mean pixel intensity of more than 3000, a standard deviation of pixel intensity of more then 2800 or skewness of less than 0.

Data analysis

sFIDA readout

For data analysis of non-artificial images only a region of interest (ROI) consisting of the central 700 pixels × 700 pixels (corresponding to 490 000 pixels per image in total) was chosen in order to minimize the effects of inhomogeneous illumination of edge regions in TIRF microscopy images.

To reduce background noise, cutoffs were determined individually for each plasma sample based on the non-spiked control. This approach accounts for donor-specific background or signal by native Aβ oligomers which may influence the readout. For Aβ-SiNaPs diluted in PBS, the cutoff was determined from PBS control. The cutoff values for each channel were

determined as the intensity, which was exceeded by 1% of total pixels. Number of colocalized pixels from both channels above the respective cutoff is in following referred to as sFIDA readout.

The effects of different anticoagulants in plasma on sFIDA readouts were studied according to the criteria described below.

Linearity of the sFIDA readout

Pearson's correlation coefficient

Pearson's correlation coefficient (ρ) was calculated with MATLAB software as a criterion for linearity of the correlation between applied concentrations of Aβ-SiNaPs and obtained sFIDA readouts according to the formula:

$$\rho = \frac{N\sum xy - \sum x \sum y}{\sqrt{[N\sum x^2 - (\sum x)^2][N\sum y^2 - (\sum y)^2]}}$$

Where x is concentration of Aβ-SiNaPs, γ is the sFIDA readout and N is the number of x,γ pairs. Prior to mean value calculation, Olkin & Pratt correction was performed on Pearson's correlation coefficients (Olkin and Pratt, 1958; Eid *et al.*, 2013). Briefly, ρ was transformed to G_i according to the formula:

$$G_i = \rho_i \left(1 + \frac{1 - \rho_i^2}{2(n_i - 1 - 3)}\right)$$

where n is the number of samples in study i. Next, the weighted mean of G_i values was calculated for studies from $i = 1, \ldots, k$ according to the formula:

$$\bar{G} = \frac{\sum_{i=1}^{k} n_i G_i}{\sum_{i=1}^{k} n_i}$$

Thus, $\bar{G}$ is an estimator for mean correlation.

Test for linearity according to Mandel (Mandel's test)

The linearity of the sFIDA readout was further investigated using Mandel's fitting test (Mandel, 1964). This method provides evidence on linearity under consideration of the residual standard deviation for the first (linear) and second order (quadratic) calibration function. The H_0 hypothesis assumes no significant difference between the residual variances of the linear and quadratic calibration function. The Mandel's test was performed as follows (Funk *et al.*, 2005; Bruggemann *et al.*, 2006): The first and second order calibration functions are calculated including the residual standard deviations s_{y_1} and s_{y_2}:

$$s_{y_1} = \sqrt{\frac{\Sigma(y_i - \hat{y}_i)^2}{N-2}}, \text{ where } \hat{y}_i = a + bx_i$$

$$s_{y_2} = \sqrt{\frac{\Sigma(y_i - \hat{y}_i)^2}{N-3}}, \text{ where } \hat{y}_i = a + bx_i + cx_i^2$$

with:

y_i: observed sFIDA readout at each concentration level *i*

$\hat{y}_i$: estimation obtained from the respective regression analysis at *i*

N: total number of measurements

Next, the difference of the variances DS^2 is calculated based on the residual standard deviation s_{y_1} and s_{y_2}:

$$DS^2 = (N-2)s_{y_1}^2 - (N-3)s_{y_2}^2$$

Finally, the test value *PW* is calculated:

$$PW = \frac{DS^2}{s_{y_2}^2}$$

For the F-test, *PW* is compared with the corresponding value of the F-distribution $F_{crit;99\%(f_1,f_2,\alpha)}$, with $f_1 = 1$ and $f_2 = N - 3$ degrees of freedom at the significance level $\alpha = 0.01$.

For $PW < F_{crit;99\%}$ H_0 is accepted. The second order calibration function will not provide a significantly better fit; the calibration function of choice is linear.

For $PW > F_{crit;99\%}$ H_0 is retained, which indicates non-linearity (Bruggemann *et al.*, 2006).

Lack-of-fit test

The Lack-of-fit test (Massart, 1997) is performed by comparing the ratio of the error due to lack of fit of the respective calibration function and the error due to pure error obtained from replicative measurements with $F_{crit;99\%}$ at (k-2) and (n-k) degrees of freedom at the significance level $\alpha = 0.01$. The H_0 hypothesis assumes no lack of fit.

The Lack-of-fit test is calculated as follows: first, the sum of squares due to pure error and due to lack of fit are calculated, respectively:

$$SS_{PE} = \sum_{i}^{k} \sum_{j}^{n_i} (y_{ij} - \bar{y}_i)^2$$

$$SS_{LOF} = \sum_{i}^{k} n_i (\bar{y}_i - \hat{y}_i)^2$$

with:

i: concentration level, *k*: number of all concentration levels, *n*: number of replicates, $\bar{y}_i$: arithmetic mean of all observed values at *i*, $\hat{y}_i$: estimation obtained from the respective regression analysis at *i*. Next, the mean squares are calculated by dividing the sum of squares by the corresponding degrees of freedom (Massart, 1997).

$$MS_{LOF} = \frac{SS_{LOF}}{df}$$

$$MS_{PE} = \frac{SS_{PE}}{df}$$

For the F-test, the test value *LOF* is calculated as the arithmetic mean of both mean squares:

$$LOF = \frac{MS_{LOF}}{MS_{PE}}$$

For $LOF < F_{crit,99\%}$ H_0 is accepted. There is no lack of fit. For $LOF > F_{crit,99\%}$ H_0 is rejected. Saturated images for which sFIDA readout reached the maximum value of 490 000 (100 pM and 10 pM Aβ-SiNaPs in EDTA plasma as well as 100 pM Aβ-SiNaPs in PBS) were excluded from this analysis.

Coefficient of variation

Coefficient of variation (CV) was calculated as a criterion for intra-assay precision using Excel software. CV was calculated for each three replicate measurements for each standard concentration and negative control. The mean for each donor and each diluent was plotted using MATLAB software. Saturated images for 100 pM and 10 pM Aβ-SiNaPs in EDTA plasma as well as 100 pM Aβ-SiNaPs in PBS were excluded from this analysis.

Limit of detection

Limit of detection (LOD) was used as a criterion for sensitivity of the sFIDA assay. LOD was calculated as the mean from sFIDA readout for 6-fold replicate measurements of negative control (neg. control) from 5 individual donors (30 negative controls in total) and respective standard deviation (σ) according to the formula:

$$LOD = \text{sFIDA readout}_{(\text{neg. control})} + 3\sigma$$

Linear calibration curves for the correlation between concentrations of Aβ-SiNaPs and sFIDA readout for LOD determination were calculated with MATLAB software. Only values within the linear range of the obtained data were included for calculating the linear calibration curves (concentrations of 10 fM, 100 fM and 1 pM for all donors and anticoagulants). Using these calibration curves, the sFIDA readouts were correlated to their respective concentration.

Acknowledgements

This work was supported by the Federal Ministry of Education and Research within the projects "Validierung des Innovationspotenzials wissenschaftlicher Forschung - VIP" (03V0641), “Kompetenznetz Degenerative Demenzen” (01GI1010A), and the JPND “Neurodegenerative Disease Research/Biomarkers for Alzheimer’s and Parkinson’s disease” (01ED1203H), as well as the Michael J. Fox Foundation for Parkinson’s Research (11084).

References

Andreasson, U., A. Perret-Liaudet, L. J. van Waalwijk van Doorn, K. Blennow, D. Chiasserini, S. Engelborghs, T. Fladby, S. Genc*, et al.* (2015). A practical guide to immunoassay method validation. Front Neurol *6*, 179.

Banks, R. E., A. J. Stanley, D. A. Cairns, J. H. Barrett, P. Clarke, D. Thompson and P. J. Selby (2005). Influences of blood sample processing on low-molecular-weight proteome identified by surface-enhanced laser desorption/ionization mass spectrometry. Clin Chem *51*, 1637-1649.

Bannach, O., E. Birkmann, E. Reinartz, K. E. Jaeger, J. P. Langeveld, R. G. Rohwer, L. Gregori, L. A. Terry*, et al.* (2012). Detection of prion protein particles in blood plasma of scrapie infected sheep. PLoS One *7*, e36620.

Biere, A. L., B. Ostaszewski, E. R. Stimson, B. T. Hyman, J. E. Maggio and D. J. Selkoe (1996). Amyloid beta-peptide is transported on lipoproteins and albumin in human plasma. J Biol Chem *271*, 32916-32922.

Birkmann, E., F. Henke, N. Weinmann, C. Dumpitak, M. Groschup, A. Funke, D. Willbold and D. Riesner (2007). Counting of single prion particles bound to a capture-antibody surface (surface-FIDA). Vet Microbiol *123*, 294-304.

Birkmann, E., O. Schafer, N. Weinmann, C. Dumpitak, M. Beekes, R. Jackman, L. Thorne and D. Riesner (2006). Detection of prion particles in samples of BSE and scrapie by fluorescence correlation spectroscopy without proteinase K digestion. Biol Chem *387*, 95-102.

Blennow, K. (2004). CSF biomarkers for mild cognitive impairment. J Intern Med *256*, 224-234.

Blennow, K., N. Mattsson, M. Scholl, O. Hansson and H. Zetterberg (2015). Amyloid biomarkers in Alzheimer's disease. Trends Pharmacol Sci *36*, 297-309.

Bruggemann, L., W. Quapp and R. Wennrich (2006). Test for non-linearity concerning linear calibrated chemical measurements. Accreditation and Quality Assurance *11*, 625-631.

Capila, I. and R. J. Linhardt (2002). Heparin-protein interactions. Angew Chem Int Ed Engl *41*, 391-412.

Chuang, C. K., S. P. Lin, Y. T. Lin and F. Y. Huang (1998). Effects of anticoagulants in amino acid analysis: comparisons of heparin, EDTA, and sodium citrate in vacutainer tubes for plasma preparation. Clin Chem *44*, 1052-1056.

Davie, E. W. and O. D. Ratnoff (1964). Waterfall Sequence for Intrinsic Blood Clotting. Science *145*, 1310-1312.

Eid, M., M. Gollwitzer and M. Schmitt (2013). Statistik und Forschungsmethoden Lehrbuch; mit Online-Materialien. Weinheim, Wiley-VCH.

Fendl, B., R. Weiss, M. B. Fischer, A. Spittler and V. Weber (2016). Characterization of extracellular vesicles in whole blood: Influence of pre-analytical parameters and visualization of vesicle-cell interactions using imaging flow cytometry. Biochem Biophys Res Commun.

Funk, W., V. Dammann and G. Donnevert (2005). Qualitätssicherung in der Analytischen Chemie Anwendungen in der Umwelt-, Lebensmittel- und Werkstoffanalytik, Biotechnologie und Medizintechnik; Weinheim, Wiley-VCH.

Funke, S. A., E. Birkmann, F. Henke, P. Gortz, C. Lange-Asschenfeldt, D. Riesner and D. Willbold (2007). Single particle detection of Aβ aggregates associated with Alzheimer's disease. Biochem Biophys Res Commun *364*, 902-907.

Funke, S. A., L. Wang, E. Birkmann and D. Willbold (2010). Single-particle detection system for Aβ aggregates: adaptation of surface-fluorescence intensity distribution analysis to laser scanning microscopy. Rejuvenation Res *13*, 206-209.

Gerlach, R. F., J. A. Uzuelli, C. D. Souza-Tarla and J. E. Tanus-Santos (2005). Effect of anticoagulants on the determination of plasma matrix metalloproteinase (MMP)-2 and MMP-9 activities. Anal Biochem *344*, 147-149.

Haass, C. and D. J. Selkoe (2007). Soluble protein oligomers in neurodegeneration: lessons from the Alzheimer's amyloid β-peptide. Nat Rev Mol Cell Biol *8*, 101-112.

Hsieh, S. Y., R. K. Chen, Y. H. Pan and H. L. Lee (2006). Systematical evaluation of the effects of sample collection procedures on low-molecular-weight serum/plasma proteome profiling. Proteomics *6*, 3189-3198.

Hubbard, R. W., J. G. Chambers, A. Sanchez, R. Slocum and P. Lee (1988). Amino acid analysis of plasma: studies in sample preparation. J Chromatogr *431*, 163-169.

Hülsemann, M., C. Zafiu, K. Kühbach, N. Luhmann, Y. Herrmann, L. Peters, C. Linnartz, J. Willbold*, et al.* (2016). Biofunctionalized silica nanoparticles: standards in amyloid-β oligomer-based diagnosis of Alzheimer's disease. J Alzheimers Dis.

Jambunathan, K. and A. K. Galande (2014). Sample collection in clinical proteomics--proteolytic activity profile of serum and plasma. Proteomics Clin Appl *8*, 299-307.

Koudinov, A., E. Matsubara, B. Frangione and J. Ghiso (1994). The soluble form of Alzheimer's amyloid β protein is complexed to high density lipoprotein 3 and very high density lipoprotein in normal human plasma. Biochem Biophys Res Commun *205*, 1164-1171.

Koudinov, A. R., T. T. Berezov, A. Kumar and N. V. Koudinova (1998). Alzheimer's amyloid β interaction with normal human plasma high density lipoprotein: association with apolipoprotein and lipids. Clin Chim Acta *270*, 75-84.

Kühbach, K., M. Hülsemann, Y. Herrmann, K. Kravchenko, A. Kulawik, C. Linnartz, L. Peters, K. Wang*, et al.* (2016). Application of an amyloid β oligomer standard in the sFIDA assay. Front Neurosci *10*, 8.

Lachno, D. R., H. Vanderstichele, G. De Groote, V. Kostanjevecki, G. De Meyer, E. R. Siemers, M. B. Willey, J. S. Bourdage*, et al.* (2009). The influence of matrix type, diurnal rhythm and sample collection and processing on the measurement of plasma β-amyloid isoforms using the INNO-BIA plasma Aβ forms multiplex assay. J Nutr Health Aging *13*, 220-225.

Leidinger, P., C. Backes, S. Rheinheimer, A. Keller and E. Meese (2015). Towards clinical applications of blood-borne miRNA signatures: the influence of the anticoagulant EDTA on miRNA abundance. PLoS One *10*, e0143321.

Madine, J., M. J. Pandya, M. R. Hicks, A. Rodger, E. A. Yates, S. E. Radford and D. A. Middleton (2012). Site-specific identification of an Aβ fibril-heparin interaction site by using solid-state NMR spectroscopy. Angew Chem Int Ed Engl *51*, 13140-13143.

Mandel, J. (1964). The statistical analysis of experimental data. New York [u.a.], Wiley Interscience.

Massart, D. L. (1997). Handbook of chemometrics and qualimetrics Elektronische Ressource. Amsterdam, New York, Elsevier.

Nguyen, K. and D. L. Rabenstein (2016). Interaction of the heparin-binding consensus sequence of β-amyloid peptides with heparin and heparin-derived oligosaccharides. J Phys Chem B *120*, 2187-2197.

Olkin, I. and J. W. Pratt (1958). Unbiased Estimation of Certain Correlation Coefficients. 201-211.

Olson, S. T. and Y. J. Chuang (2002). Heparin activates antithrombin anticoagulant function by generating new interaction sites (exosites) for blood clotting proteinases. Trends Cardiovasc Med *12*, 331-338.

Parvy, P. R., J. I. Bardet and P. P. Kamoun (1983). EDTA in vacutainer tubes can interfere with plasma amino acid analysis. Clin Chem *29*, 735.

Ribeiro, A., T. Ritter, M. Griffin and R. Ceredig (2016). Development of a flow cytometry-based potency assay for measuring the *in vitro* immunomodulatory properties of mesenchymal stromal cells. Immunol Lett *177*: 38-46.

Riches, P., R. Gooding, B. C. Millar and A. W. Rowbottom (1992). Influence of collection and separation of blood samples on plasma IL-1, IL-6 and TNF-α concentrations. J Immunol Methods *153*, 125-131.

Safar, J. G., H. Wille, M. D. Geschwind, C. Deering, D. Latawiec, A. Serban, D. J. King, G. Legname*, et al.* (2006). Human prions and plasma lipoproteins. Proc Natl Acad Sci USA *103*, 11312-11317.

Sanagi, M. M., Z. Nasir, S. L. Ling, D. Hermawan, W. A. Ibrahim and A. A. Naim (2010). A practical approach for linearity assessment of calibration curves under the International Union of Pure and Applied Chemistry (IUPAC) guidelines for an in-house validation of method of analysis. J AOAC Int *93*, 1322-1330.

Selkoe, D. J. (1991). The molecular pathology of Alzheimer's disease. Neuron *6*, 487-498.

Van Loco, J., M. Elskens, C. Croux and H. Beernaert (2002). Linearity of calibration curves: use and misuse of the correlation coefficient. Accreditation and Quality Assurance *7*, 281-285.

Vanderstichele, H., E. Van Kerschaver, C. Hesse, P. Davidsson, M. A. Buyse, N. Andreasen, L. Minthon, A. Wallin*, et al.* (2000). Standardization of measurement of β-amyloid(1-42) in cerebrospinal fluid and plasma. Amyloid *7*, 245-258.

Wang-Dietrich, L., S. A. Funke, K. Kuhbach, K. Wang, A. Besmehn, S. Willbold, Y. Cinar, O. Bannach*, et al.* (2013). The amyloid-β oligomer count in cerebrospinal fluid is a biomarker for Alzheimer's disease. J Alzheimers Dis *34*, 985-994.

Watson, D. J., A. D. Lander and D. J. Selkoe (1997). Heparin-binding properties of the amyloidogenic peptides Aβ and amylin. Dependence on aggregation state and inhibition by Congo red. J Biol Chem *272*, 31617-31624.

Wimo, A., L. Jonsson, J. Bond, M. Prince, B. Winblad and I. Alzheimer Disease (2013). The worldwide economic impact of dementia 2010. Alzheimer's Dement *9*, 1-11 e13.

Tables and figures

Table 1 Analysis on linearity of sFIDA readout from Aβ-SiNaP dilution series.

	Pearson	Mandel's test		Lack-of-fit test (LRM)		Lack-of-fit test (QRM)	
	ρ	PW	F	LOF	F	LOF	F
EDTA 1	0.97	0.88	9.33	3.94	7.21	0.17	7.21
EDTA 2	0.98	1.16	10.04	6.35	8.02	0.12	8.02
EDTA 3	0.99	1.71	9.33	3.94	7.21	0.08	7.21
EDTA 4	0.78	0.13	9.33	3.17	7.21	2.33	7.21
EDTA 5	0.97	1.12	9.33	5.04	7.21	0.15	7.21
Citrate 1	0.1	138.29	8.28	52.22	4.89	1.88	4.89
Citrate 2	0.64	127.13	8.28	36.96	4.89	0.63	4.89
Citrate 3	0.19	204.31	8.28	56.76	4.89	0.34	4.89
Citrate 4	0.5	131.22	8.28	33.64	4.89	0.58	4.89
Citrate 5	0.42	69.77	8.28	21.01	4.89	0.86	4.89
Heparin 1	0.16	10.36	8.28	4.62	4.89	1.86	4.89
Heparin 2	0.87	46.14	8.28	11.79	4.89	5.80	4.89
Heparin 3	0.77	6.45	8.28	2.90	4.89	1.24	4.89
Heparin 4	0.70	3.92	8.28	2.36	4.89	1.58	4.89
Heparin 5	0.69	12.04	8.28	5.27	4.89	2.09	4.89
PBS 1	0.92	0.14	9.33	1.74	7.21	0.47	7.21
PBS 2	0.98	0.12	9.33	0.18	7.21	0.16	7.21
PBS 3	0.94	0.66	8.68	3.89	5.74	0.46	5.74

Pearson's correlation coefficient ρ, Mandel's test as well as Lack-of-fit test was calculated to analyze the linearity of sFIDA readout from SiNaP dilution series at a significance level of 99%. For the Mandel-test H_0 assumes no significant difference between the residual variances. For PW < F H_0 is accepted, the calibration function of choice is linear. For the

Lack-of-fit test H_0 assumes that the applied model is appropriate, lack of fit occurs at LOF > $F_{crit,99\%}$.

Table 2 Summary of analysis on the effect of different anitcoagulants on assay outcome parameters.

Anticoagulant	ρ	CV [%]	LOD [fM]
EDTA	0.94	28	16
citrate	0.37	39	19
heparin	0.64	67	34
PBS	0.94	51	27

The assay outcome was evaluated by means of three parameters: the linearity of the sFIDA readout as a function of applied Aβ-SiNaP concentration (mean Pearson's correlation coefficient ρ), the mean coefficient of variation (CV) as well as the mean limit of detection (LOD).

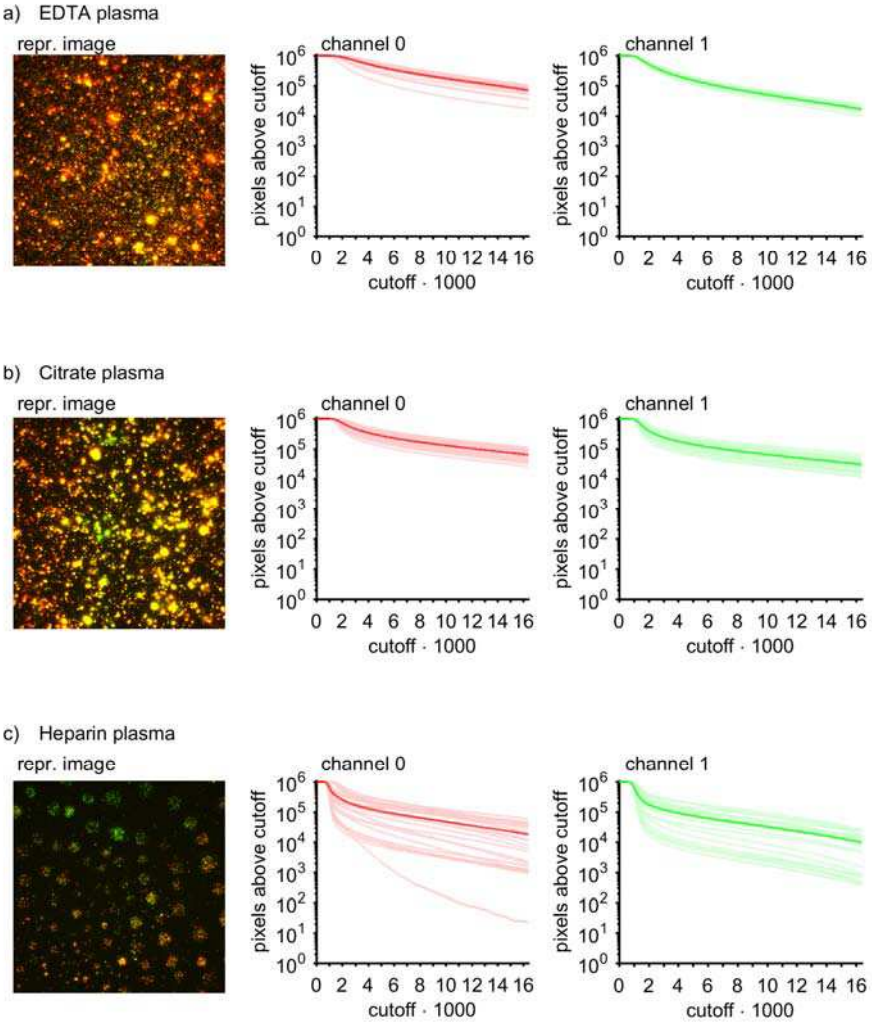

Figure 1 Representative images and cumulative histograms for 1 pM Aβ-SiNaP spiked in EDTA, citrate and heparin plasma.

1 pM Aβ-SiNaP was spiked in blood plasma treated with different anticoagulants from a single donor and subsequently applied to sFIDA assay. A representative image as a composition of channel 0 (exc.: 635 nm, em.: 705 nm) and channel 1 (exc.: 488 nm, em.: 525 nm) is given for (a) EDTA, (b) citrate and (c) heparin-treated plasma, respectively (left hand), as well as cumulative intensity histograms for channel 0 (middle) and channel 1 (right hand). Cumulative histograms for single images are depicted in light color whereas the mean cumulative histogram is depicted in dark color. The variation in intensity distribution between the images is higher for heparin compared to EDTA and citrate.

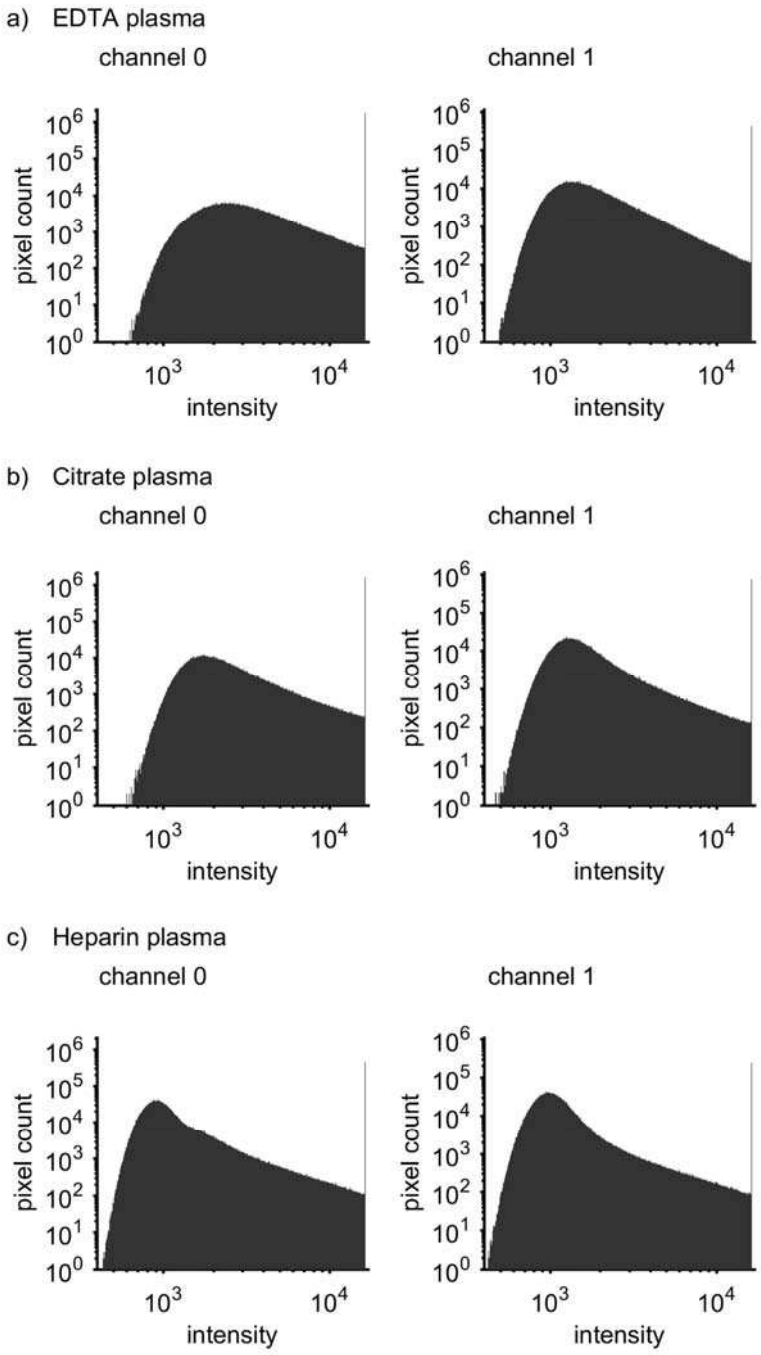

Figure 2 Intensity distribution for images obtained from 1 pM Aβ-SiNaPs spiked in EDTA, citrate and heparin plasma following sFIDA assay.

For channel 0 (exc.: 635 nm, em.: 705 nm) the major peak in intensity distribution for EDTA is approximately at 2400, for citrate at 1700 and for heparin plasma at 900 on a 14-bit grayscale, and for channel 1 (exc.: 488 nm, em.: 525 nm) at approximately 1300, 1300 and 1000, respectively. For channel 0 the major peak is approximately at 2400, for citrate at 1700 and for heparin plasma at 900 on a 14-bit grayscale, and for channel 1 at approximately 1300, 1300 and 1000, respectively.

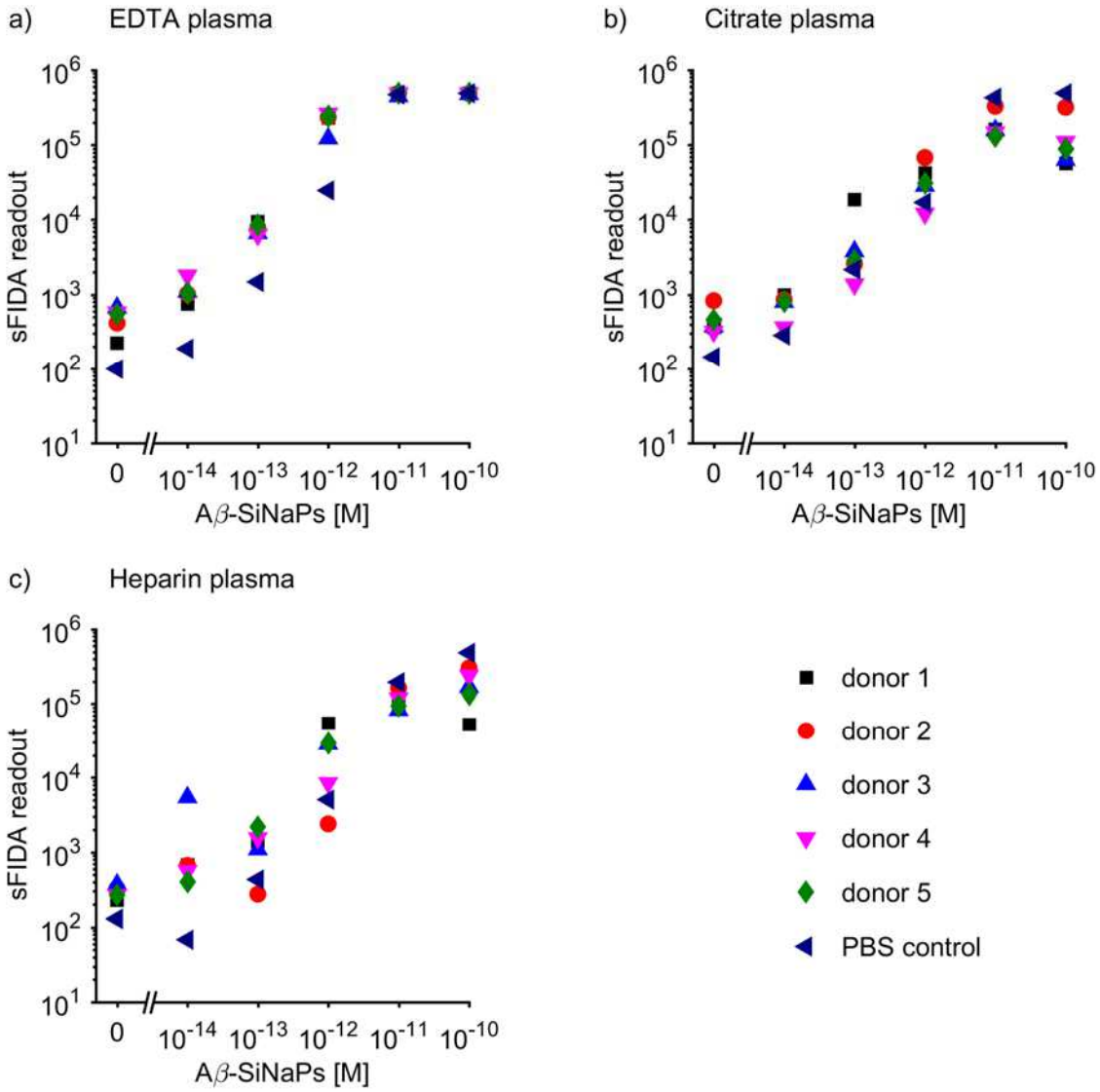

Figure 3 sFIDA readout for Aβ-SiNaPs spiked in EDTA, citrate and heparin plasma from five individual donors as well as in PBS.

Aβ-SiNaPs were serially diluted to 100 pM, 10 pM, 1 pM, 100 fM and 10 fM. As negative controls, non-spiked plasma samples were used (respective 0 M Aβ-SiNaP data points). Black rectangular symbols represent the sFIDA readout for donor 1, red circular symbols for donor 2, blue up-top triangular symbols for donor 3, magenta down-top triangular symbols for donor 4, green rhombical symbol for donor 5 and dark blue left-top triangular symbols for PBS control.

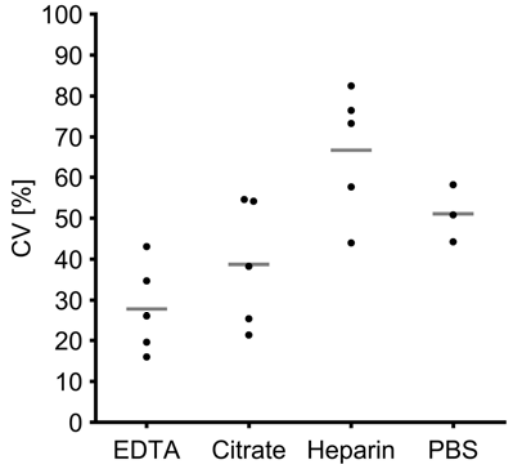

Figure 4 Coefficient of variation (CV) of sFIDA measurements for Aβ-SiNaPs diluted in EDTA, citrate and heparin plasma from five individual human donors.

The mean coefficient of variation (CV[%]) for the sFIDA readout was obtained for Aβ dilution series spiked in plasma samples from five different donors. The CV[%] was calculated as the standard deviation weighted by the mean sFIDA readout. The lowest and highest mean LOD is gained from EDTA and heparin treated blood plasma, respectively.

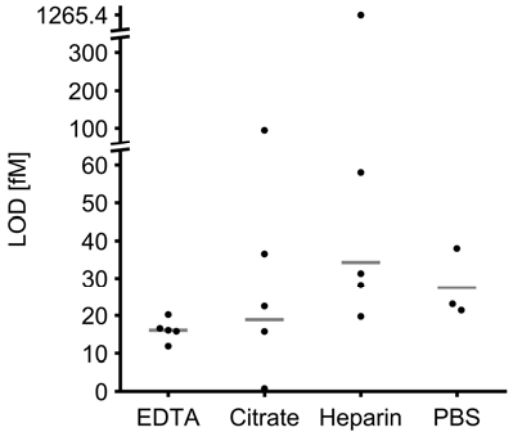

Figure 5 Limit of detection (LOD) from sFIDA measurements of Aβ-SiNaPs spiked in EDTA, citrate and heparin plasma from five donors as well as in PBS.

The mean limit of detection (LOD) for Aβ-SiNaPs spiked in blood plasma was obtained for six replicate measurements of each dilution series in samples from five different donors. The LOD was calculated from the sFIDA readout from the respective negative control plus three times the standard deviation. The lowest mean LOD of 16 fM was obtained for Aβ-SiNaPs spiked in EDTA plasma followed by 19 fM (incl. outlier: 34 fM) for citrate, 27 fM for PBS and 34 fM (incl. outlier: 280 fM) for heparin.

3 Discussion

Amyloid plaques are considered one of the major pathological hallmarks of Alzheimer's disease. The role of Aβ in AD pathology is well described in the amyloid cascade hypothesis, which states that Aβ plays a crucial role in the disease development and progression. For a long time, Aβ fibrils were believed to cause neuronal death and thus cognitive deficits. However, several studies have shown a poor correlation between disease progression and amount of aggregated Aβ. Moreover, amyloid plaques were found in brains of older individuals without any symptoms. These findings triggered the formulation of the theory for neurotoxicity of small soluble Aβ species rather than fibrils. Starting in the nineties, a large number of studies showed increased neurotoxicity of oligomers compared to fibrils and the evidence continues to grow. The size of toxic Aβ assemblies consisting of 3 to 24 monomers was estimated by AFM, however, neurotoxicity of dimers and higher molecular weight (HMW) oligomers has also been reported. Further insights on morphology and certain size of pathologic Aβ species remain to be elucidated [87].

Based on these findings, oligomeric Aβ has become a target molecule as a potential biomarker. Several approaches have been developed for the detection of oligomeric Aβ including method of seeded polymerization combined with FCS, oligomer specific ELISA which use either conformational antibodies or the same Aβ specific antibody for capturing and detection, nanotechnologies and FRET combined with flow cytometry as well as the sFIDA assay used in this study. The results on Aβ detection and quantification attained by these methods are inconsistent. Several reasons can be discussed regarding this issue. Firstly, different Aβ species are detected by different methods such protofibrils or HMW oligomer specific ELISAs [88, 89]. Secondly, BSA which is used in some studies as a blocking buffer may interfere with Aβ detection, since it has been shown that BSA binds Aβ [60]. Thirdly, an issue that has been discussed for ELISAs is human anti-mouse antibodies (HAMAs) which may be present in 10 to 40 % of human sam-

ples. These heterophilic antibodies may cross-link capture and detection antibodies and thus produce a false positive signal [90, 91]. Fourthly, the collection and pretreatment of CSF or plasma samples may play a crucial role for Aβ detection. Aβ is known to bind to plastic, thus the choice of tube material for samples collection needs to be standardized in respect to possible Aβ loss due to Aβ interactions with the material [92]. Fifthly, several studies report higher Aβ levels in EDTA plasma compared to citrate and heparin [93, 94]. These findings emphasize the importance to establish standardized protocols for sample handling and treatment prior to Aβ oligomer detection.
Furthermore, one major deficiency of research on Aβ oligomer concentration in body fluids is the absence of a reliable calibration standard, which would allow inter- and intra-assay comparability and calibration of the assays. In following, currently used standards and their characteristics are reviewed and compared with stabilized CB oligomers and Aβ-SiNaP presented in this study.

3.1 Literature review of published standards

3.1.1 Aβ derived diffusible ligands (ADDLs)

In 1998, Lambert *et al.* have presented a study on neurotoxicity of oligomeric Aβ species referred to as Aβ-derived diffusible ligands (ADDLs) [83]. They reported that ADDLs are a soluble and highly toxic Aβ species. Three protocols were proposed for preparation of soluble and fibril-free ADDLs. Aβ_{1-42} was incubated 1. with clusterin which acted as chaperone for Aβ misfolding, 2. in cold F12 medium and 3. in 37 °C brain slice culture medium. ADDLs prepared in F12 medium were used as standard reference in several studies for Aβ oligomer quantification in body fluids. Their characterization by atomic force microscopy (AFM) revealed globular structures of approximately 4.8 to 5.7 nm along the z-axis. Nondenaturating electrophoresis showed oligomeric species with predominant size of 27 kDa and a weaker band at 17 kDa. Similar sizes of 22 kDa and 17 kDa were obtained by Western blot. The authors stated the stability of ADDLs for at least 24 h.
In the following three completely different methods for Aβ oligomer quantification are described, where the ADDLs prepared in F12 medium were used for assay calibration.

In 2004, Georganopoulu *et al.* measured 30 CSF samples from AD patients and healthy individuals using an ultrasensitive bio-barcode assay [73]. They were able to distinguish AD samples from age-matched non-demented controls. Here, magnetic microparticles (MMP) coated with ADDL specific monoclonal antibody bind to ADDLs, which are then added to gold nanoparticles (AuNP) modified with DNA and an ADDL specific polyclonal antibody. Using a magnet the sandwich complexes of MMP-ADDL-AuNP are separated from the sample and the DNA is released from the complex. The barcode DNA is then quantified by scanometric detection method. The authors reported a correlation of the assay results with the concentration of applied ADDLs with a limit of detection of approximately 100 aM. At concentrations above 500 fM the linearity of the assay shifted to a plateau.

In 2007, Santos *et al.* reported a high reliability and reproducibility of a method for Aβ oligomer quantification in 174 CSF samples of non-demented individuals based on fluorescence resonance energy transfer (FRET) combined with flow cytometry [75]. Here, Aβ samples are incubated with Aβ specific antibodies labeled with two different fluorescent dyes: a donor and an acceptor. Only if the two detection antibodies are closer than 10 nm to each other (bind to the same oligomer) the energy transfer from a donor to an acceptor molecule can take place upon excitation of the donor molecule and emission of acceptor molecule is detected by flow cytometry. For assay calibration with ADDLs, they reported a poor reproducibility of the measurements due to instability of the prepared oligomers and used fibrils instead as reference standard. The detection limit of the assay was in the femtomolar range of monomer concentration. The determination was based on approximation of an average fibril size from several hundreds to thousands of monomers.

In 2014, Savage *et al.* reported 80 % sensitivity and 88 % specificity for differentiating 63 AD patients from 54 healthy controls by their CSF samples in an oligomer specific two-site ELISA using Erenna platform [72]. In this flow-based detection method, paramagnetic particles coated with monoclonal oligomer specific antibody (MP) bind to Aβ. Upon a magnetic bed MPs are retained while unbound material is removed. After addition of detection antibody, MP-Aβ-antibody complexes are detected on the Erenna instrument. Characteristics of synthetic oligomers used for the calibration revealed a HMW species enriched mixture with sizes ranging from 310 to 7700 kDa. The limit of detection for Aβ oligomers in human CSF was 0.09 pg/ml. The authors evaluated the used standard as a "dynamic mixture of oligomers and monomers" which, however, did not show any "significant change after prolonged storage at -80 °C".

In 2002, Dahlgren *et al.* demonstrated that oligomers are 10-fold more toxic than fibrils and 40-fold more toxic than monomeric Aβ [85]. For this study, Aβ oligomers were prepared according to the following protocol: solving of Aβ in HFIP, vacuum drying and resuspension in DMSO preceded the dilution in F12 medium. AFM measurements revealed globular structures with a size of approximately 2 to 5 nm in z-height indicating a molecular mass range from 10 to 100 kDa. The authors report heterogeneous oligomer size distribution by AFM but absence of fibrils and large aggregates.
The same protocol was used for standard preparation by Fukumoto *et al.* to calibrate a HMW oligomer specific ELISA [89]. Significant higher Aβ levels were detected in 25 AD or MCI CSF samples compared to 25 age-matched controls. Here, the same Aβ specific monoclonal antibody was used as capture and detection antibody. Characterization of the standard reference by immunoblotting revealed an average mass of majority of Aβ oligomer species of 50 kDa, ranging from 40 to 70 kDa. Taking into consideration that the solution may contain not only oligomers, but also protofibrils, the authors refer to the prepared oligomers as "parent" oligomer mixture.

In the same year of 2002, in his article W. Klein discussed the neurotoxicity mechanism of ADDLs and presented a slightly different protocol for preparation of ADDLs in comparison to Dahlgreen *et al.* [84]. Aβ oligomer characteristics by AFM and SDS-PAGE revealed heterogeneity of the prepared Aβ species, indicating presence of trimers to 24-mers with an average molecular weight of 108 kDa. Oligomer stability for 24 h at 1 μM and 37 °C and absence of protofibrils were reported for the obtained Aβ species. However, the authors emphasize an eventual shift from tetramers to 12-24-mers.
Zhou *et al.* prepared oligomers according to the procol proposed by W. Klein to calibrate a sandwich-ELISA for the detection of amyloid-β oligomers in plasma. In their study, they investigated 44 plasma samples from AD patients and 22 from control donors. They were able to differentiate between samples from AD patients and non-demented controls using an oligomer specific detection antibody which binds LMW oligomers between 10 to 18 kDa and HMW species ranging from 50 kDa to >150 kDa. Western blot analysis of synthetic Aβ species used as standard revealed oligomers with approximately 10, 16 and 20 kDa indicating presence of predominantly dimers and pentamers.

3.1.2 Multimers and oligomer enriched samples

Two different groups used similar oligomer preparation to calibrate two distinct methods for Aβ oligomer detection in CSF [70, 74]. In both studies, synthetic Aβ was dissolved in DMSO prior to dilution and incubation in PBS. None of the groups presented characteristics of the obtained Aβ species.
However, Pietschke *et al.* refer to the prepared Aβ as multimers, thus indicating unknown oligomer composition or/and inhomogeneous size distribution of the Aβ species [74]. They presented the detection of single amyloid β aggregates in CSF of AD patients using the process of seeded polymerization in combination with FCS. Based on stronger signals obtained for Aβ aggregates in CSF from AD patients, 15 AD samples could be differentiated from 19 age-matched controls.
In 2013, Bruggink *et al.* could not detect any differences between CSF samples of AD and healthy individuals [70]. Aβ oligomers were quantified using an ELISA with the same capture and detection antibody. These findings were explained by LMW oligomer (10 to 25 kDa) specificity of the method. The limit of detection was 2.2 pg/mL, calculated for synthetic oligomers prepared as described above to which the authors refer as "oligomer-enriched" samples.

3.1.3 Aβ dimers

A different approach for preparation of standard molecules is the coupling of two antigen molecules via a disulfide bond. Two studies presented their results on Aβ oligomer detection in body fluids using these particular molecules.
In 2009, W. Xia *et al.* reported the detection of Aβ oligomers and the correlation of Aβ monomer with oligomer concentrations in plasma of 36 AD patients and 10 control donors using a sandwich-ELISA, where the same N-terminal antibody was used for capturing and detection of the target [86]. Also a decrease in Aβ monomer and oligomer levels in plasma was shown over a 1- to 2-year period in AD patients. For assay calibration, synthetic Aβ_{1-40}Ser26Cys was cross-linked via disulfide bridges by atmospheric oxidation in ammonium bicarbonate for four days followed by a disassembly of aggregates by incubation of the cross-linked dimer in guanidine hydrochloride and TRIS hydrochlorid. Homogeneous size distribution was achieved by SEC separation of dimers from monomers

and other Aβ species.
The same standard molecules were used by Esparza *et al.* for the development of a single molecule counting ELISA for Aβ oligomer detection in aqueous cortical lysates and CSF, where the same N-terminal antibody was used for capturing and detection of Aβ [69]. After washing to remove unbound antibodies, the detection antibody is eluted and measured on the Erenna instrument by spot illumination and single photon count. With this assay, the authors demonstrated a correlation between Aβ oligomer concentration and plaque deposits in frontal cortex samples from AD patients, but could not detect Aβ oligomers in CSF samples. The concentration of detected Aβ oligomers was calculated in units of dimer equivalents using the calibration curve. An LOD of 1.56 pg/ml was reported for the assay.

3.1.4 Multiple antigen peptides (MAPs)

Another approach for preparing reference standards is the construction of multiple antigen peptides (MAPs). Using this technique, desired epitopes are linked to a core branching molecule. In 2012, T. Kasai *et al.* published the development of a calibration standard for the oligomer specific single antibody sandwich-ELISA (SAS-ELISA described by Fukumoto *et al.* [89]) [95]. The amine groups of a lysine core were maleimide-linked to the N-terminus of the monomeric epitope. As epitope, a linear peptide was chosen, consiting of Aβ_{1-10} at C-terminus and an N-terminal 'linker sequence' CGGGSG. An 8-MAP and a 16-MAP were tested for their usability as a standard. The calibration curve obtained from the measurements with 16-MAP was reported to cover the concentration range of Aβ oligomers detected in CSF, serum and plasma. Stability of 16-MAPS was reported for at least two freeze-thaw cycles. Intra- and inter-assay variability of 10 %, determined by the coefficient of variation, indicates usability of 16-MAP as a stadard for longitudinal studies.
In 2013, T. Kasai *et al.* detected HMW Aβ oligomers in CSF and serum samples from healthy individuals using SAS-ELISA [71]. They reported a correlation of Aβ oligomer levels in CSF and serum samples in non-demented matched individuals, but no correlation of total Aβ_{1-42} and Aβ_{1-40} between CSF and serum. The newly developed standard 16-MAP for was used for inter- and intra-assay calibration.

3.2 Standards presented in this study

3.2.1 Application of stabilized Aβ oligomers in the sFIDA

Stabilized Aβ oligomers obtained from Crossbeta (CB oligomers) were serially diluted in PBS, CSF and EDTA plasma fraction and measured in the sFIDA assay. According to the manufacturer, CB oligos exhibit following characteristics: homogeneous population with a hydrodynamic radius of 12 nm as determined by dynamic light scattering (DLS), >85 % β-sheet content as measured by circular dichroism (CD), predominantly monomer-free oligomer mixture as determined by AFM. One oligomer consists of approximately 220 Aβ_{1-42} monomers. The stability of CB oligomers was demonstrated in PBS for 56 days, in F12 medium and in HEPES buffer for 7 days at 4 °C, and in F12 medium and HEPES buffer for 24 h at 37 °C [96]. Correlation of the sFIDA readout with CB oligomer concentration was observed for all matrices down to femtomolar range. LODs obtained for CB oligomers were 22 fM in PBS, 18 fM in CSF and 14 fM in plasma fraction.

3.2.2 Synthesis and characterization of Aβ-SiNaP

Furthermore, this study presents the synthesis, characterization and performance of Aβ-coated silica nanoparticles (Aβ-SiNaP) in sFIDA assay. Aβ-SiNaP were prepared by biofunctionalization of SiNaP synthesized according to the Stöber process. The diameter of bare SiNaP of approximately 24 nm was determined by transmission electron microscopy (TEM). SiNaP were silanized with APTES to coat the surface with primary amine groups. Subsequent reaction with succinic anhydrid resulted in carboxylated SiNaP, which were activated by EDC/NHS for the final covalent coupling of Aβ_{1-42} to the particle surface. The successful coupling was demonstrated by Fourier transform infrared spectroscopy (FTIR). The concentration of Aβ_{1-42} on the surface of SiNaP was determined by BCA assay as 24 μg/ml in 1 mg/ml SiNaP solution. This concentration corresponds to 44 peptides per 24 nm SiNaP.
Aβ-SiNaP were firstly tested in water and CSF. Correlation between SiNaP concentration and sFIDA readout was shown down to femtomolar range. sFIDA measurements

on stability of Aβ-SiNaP revealed stability over a period of four months when Aβ-SiNaP were stored in water at 4 °C.

3.2.3 Application of Aβ-SiNaP in the sFIDA assay

Additionally, Aβ-SiNaP were used to determine the most suitable anti-coagulant for Aβ oligomer detection in plasma. The batch of Aβ-SiNaP used in this study had following characteristics: 30 nm of SiNaP core (as determined by TEM) and 36 Aβ molecules per nanoparticle (as determined by BCA assay). A correlation of Aβ-SiNaP concentration with sFIDA readout was shown in PBS, EDTA-, citrate- and heparin-plasma. Based on calculated linearity of the correlation between applied concentrations of SiNaP and the determined sFIDA readouts, coefficient of variation and limit of detection, the results showed that EDTA is the anti-coagulant of choice for quantification of Aβ oligomer levels in human plasma using the sFIDA assay. LOD obtained for Aβ-SiNaP spiked in EDTA plasma was 2.6 pg/ml based on Aβ monomer concentration coated to SiNaP.

3.3 Comparison of presented Aβ species as reference standards

In order to attain more consistency in results for Aβ oligomer quantification and to allow comparability of different quantification methods, a reliable standard is required which resembles characteristics of Aβ oligomers. Furthermore, this standard should be stable for a certain period of time to ensure assay reproducibility in longitudinal intra- and inter-assay studies.

The reviewed methods for Aβ oligomer preparation offer several standards for assay calibration such as ADDLs, multimers and oligomer-enriched samples, Aβ dimers and 16-MAPs. In our study, stabilized CB oligomers and $A\beta_{1-42}$-coated SiNaP were proposed as suitable standards for the Aβ oligomer detection in the sFIDA assay.

ADDLs are the most commonly used standard for assay calibration. However, discussed studies present different characteristics of prepared Aβ oligomers. The size of oligomeric

Aβ species prepared accordingly to different protocols varies from 10 to 7700 kDa. Even if the same protocol for oligomer preparation was used, significant differences in oligomer characteristics have been reported by different groups. For example, ADDLs prepared according to the protocol proposed by Lambert *et al.* have sizes between 17 and 27 kDa according to Lambert *et al.*, whereas Savage *et al.* report a size distribution in the range between 310 to 7700 kDa. The stability of at least 24 h reported by Lambert *et al.* was not achieved by Santos *et al.*. Instead, Santos *et al.* pointed out poor reproducibility obtained with prepared oligomers, which were therefore replaced by fibrils. Aβ fibrils exhibit higher stability compared to oligomers, but they are significantly larger. In contrast, although Savage *et al.* refer to prepared Aβ oligomers as 'dynamic mixture', they report stability after prolonged storage at -80 °C.
Also, for ADDLs prepared according to the same protocol, Dahlgreen *et al.* report oligomer size distribution between 10 and 100 kDa, whereas Fukumoto *et al.* published the size range from 40 to 70 kDa.
Similarly, the oligomer preparation proposed by Klein, revealed a heterogeneous mixture of trimers to 24-mers in his study, whereas Zhou *et al.* reported predominantly dimers and pentamers in their oligomer mixture prepared by the same protocol. Often, information on standards and especially their stability is insufficient. Studies by Pietschke *et al.* and Bruggink *et al.* lack any oligomer characterization. However, their description of prepared Aβ mixtures as multimers and oligomer-enriched samples, respectively, indicates heterogeneous size distribution.
On the one hand, the heterogeneity of Aβ oligomer mixtures may be interpreted as advantage for quantification of oligomeric Aβ species in body fluids, since the size distribution of endogenous Aβ oligomers is not exactly known, but supposed to vary over a wide range. However, the dynamic equilibrium between the different Aβ species often results in poor reproducibility over time. Moreover, if the composition of oligomer mixture differs for each preparation according to the same protocol, a standard is required, which is simple and reproducible in preparation. This evidence indicates that Aβ oligomers do not represent a reliable standard for assay calibration.

In contrast to ADDLs, $A\beta_{1-40}$ dimers separated by SEC have a defined size and morphology. The stability of these molecules is guaranteed by cross-linking and by use of $A\beta_{1-40}$ which is less prone to aggregation compared to $A\beta_{1-42}$. Due to the very small size, these Aβ species are suitable standards only for quantitation of LMW oligomers.

Another issue is that the dimers consist of $A\beta_{1-40}$, whereas the main component of endogenous Aβ oligomers is $A\beta_{1-42}$ with eventually a small amount of $A\beta_{1-40}$, since $A\beta_{1-40}$ was found in amyloid plaques. Thus, the dimers do not fulfill the requirements of a universally applicable standard, either.

Finally, the 16-MAPs presented by T. Kasai *et al.* seem to be the most promising candidates among the discussed standards. 16-MAPs provide a defined size and a known number of epitopes. The authors report stability against freeze/thaw cycles as well as inter- and intra-assay variability of less than 10 %. These characteristics make them a reliable standard.

The stabilized CB oligomers consisting of 220 Aβ monomers measured in the sFIDA assay in this study are a suitable standard for detection of HMW oligomers. CB oligomers do not contain Aβ monomers and are stable for 56 days in PBS and 1 week in F12 medium or HEPES at 4 °C and 24 h in F12 medium or HEPES buffer at 37 °C, thus providing much higher stability than the discussed ADDLs. However, these standards do not resemble LMW oligomers such as trimers to 24-mers which are considered the most toxic species in AD pathology.

Aβ-SiNaP which were synthesized, characterized and validated in the sFIDA assay within the scope of this study, revealed pronounced advantages compared to Aβ oligomers and dimers and share some similarities with 16-MAPs. Both Aβ-SiNaP and 16-MAPs are particles with defined sizes. Most prominent difference between them and other standards is flexibility in number and choice of epitopes. Thus, a synthesis of hybrid standards consisting of, for example $A\beta_{1-42}$ and tau, which can be used in studies for the exploration of hybrid aggregates as biomarkers, is possible for both standards. The reported stability of four months for Aβ-SiNaP in water at 4 °C and stability of 16-MAPs against freeze/thaw cycles make both standards excellent candidates for long-term studies.
Moreover, it is possible for Aβ-SiNaP to vary the size of the silica cores by adjusting the reaction conditions in the Stöber synthesis from nano- to micrometer range. The spherical geometry of Aβ-SiNaP allows an even distribution of Aβ epitopes compared to the

branched Aβ epitopes in MAPs. Thus, the introduction of higher dimension hierarchies minimizes sterical effects which might decrease the accessibility of Aβ epitopes on the sphere surface. The shortcomings of Aβ-SiNaP presented in this study is the fact that the size of silica cores and number of Aβ epitopes might slightly vary batch-to-batch. In contrast, size and number of epitopes in 16-MAPs produced by custom peptide synthesis is always exactly defined. Also, Aβ-SiNaP with approximately 40 epitopes do not resemble LMW oligomers, and are more suitable for the detection of larger soluble Aβ species. However, further validation experiments for both standards are required to ensure inter- and intra-assay comparability.

Standards reviewed and described in this study differ strongly in their characteristics such as size distribution, composition, morphology and stability. Taking into consideration that a reliable standard ideally represents the analyte in its size, properties and interaction with the matrix where it is measured, it can be concluded, that ADDLs resemble the dynamic nature of Aβ oligomers best, cross-linked $A\beta_{1-40}$-dimers are suitable for detection of very small Aβ oligomers, but do not represent the interaction of $A\beta_{1-42}$ with the matrix, 16-MAPs are in the size range with toxic 3 to 24-mers, stabilized CB oligomers and Aβ-SiNaP resemble HMW oligomers. The characteristics of the standard molecules should be taken into account for prospective applications which depend on the technique used for AD diagnosis.

Bibliography

[1] A. Alzheimer. über eine eigenartige erkrankung der hirnrinde. *Centralblatt fur Nervenheilkunde Psychiatrie*, 30:177–179, 1907.

[2] T. G. Beach, S. E. Monsell, L. E. Phillips, and W. Kukull. Accuracy of the clinical diagnosis of alzheimer disease at national institute on aging alzheimer's disease centers, 2005–2010. *Journal of Neuropathology and Experimental Neurology*, 71(4):266–273, 2012.

[3] E. Karran, M. Mercken, and B. D. Strooper. The amyloid cascade hypothesis for alzheimer's disease: an appraisal for the development of therapeutics. *Nature Reviews Drug Discovery*, 10:698–712, 2011.

[4] S. W. Pimplikar. Reassessing the amyloid cascade hypothesis of alzheimer's disease. *The International Journal of Biochemistry & Cell Biology*, 41(6):1261 – 1268, 2009.

[5] H. Hampel and S. Lista. Alzheimer disease: From inherited to sporadic ad—crossing the biomarker bridge. *Nature Reviews Neurology*, 8:598–600, 2012.

[6] K. Blennow. Csf biomarkers for mild cognitive impairment. *Journal of Internal Medicine*, 256(3):224–234, 2004.

[7] K. Blennow, H. Hampel, M. Weiner, and H. Zetterberg. Cerebrospinal fluid and plasma biomarkers in alzheimer disease. *Nature Reviews Neurology*, 6:131–144, 2010.

[8] https://knowingneurons.files.wordpress.com/2012/11/brainatrophy_600.jpg.

[9] http://t.jwwb.nl/4xlayjxyr_dkg6mdpn-ovaid8iu=/382x0/http://f.jwwb.nl/public/0/5/2/braininjury-explanation/alz-cells.large.jpg.

[10] P. Scheltens, F. Barkhof, D. Leys, E. C. Wolters, R. Ravid, and W. Kamphorst. Histopathologic correlates of white matter changes on mri in alzheimer's disease and normal aging. *Neurology*, 45(5):883–888, 1995.

[11] N. C. Fox and P. A. Freeborough. Brain atrophy progression measured from registered serial mri: Validation and application to alzheimer's disease. *Journal of Magnetic Resonance Imaging*, 7(6):1069–1075, 1997.

[12] G. B. Frisoni, N. C. Fox, C. R. Jack Jr, P. Scheltens, and P. M. Thompson. The clinical use of structural mri in alzheimer disease. *Nature Reviews Neurology*, 6:67–77, 2010.

[13] K. L. Double, G. M. Halliday, J. J. Krill, J. A. Harasty, K. Cullen, W. S. Brooks, H. Creasey, and G. A. Broe. Topography of brain atrophy during normal aging and alzheimer's disease. *Neurobiology of Aging*, 17(4):513 – 521, 1996.

[14] N. Andreasen and K. Blennow. Csf biomarkers for mild cognitive impairment and early alzheimer's disease. *Clinical Neurology and Neurosurgery*, 107(3):165 – 173, 2005.

[15] K. Blennow and H. Zetterberg. Cerebrospinal fluid biomarkers for alzheimer's disease. *Journal of Alzheimer's disease : JAD*, 18(2):413—417, 2009.

[16] D. R. Thal, U. Rüb, M. Orantes, and H. Braak. Phases of aβ-deposition in the human brain and its relevance for the development of ad. *Neurology*, 58(12):1791–1800, 2002.

[17] E. Portelius, N. Bogdanovic, M. K. Gustavsson, I. Volkmann, G. Brinkmalm, H. Zetterberg, B. Winblad, and K. Blennowfox. Mass spectrometric characterization of brain amyloid beta isoform signatures in familial and sporadic alzheimer's disease. *Acta Neuropathologica*, 120(2):185–193, 2010.

[18] H. Crystal, D. Dickson, P. Fuld, D. Masur, R. Scott, M. Mehler, J. Masdeu, C. Kawas, M. Aronson, and L. Wolfson. Clinico-pathologic studies in dementia: Nondemented subjects with pathologically confirmed alzheimer's disease. *Neurology*, 38:1682–1687, 1988.

[19] I. R. A. Mackenzie, R. S. McLachlan, C. S. Kubu, and L. A. Miller. Prospective neuropsychological assessment of nondemented patients with biopsy proven senile plaques. *Neurology*, 46(2):425–429, 1996.

[20] J. Näslund, V. Haroutunian, R. Mohs, K. L. Davis, P. Davies, P. Greengard, and J. D. Buxbaum. Correlation between elevated levels of amyloid β-peptide in the brain and cognitive decline. *JAMA*, 283(12):1571–1577, 2000.

[21] C. Bancher, C. Brunner, H. Lassmann, H. Budka, K. Jellinger, G. Wiche, F. Seitelberger, I. Grundke-Iqbal, K. Iqbal, and H. M. Wisniewski. Accumulation of abnormally phosphorylated τ precedes the formation of neurofibrillary tangles in alzheimer's disease. *Brain Research*, 477(1):90 – 99, 1989.

[22] A. C. Alonso, I. Grundke-Iqbal, and K. Iqbal. Alzheimer's disease hyperphosphorylated tau sequesters normal tau into tangles of filaments and disassembles microtubules. *Nature Medicine*, 2:783 – 787, 1996.

[23] H. A. Pearson and C. Peers. Physiological roles for amyloid β peptides. *The Journal of Physiology*, 575(1):5–10, 2006.

[24] J. E. Morley, S. A. Farr, W. A. Banks, S. N. Johnson, K. A. Yamada, and L. Xu. A physiological role for amyloid-β protein: Enhancement of learning and memory. *Journal of Alzheimer's Disease*, 19(2):441–449, 2010.

[25] M. d. C. Cárdenas-Aguayo, M. d. C. Silva-Lucero, B. Jiménez-Ramos M. Cortes-Ortiz, L. Gómez-Virgilio, G. Ramírez-Rodríguez, E. Vera-Arroyo, R. Fiorentino-Pérez, U. García, J. Luna-Muñoz, and M. A. Meraz-Ríos. Physiological role of amyloid beta in neural cells: The cellular trophic activity. *Neurochemistry*, pages 1–25, 2014.

[26] M. Shoji, T. E. Golde, J. Ghiso, T. T. Cheung, S. Estus, L. M. Shaffer, X. D. Cai, D. M. McKay, R. Tintner, and B. Frangione. Production of the alzheimer amyloid beta protein by normal proteolytic processing. *Science*, 258(5079):126–129, 1992.

[27] H.-C. Huang and Z.-F. Jiang. Accumulated amyloid-β peptide and hyperphosphorylated tau protein: Relationship and links in alzheimer's disease. *Journal of Alzheimer's Disease*, 16:15–27, 2009.

[28] S. F. Lichtenthaler. Alpha-secretase cleavage of the amyloid precursor protein: Proteolysis regulated by signaling pathways and protein trafficking. *Current Alzheimer Research*, 9(2):165 – 177, 2011.

[29] L. K. Simmons, P. C. May, K. J. Tomaselli, R. E. Rydel, K. S. Fuson, E. F. Brigham, S. Wright, I. Lieberburg, G. W. Becker, and D. N. Brems. Secondary structure of amyloid beta peptide correlates with neurotoxic activity in vitro. *Molecular Pharmacology*, 45(3):373–379, 1994.

[30] C. J. Pike, A. J. Walencewicz-Wasserman, J. Kosmoski, D. H. Cribbs, C. G. Glabe, and C. W. Cotman. Structure-activity analyses of β-amyloid peptides: Contributions of the β25–35 region to aggregation and neurotoxicity. *Journal of Neurochemistry*, 64(1):253–265, 1995.

[31] G. Bitan, M. D. Kirkitadze, A. Lomakin, S. S. Vollers, G. B. Benedek, and D. B. Teplow. Amyloid β-protein (aβ) assembly: Aβ40 and aβ42 oligomerize through distinct pathways. *PNAS*, 100(1):330–335, 2003.

[32] R. Vassar, B. D. Bennett, S. Babu-Khan, S. Kahn, E. A. Mendiaz, P. Denis, D. B. Teplow, S. Ross, P. Amarante, R. Loeloff, Y. Luo, S. Fisher, J. Fuller, S. Edenson, J. Lile, M. A. Jarosinski, A. L. Biere, E. Curran, T. Burgess, J.-C. Louis, F. Collins, J. Treanor, G. Rogers, and M. Citron. β-secretase cleavage of alzheimer's amyloid precursor protein by the transmembrane aspartic protease bace. *Science*, 286(5440):735–741, 1999.

[33] F. Kamenetz, T. Tomita, H. Hsieh, G. Seabrook, D. Borchelt, T. Iwatsubo, S. Sisodia, and R. Malinow. App processing and synaptic function. *Neuron*, 37(6):925 –

937, 2003.

[34] M. Verma, A. Vats, and V. Taneja. Toxic species in amyloid disorders: Oligomers or mature fibrils. *Annals of Indian Academy of Neurology*, 18(2):138–145, 2015.

[35] L. C. Serpell. Alzheimer's amyloid fibrils: structure and assembly. *Biochimica et Biophysica Acta (BBA) - Molecular Basis of Disease*, 1502(1):16–30, 2000.

[36] S. I. A. Cohen, S. Linse, L. M. Luheshi, E. Hellstrand, D. A. White, L. Rajah, D. E. Otzen, M. Vendruscolo, C. M. Dobson, and T. P. J. Knowlesa. Proliferation of amyloid-β-42 aggregates occurs through a secondary nucleation mechanism. *PNAS*, 110(24):9758–9763, 2013.

[37] C. Haass and D. J. Selkoe. Soluble protein oligomers in neurodegeneration: lessons from the alzheimer's amyloid bold beta-peptide. *Nature Reviews Molecular Cell Biology*, 8:101–112, 2007.

[38] J. P. Cleary, D. M. Walsh, J. J. Hofmeister, G. M. Shankar, M. A. Kuskowski, D. J. Selkoe, and K. H. Ashe. Natural oligomers of the amyloid beta protein specifically disrupt cognitive function. *Nature Neuroscience*, 8:79–84, 2004.

[39] Dennis J. Selkoe. Soluble oligomers of the amyloid β-protein impair synaptic plasticity and behavior. *Behavioural Brain Research*, 192(1):106 – 113, 2008. Biobehavioural Plasticity.

[40] R. A. Armstrong. The pathogenesis of alzheimer's disease: A reevaluation of the "amyloid cascade hypothesis". *International Journal of Alzheimer's Disease*, 2011:6 pages, 2011.

[41] C. Reitz. Alzheimer's disease and the amyloid cascade hypothesis: A critical review. *International Journal of Alzheimer's Disease*, 2012:11 pages, 2012.

[42] M. F. Folstein, S. E. Folstein, and P. R. McHugh. "mini-mental state": A practical method for grading the cognitive state of patients for the clinician. *Journal of Psychiatric Research*, 12(3):189–198, 1975.

[43] M. S. Huckman, J. H. Fox, and R. G. Ramsey. Computed tomography in the diagnosis of degenerative diseases of the brain. *Seminars in Roentgenology*, 12(1):63 – 75, 1977.

[44] M. J. de Leon, S. H. Ferris, A. E. George, B. Reisberg, I. I. Kricheff, and S. Gershon. Computed tomography evaluations of brain-behavior relationships in senile d dementia of the alzheimer's type. *Neurobiology of Aging*, 1(1):69 – 79, 1980.

[45] N. L. Foster, T. N. Chase, P. Fedio, N. J. Patronas, R. A. Brooks, and G. D. Chiro. Focal cortical changes shown by positron emission tomography. *Neurology*, 33(8), 1983.

[46] K. Herholz. Fdg pet and differential diagnosis of dementia. *Alzheimer Disease & Associated Disorders*, 9(1):6–16, 1995.

[47] P. L. McGeer, H. Kamo, R. Harrop, D. K. Li, H. Tuokko, E. G. McGeer, M. J. Adam, W. Ammann, B. L. Beattie, and D. B. Calne. Positron emission tomography in patients with clinically diagnosed alzheimer's disease. *CMAJ: Canadian Medical Association Journal*, 134(6):597–607, 1986.

[48] R. A. Sperling, J. F. Bates, E. F. Chua, A. J. Cocchiarella, D. M. Rentz, B. R. Rosen, D. L. Schacter, and M. S. Albert. fmri studies of associative encoding in young and elderly controls and mild alzheimer's disease. *J Neurol Neurosurg Psychiatry*, 74(1):44–50, 2003.

[49] R. Sperling. Functional mri studies of associative encoding in normal aging, mild cognitive impairment, and alzheimer's disease. *Annals of the New York Academy of Sciences*, 1097(1):146–155, 2007.

[50] W. E. Klunk, H. Engler, A. Nordberg, Y. Wang, G. Blomqvist, D. P. Holt, M. Bergström, I. Savitcheva, G.-F. Huang, S. Estrada, B. Ausen, M. L. Debnath, J. Barletta, J. C. Price, J. Sandell, B. J. Lopresti, Anders Wall, P. Koivisto, G. Antoni, C. A. Mathis, , and B. Långström. Imaging brain amyloid in alzheimer's disease with pittsburgh compound-b. *Annals of Neurology*, 55(3):306–319, 2004.

[51] J. C. Morris, C. M. Roe, E. A. Grant, D. Head, M. Storandt, A. M. Goate, A. M. Fagan, D. M. Holtzman, and M. A. Mintun. Pittsburgh compound b imaging and prediction of progression from cognitive normality to symptomatic alzheimer disease. *Archives of Neurology*, 66(12):1469–1475, 2009.

[52] M. A. Butters, W. E. Klunk, C. A. Mathis, J. C. Price, S. K. Ziolko, J. A. Hoge, N. D. Tsopelas, B. J. Lopresti, C. F. Reynolds, S. T. DeKosky, and C. C. Meltzer. Imaging alzheimer pathology in late-life depression with pet and pittsburgh compound-b. *Alzheimer Dis Assoc Disord.*, 22(3):261–268, 2008.

[53] S. Lista, F. Faltraco, D. Prvulovic, and H. Hampel. Blood and plasma-based proteomic biomarker research in alzheimer's disease. *Progress in Neurobiology*, 101–102:1 – 17, 2013.

[54] S. Ray, M. Britschgi, C. Herbert, Y. Takeda-Uchimura, A. Boxer, K. Blennow, L. F. Friedman, D. R. Galasko, M. Jutel, A. Karydas, J. A. Kaye, J. Leszek, B. L. Miller, L. Minthon, J. F. Quinn, G. D. Rabinovici, W. H. Robinson, M. N. Sabbagh, Y. T. So, D. L. Sparks, M. Tabaton, J. Tinklenberg, J. A. Yesavage, R. Tibshirani, and T. Wyss-Coray. Classification and prediction of clinical alzheimer's diagnosis based on plasma signaling proteins. *Nature Medicine*, 13:1359 – 1362, 2007.

[55] M. C. Irizarry. Biomarkers of alzheimer disease in plasma. *NeuroRX*, 1(2):226 – 234, 2004. Biomarkers and Surrogates.

[56] H. M. Snyder, M. C. Carrillo, F. Grodstein, K. Henriksen, A. Jeromin, S. Lovestone, M. M. Mielke, S. O'Bryant, M. Sarasa, M. Sjøgren, H. Soares, J. Teeling, E. Trushina, M. Ward, T. West, L. J. Bain, D. W. Shineman, M. Weiner, and H. M. Fillit. Developing novel blood-based biomarkers for alzheimer's disease. *Alzheimer's & Dementia*, 10(1):109 – 114, 2014.

[57] E. S. Oh, J. C. Troncoso, and S. M. Fangmark Tucker. Maximizing the potential of plasma amyloid-beta as a diagnostic biomarker for alzheimer's disease. *Neuro-Molecular Medicine*, 10(3):195–207, 2008.

[58] A. Koudinov, E. Matsubara, B. Frangione, and J. Ghiso. The soluble form of

alzheimer's amyloid β protein is complexed to high density lipoprotein 3 and very high density lipoprotein in normal human plasma. *Biochemical and Biophysical Research Communications*, 205(2):1164 – 1171, 1994.

[59] A. R. Koudinov, T. T. Berezov, A. Kumar, and N. V. Koudinova. Alzheimer's amyloid β interaction with normal human plasma high density lipoprotein: association with apolipoprotein and lipids. *Clinica Chimica Acta*, 270(2):75 – 84, 1998.

[60] A. L. Biere, B. Ostaszewski, E. R. Stimson, B. T. Hyman, J. E. Maggio, and D. J. Selkoe. Amyloid β-peptide is transported on lipoproteins and albumin in human plasma. *Journal of Biological Chemistry*, 271(51):32916–32922, 1996.

[61] Y.-M. Kuo, M. R. Emmerling, H. C. Lampert, S. R. Hempelman, T. A. Kokjohn, A. S. Woods, R. J. Cotter, and A. E. Roher. High levels of circulating aβ42 are sequestered by plasma proteins in alzheimer's disease. *Biochemical and Biophysical Research Communications*, 257(3):787 – 791, 1999.

[62] Y.-M. Kuo, T. A. Kokjohn, W. Kalback, D. Luehrs, D. R. Galasko, N. Chevallier, E. H. Koo, M. R. Emmerling, and A. E. Roher. Amyloid-β peptides interact with plasma proteins and erythrocytes: Implications for their quantitation in plasma. *Biochemical and Biophysical Research Communications*, 268(3):750 – 756, 2000.

[63] R. C. Dodel, Y. Du, C. Depboylu, H. Hampel, L. Frölich, A. Haag, U. Hemmeter, S. Paulsen, S. J. Teipel, S. Brettschneider, A. Spottke, C. Nölker, H. J. Möller, X. Wei, M. Farlow, N. Sommer, and W. H. Oertel. Intravenous immunoglobulins containing antibodies against β-amyloid for the treatment of alzheimer's disease. *J Neurol Neurosurg Psychiatry*, 75:1472–1474, 2004.

[64] W. Q. Qiu, D. M. Walsh, Z. Ye, K. Vekrellis, J. Zhang, M. B. Podlisny, M. R. Rosner, A. Safavi, L. B. Hersh, and D. J. Selkoe. Insulin-degrading enzyme regulates extracellular levels of amyloid β-protein by degradation. *The Journal of Biological Chemistry, 273, 32730-32738*, 273:32730–32738, 1998.

[65] J. J. Kulstad, P. S. Green, D. G. Cook, G. S. Watson, M. A. Reger, L. D. Baker, S. R. Plymate, S. Asthana, K. Rhoads, P. D. Mehta, and S. Craft. Differential modula-

tion of plasma β-amyloid by insulin in patients with alzheimer disease. *Neurology*, 66(10):1506–1510, 2006.

[66] A. D. Watt, K. A. Perez, A. R. Rembach, C. L. Masters, V. L. Villemagne, and K. J. Barnham. Variability in blood-based amyloid-beta assays: the need for consensus on pre-analytical processing. *Journal of Alzheimer's disease : JAD*, 30(2):323—336, 2012.

[67] H. Tammen, I. Schulte, R. Hess, C. Menzel, M. Kellmann, T. Mohring, and P. Schulz-Knappe. Peptidomic analysis of human blood specimens: Comparison between plasma specimens and serum by differential peptide display. *Proteomics*, 5:3414–3422, 2005.

[68] A. S. Funke. Detection of soluble amyloid-beta oligomers and insoluble high-molecular-weight particles in csf: Development of methods with potential for diagnosis and therapy monitoring of alzheimer's disease. *International Journal of Alzheimer's Disease*, 2011:1–8, 2011.

[69] T. J. Esparza, H. Zhao, J. R. Cirrito, N. J. Cairns, R. J. Bateman, D: M. Holtzman, and D. L. Brody. Amyloid-beta oligomerization in alzheimer dementia versus high-pathology controls. *Annals of Neurology*, 73(1):104–119, 2013.

[70] K. A. Bruggink, W. Jongbloed, E. A. L. M. Biemans, R. Veerhuis, J. A. H. R. Claassen, H. B. Kuiperij, and M. M. Verbeek. Amyloid-β oligomer detection by elisa in cerebrospinal fluid and brain tissue. *Analytical Biochemistry*, 433(2):112 – 120, 2013.

[71] T. Kasai, T. Tokuda, M. Taylor, M. Kondo, D. M.A. Mann, P. G. Foulds, M. Nakagawa, and D. Allsop. Correlation of aβ oligomer levels in matched cerebrospinal fluid and serum samples. *Neuroscience Letters*, 551:17 – 22, 2013.

[72] M. J. Savage, J. Kalinina, A. Wolfe, K. Tugusheva, R. Korn, T. Cash-Mason, J. W. Maxwell, N. G. Hatcher, S. J. Haugabook, G. Wu, B. J. Howell, J. J. Renger, P. J. Shughrue, and A. McCampbell. A sensitive aβ oligomer assay discriminates

alzheimer's and aged control cerebrospinal fluid. *The Journal of Neuroscience*, 34(8):2884 –2897, 2014.

[73] D. G. Georganopoulou, L. Chang, J.-M. Nam, C. S. Thaxton, E. J. Mufson, W. L. Klein, and C. A. Mirkin. Nanoparticle-based detection in cerebral spinal fluid of a soluble pathogenic biomarker for alzheimer's disease. *PNAS*, 102(7):2273–2276, 2005.

[74] M. Pitschke, R. Prior, M. Haupt, and D. Riesner. Detection of single amyloid beta-protein aggregates in the cerebrospinal fluid of alzheimer's patients by fluorescence correlation spectroscopy. *Nature Medicine*, 4:832 – 834, 1998.

[75] A. N. Santos, S. Torkler, D. Nowak, C. Schlittig, M. Goerdes, T. Lauber, L. Trischmann, M. Schaupp, M. Penz, F.-W. Tiller, and G. Böhm. Detection of amyloid-β oligomers in human cerebrospinal fluid by flow cytometry and fluorescence resonance energy transfer. *Journal of Alzheimer's Disease*, 11:117–125, 2007.

[76] E. Birkmann, O. Schäfer, N. Weinmann, C. Dumpitak, M. Beekes, R. Jackman, L. Thorne, and D. Riesner. Detection of prion particles in samples of bse and scrapie by fluorescence correlation spectroscopy without proteinase k digestion. *Biological Chemistry*, 387(1):95–102, 2006.

[77] E. Birkmann, F. Henke, N. Weinmann, C. Dumpitak, M. Groschup, A. Funke, D. Willbold, and D. Riesner. Counting of single prion particles bound to a capture-antibody surface (surface-fida). *Veterinary Microbiology*, 123(4):294 – 304, 2007.

[78] S. A. Funke, E. Birkmann, F. Henke, P. Görtz, C. Lange-Asschenfeldt, D. Riesner, and D. Willbold. Single particle detection of aβ aggregates associated with alzheimer's disease. *Biochemical and Biophysical Research Communications*, 364(4):902 – 907, 2007.

[79] S. A. Funke, L. Wang, E. Birkmann, and D. Willbold. Single-particle detection system for aβ aggregates: Adaptation of surface-fluorescence intensity distribu-

tion analysis to laser scanning microscopy. *Rejuvenation Research*, 13(2-3):206–209, 2010.

[80] L. Wang-Dietrich, S. A. Funke, K. Kühbach, K. Wang, A. Besmehn, S. Willbold, Y. Cinar, O. Bannach, E. Birkmann, and D. Willbold. The amyloid-β oligomer count in cerebrospinal fluid is a biomarker for alzheimer's disease. *Journal of Alzheimer's Disease*, pages 1–10, 2012.

[81] R. Jacobson. Principle and methods of validation of diagnostic assays for infectious diseases. *OIE (Ed.), Manual of Diagnostic Tests and Vaccines for Terrestrial Animals (Terrestrial Manual), OIE*, page p15, 2009.

[82] U. Andreasson, A. Perret-Liaudet, L. J. C. van Waalwijk van Doorn, K. Blennow, D. Chiasserini, S. Engelborghs, T. Fladby, S. Genc, N. Kruse, H. Bea Kuiperij, L. Kulic, P. Lewczuk, B. Mollenhauer, B. Mroczko, L. Parnetti, E. Vanmechelen, M. M. Verbeek, B. Winblad, H. Zetterberg, M. Koel-Simmelink, and C. E. Teunissen. A practical guide to immunoassay method validation. *Frontiers in Neurology. 2015;6:179*, 6(179), 2015.

[83] M. P. Lambert, A. K. Barlow, B. A. Chromy, C. Edwards, R. Freed, M. Liosatos, T. E. Morgan, I. Rozovsky, B. Trommer, K. L. Viola, P. Wals, C. Zhang, C. E. Finch, G. A. Krafft, and W. L. Klein. Diffusible, nonfibrillar ligands derived from aβ1–42 are potent central nervous system neurotoxins. *PNAS*, 95(11):6448–6453, 1998.

[84] W. L. Klein. Aβ toxicity in alzheimer's disease: globular oligomers (addls) as new vaccine and drug targets. *Neurochemistry International*, 41(5):345 – 352, 2002.

[85] K. N. Dahlgren, A. M. Manelli, W. B. Stine Jr., L. K. Baker, G. A. Krafft, and M. J. LaDu. Oligomeric and fibrillar species of amyloid-β peptides differentially affect neuronal viability. *The Journal of Biological Chemistry*, 277:32046–32053, 2002.

[86] W. Xia, T. Yang, G. Shankar, I. M. Smith, Y. Shen, D. M. Walsh, and D. J. Selkoe. A specific enzyme-linked immunosorbent assay for measuring β-amyloid protein

oligomers in human plasma and brain tissue of patients with alzheimer disease. *Archives of Neurology*, 66(2):190–199, 2009.

[87] G. A. Krafft and W. L. Klein. ADDLs and the signaling web that leads to alzheimer's disease. *Neuropharmacology*, 59(4–5):230 – 242, 2010. Alzheimers Disease.

[88] H. Englund, D. Sehlin, A.-S. Johansson, L. N. G. Nilsson, P. Gellerfors, S. Paulie, L. Lannfelt, and F. E. Pettersson. Sensitive elisa detection of amyloid-β protofibrils in biological samples. *Journal of Neurochemistry*, 103(1):334–345, 2007.

[89] H. Fukumoto, T. Tokuda, T. Kasai, N. Ishigami, H. Hidaka, M. Kondo, D. Allsop, and M. Nakagawak. High-molecular-weight β-amyloid oligomers are elevated in cerebrospinal fluid of alzheimer patients. *The FASEB Journal*, 24(8):2716–2726, 2010.

[90] L. J. Kricka. Human anti-animal antibody interferences in immunological assays. *Clinical Chemistry*, 45(7):942–956, 1999.

[91] D. Sehlin, S. Söllvander, S. Paulie, R. Brundin, M. Ingelsson, L. Lannfelt, F. E. Pettersson, and H. Englund. Interference from heterophilic antibodies in amyloid-β oligomer elisas. *Journal of Alzheimer's Disease*, 21(4):1295–1301, 2010.

[92] P. Lewczuk, G. Beck, H. Esselmann, R. Bruckmoser, R. Zimmermann, M. Fiszer, M. Bibl, J. M. Maler, J. Kornhuber, , and J. Wiltfang. Effect of sample collection tubes on cerebrospinal fluid concentrations of tau proteins and amyloid β peptides. *Clinical Chemistry*, 52(2):332–334, 2006.

[93] D.R. Lachno, H. Vanderstichele, G. De Groote, V. Kostanjevecki, G. De Meyer, E.R. Siemers, M.B. Willey, J.S. Bourdage, R.J. Konrad, and R.A. Dean. The influence of matrix type, diurnal rhythm and sample collection and processing on the measurement of plasma β-amyloid isoforms using the inno-bia plasma aβ forms multiplex assay. *JNHA - The Journal of Nutrition, Health and Aging*, 13(3):220–225, 2009.

[94] H. Vanderstichele, E. V. Kerschaver, C. Hesse, P. Davidsson, M.-A. Buyse, N. Andreasen, L. Minthon, A. Wallin, K. Blennow, and E. Vanmechelen. Standardization of measurement of β-amyloid(1-42) in cerebrospinal fluid and plasma. *Amyloid: The Journal of Protein Folding Disorders*, 7:245–258, 2000.

[95] T. Kasai, T. Tokuda, M. Taylor, M. Nakagawa, and D. Allsop. Utilization of a multiple antigenic peptide as a calibration standard in the ban50 single antibody sandwich elisa for aβ oligomers. *Biochemical and Biophysical Research Communications*, 422(3):375 – 380, 2012.

[96] F. van der Vegt F. van Diggelen W. Grievink E. C. de Boer I. C. Schut J. D. J. Vis E. Vaccalluzzo-Hoogveld G. A. P. H. Scheefhals Elizabeth C. de Boer Ivar C. Schut Joost D.J. Vis Emily A. W. J. W. Tepper, I. J. Vereyken. Stabilized aβ oligomers as reliable and disease relevant reference standards in alzheimer's biomarker assays. http://www.crossbeta.com/uploads/crossbeta_poster_biomarkers_nov_2014.pdf.